ME-forskerens ABC

Her er en alfabetisk liste over vigtige gener / proteiner, som er påvirkede i ME sygdomsmekanismen.

internt notat 10. april 2018 HSN

	antal sider
A, Coenzym A	(4)
ABCC1	
ACACA	(2)
ACAD8	(2)
ACOT7	
ACOT11/STARD14	(8)
ACSF3 og B-celler	(6)
ACSL1	
AGXT2L2	
AMACR	(7)
AMPK	
ATP5A1	
ATP10A	
BCKDK	
BLVRA	
CAB39L	
CBFA2T2	
CBFA2T3	
CLYBL	(3)
COX10	
CYB5R2	
CYB5R3	
D2HGDH	(5)
DECR1	
ETFB	(6)
FADS2	
FAM13A	(2)
FKBP5	(3)
HADH	
HMGCL	
OSBPL6	
OXNAD1	(2)
PFKFB3	
PHYH	
POR	
PPCDC	(2)
SORCS2	
SORL1	
SORT1	
UCP2	(2)
UCP3	

WIKIPEDIA Mit navn er A, co-enzym A (CoA)

Coenzyme A

Coenzyme A (**CoA**, **CoASH**, or **HSCoA**) is a coenzyme, notable for its role in the synthesis and oxidation of fatty acids, and the oxidation of pyruvate in the citric acid cycle. All genomes sequenced to date encode enzymes that use coenzyme A as a substrate, and around 4% of cellular enzymes use it (or a thioester, such as acetyl-CoA) as a substrate. In humans, CoA biosynthesis requires cysteine, pantothenate, and adenosine triphosphate (ATP).[1]

De understregede processer er alle påvirkede i ME.

Contents

Discovery of structure

The structure of coenzyme A was identified in the early 1950s at the Lister Institute, London, together by Fritz Lipmann and other workers at Harvard Medical School and Massachusetts General Hospital.[2] Lipmann initially intended to study acetyl transfer in animals, and from these experiments he noticed a unique factor that was not present in enzyme extracts but was evident in all organs of the animals. He was able to isolate and purify the factor from pig liver and discovered that its function was related to a coenzyme that was active in choline acetylation.[3] The coenzyme was named coenzyme A to stand for "activation of acetate." In 1953, Fritz Lipmann won the Nobel Prize in Physiology or Medicine "for his discovery of co-enzyme A and its importance for intermediary metabolism".[3][4]

Coenzyme A

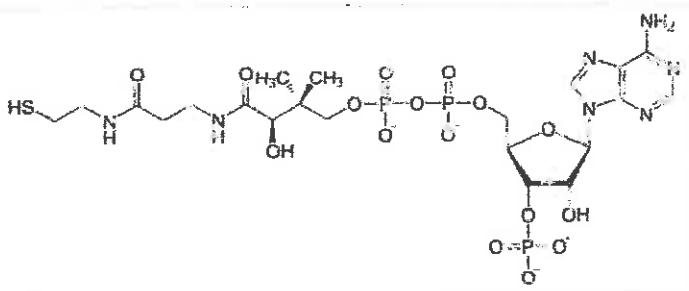

Identifiers	
CAS Number	85-61-0 (http://www.commonchemistry.org/ChemicalDetail.aspx?ref=85-61-0)
3D model (JSmol)	Interactive image (https://chemapps.stolaf.edu/jmol/jmol.php?model=O%3DC%28NCCS%29CCNC%28%3DO%29C%28O%29C%28C%29%28C%29COP%28%3DO%29%28O%29OP%28%3DO%29%28O%29OC%5BC%40H%5D3O%5BC%40%40H%5D%28n2cnc1c%28ncnc12%29N%29%5BC%40H%5D%28O%29%5BC%40%40H%5D3OP%28%3DO%29%28O%29O)
ChEBI	CHEBI:15346 (https://www.ebi.ac.uk/chebi/searchId.do?chebiId=15346)
ChEMBL	ChEMBL1213327 (https://www.ebi.ac.uk/chembldb/index.php/compound/inspect/ChEMBL1213327)
ChemSpider	6557 (http://www.chemspider.com/Chemical-Structure.6557.html)
DrugBank	DB01992 (https://www.drugban

mixed disulfides, such as CoA-S-S-glutathione, are commonly noted contaminants in commercial preparations of CoA.[18] Free CoA can be regenerated from CoA disulfide and mixed CoA disulfides with reducing agents such as DTT or BME.

side 4 i Wikipedia har en liste over

Non-exhaustive list of Coenzyme A-activated Acyl Groups

vigtige Coenzym A forbindelser

- Acetyl-CoA
- Fatty acyl-CoA (activated form of all fatty acids; only the CoA esters are substrates for important reactions such as mono-, di- and triacylglycerol synthesis, carnitine palmitoyl transferase, and cholesterol esterification)
  - Propionyl-CoA
  - Butyryl-CoA
  - Myristoyl-CoA
  - Crotonyl-CoA
- Acetoacetyl-CoA
- Coumaroyl-CoA (used in flavonoid and stilbenoid biosynthesis)
- Benzoyl-CoA
- Phenylacetyl-CoA
- Acyl derived from dicarboxylic acids
  - Malonyl-CoA (important in chain elongation in fatty acid biosynthesis and polyketide biosynthesis)
  - Succinyl-CoA (used in heme biosynthesis)
  - Hydroxymethylglutaryl-CoA (used in isoprenoid biosynthesis)
  - Pimelyl-CoA (used in biotin biosynthesis)

Klik på Malonyl-CoA og læs: Malonyl CoA inhibits fatty acids from associating with carnitine by regulating the enzyme carnitine acyltransferase, thereby preventing them from entering the mitochondria, where fatty acid oxidation and degradation occur.

References

1. Matthew Daugherty; Boris Polanuyer; Michael Farrell; Michael Scholle; Athanasios Lykidis; Valérie de Crécy-Lagard; Andrei Osterman (2002). "Complete Reconstitution of the Human Coenzyme A Biosynthetic Pathway via Comparative Genomics". *The Journal of Biological Chemistry*. 277 (24): 21431–21439. doi:10.1074/jbc.M201708200 (https://doi.org/10.1074%2Fjbc.M201708200). PMID 11923312 (https://www.ncbi.nlm.nih.gov/pubmed/11923312).
2. Baddiley, J.; Thain, E. M.; Novelli, G. D.; Lipmann, F. (1953). "Structure of Coenzyme A". *Nature*. 171 (4341): 76. doi:10.1038/171076a0 (https://doi.org/10.1038%2F171076a0).
3. Kresge, Nicole; Simoni, Robert D.; Hill, Robert L. (2005-05-27). "Fritz Lipmann and the Discovery of Coenzyme A" (http://www.jbc.org/content/280/21/e18). *Journal of Biological Chemistry*. 280 (21): e18–e18. ISSN 0021-9258 (https://www.worldcat.org/issn/0021-9258).
4. "Fritz Lipmann - Facts". Nobelprize.org. Nobel Media AB 2014. Web. 8 Nov 2017. <http://www.nobelprize.org/nobel_prizes/medicine/laureates/1953/lipmann-facts.html>
5. "Vitamin B5 (Pantothenic acid)" (http://www.umm.edu/health/medical/altmed/supplement/vitamin-b5-pantothenic-acid). *University of Maryland Medical Center*. Retrieved 2017-11-03.
6. "Pantothenic Acid (Vitamin B5): MedlinePlus Supplements" (https://medlineplus.gov/druginfo/natural/853.html). *medlineplus.gov*. Retrieved 2017-12-10.
7. LEONARDI, ROBERTA; JACKOWSKI, SUZANNE (April 2007). "Biosynthesis of Pantothenic Acid and Coenzyme A" (https://www.ncbi.nlm.nih.gov/pmc/articles/PMC4950986). *EcoSal Plus*. 2 (2). doi:10.1128/ecosalplus.3.6.3.4 (https://doi.org/10.1128%2Fecosalplus.3.6.3.4). ISSN 2324-6200 (https://www.worldcat.org/issn/2324-6200). PMC 4950986 (https://www.ncbi.nlm.nih.gov/pmc/articles/PMC4950986). PMID 26443589 (https://www.ncbi.nlm.nih.gov/pubmed/26443589).
8. Leonardi R, Zhang YM, Rock CO, Jackowski S (2005). "Coenzyme A: back in action". *Progress in Lipid Research*. 44 (2-3): 125–153. doi:10.1016/j.plipres.2005.04.001 (https://doi.org/10.1016%2Fj.plipres.2005.04.001). PMID 15893380 (https://www.ncbi.nlm.nih.gov/pubmed/15893380).

På reference listen er også artiklen, som der er uddrag af på side 3+4

A: Coenzym 1 side 2

Biochemical Journal (2017) 474 2489–2508
DOI: 10.1042/BCJ20170129

PORTLAND PRESS

Research Article

Protein CoAlation: a redox-regulated protein modification by coenzyme A in mammalian cells

Yugo Tsuchiya[1], Sew Yeu Peak-Chew[2], Clare Newell[1], Sharitta Miller-Aidoo[1], Sriyash Mangal[1,3], Alexander Zhyvoloup[1], Jovana Baković[1], Oksana Malanchuk[4], Gonçalo C. Pereira[5], Vassilios Kotiadis[5], Gyorgy Szabadkai[5], Michael R. Duchen[5], Mark Campbell[6], Sergio Rodriguez Cuenca[6], Antonio Vidal-Puig[6], Andrew M. James[7], Michael P. Murphy[7], Valeriy Filonenko[4], Mark Skehel[2] and Ivan Gout[1,4]

[1]Department of Structural and Molecular Biology, University College London, London WC1E 6BT, U.K.; [2]Biological Mass Spectrometry & Proteomics Cell Biology, MRC Laboratory of Molecular Biology, Cambridge CB2 0QH, U.K.; [3]Department of Biology II, Ludwig-Maximilians-Universität München, Planegg-Martinsried 82152, Germany; [4]Institute of Molecular Biology and Genetics, National Academy of Sciences of Ukraine, Kyiv 03680, Ukraine; [5]Department of Cell and Developmental Biology, University College London, London WC1E 6BT, U.K.; [6]Wellcome Trust–MRC Institute of Metabolic Science and MRC Metabolic Diseases Unit, Addenbrooke's Hospital, Cambridge CB2 0QQ, U.K.; and [7]MRC Mitochondrial Biology Unit, Wellcome Trust, MRC Building, University of Cambridge, Cambridge CB2 0XY, U.K.

Correspondence: Ivan Gout (i.gout@ucl.ac.uk)

OPEN ACCESS

Coenzyme A (CoA) is an obligatory cofactor in all branches of life. CoA and its derivatives are involved in major metabolic pathways, allosteric interactions and the regulation of gene expression. Abnormal biosynthesis and homeostasis of CoA and its derivatives have been associated with various human pathologies, including cancer, diabetes and neurodegeneration. Using an anti-CoA monoclonal antibody and mass spectrometry, we identified a wide range of cellular proteins which are modified by covalent attachment of CoA to cysteine thiols (CoAlation). We show that protein CoAlation is a reversible post-translational modification that is induced in mammalian cells and tissues by oxidising agents and metabolic stress. Many key cellular enzymes were found to be CoAlated *in vitro* and *in vivo* in ways that modified their activities. Our study reveals that protein CoAlation is a widespread post-translational modification which may play an important role in redox regulation under physiological and pathophysiological conditions.

Introduction

Coenzyme A (CoA) is a ubiquitous and essential cellular cofactor synthesised from cysteine, pantothenate (Vitamin B5) and ATP in a pathway conserved in all cells. CoA functions as a master acyl group carrier and a carbonyl-activating group, resulting in numerous metabolically active thioester derivatives, including acetyl CoA, malonyl CoA, succinyl CoA and 3-hydroxy-3-methylglutaryl CoA, among many others. CoA and its derivatives play important roles in a diverse range of cellular processes, including the Krebs cycle, the synthesis and oxidation of fatty acids, ketogenesis, biosynthesis of cholesterol and acetylcholine, regulation of gene expression and cellular metabolism via protein acetylation and others [1–4]. The size of the CoA pool (CoA and all its derivatives) varies widely among mammalian cells and tissues, being largest in the liver, heart and kidney. The subcellular distribution of the CoA pool reflects its diverse roles and varies from 20–140 μM in the cytosol to 2.2–5 mM in the mitochondria [1]. The level of CoA and the ratio between CoA and its thioesters (acyl CoA) in mammalian cells and tissues are tightly regulated by extracellular stimuli, nutrients, intracellular metabolites and stresses. Insulin, glucose, fatty acids and pyruvate all decrease CoA biosynthesis, whereas fasting, glucagon, glucocorticoids and hypolipidaemic drugs have the opposite effect [5–9]. Changes in the size of the CoA pool have also been reported in pathological conditions, such as diabetes and cancer [10,11]. Mutations in pantothenate kinase 2 (*PANK2*) and CoA synthase (*COASY*), which are rate-limiting enzymes in the CoA biosynthetic pathway, are associated with a severe

Received: 17 February 2017
Revised: 23 March 2017
Accepted: 24 March 2017

Accepted Manuscript online: 24 March 2017
Version of Record published: 11 July 2017

Side 3 A: coenzym A

PORTLAND PRESS

Biochemical Journal (2017) 474 2489–2508
DOI: 10.1042/BCJ20170129

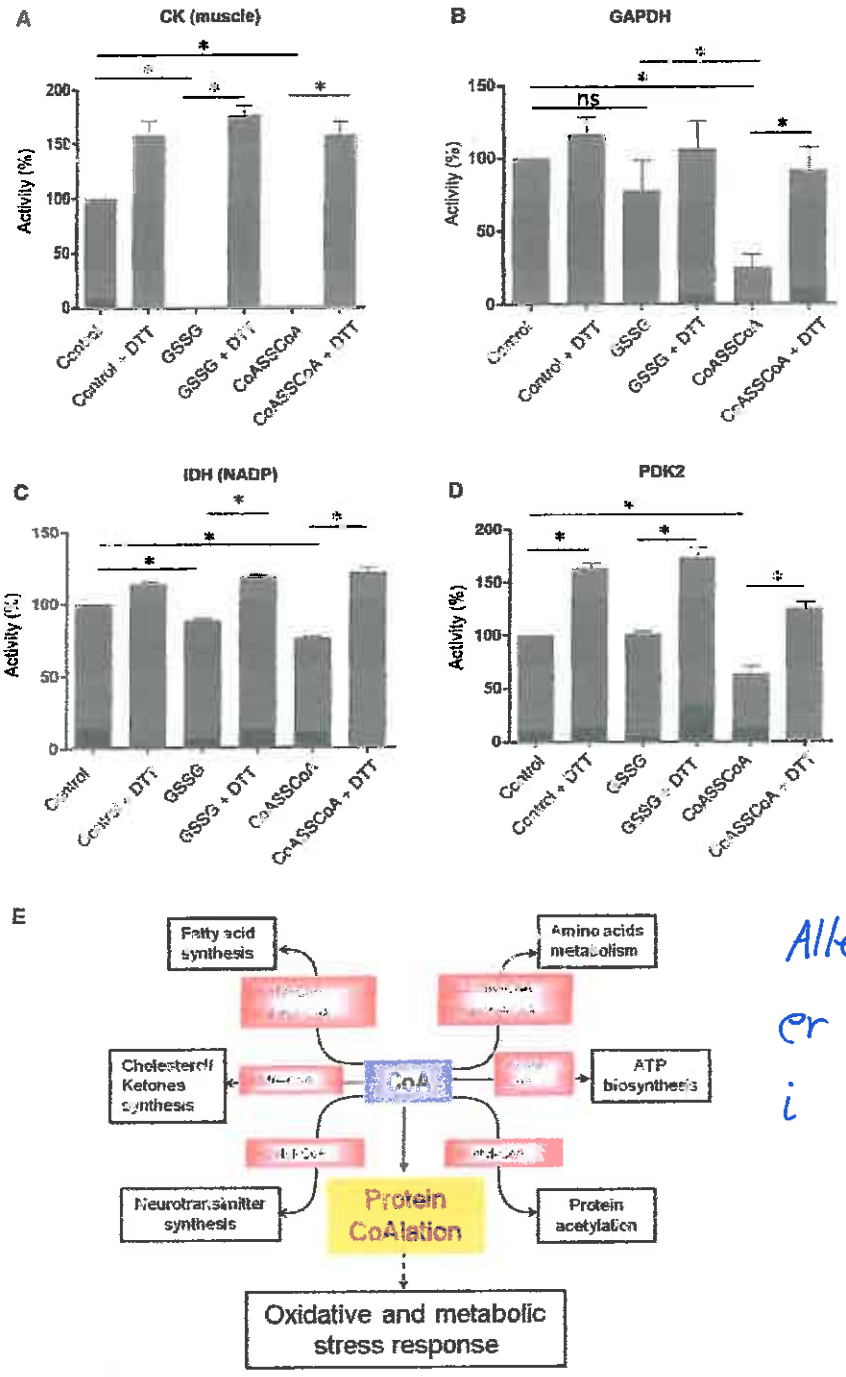

Alle processer er påvirkede i ME.

Figure 6. Catalytic activities of CK, GAPDH, IDH and PDK2 are modulated by CoAlation.

(**A–D**) CK, GAPDH purified from skeletal muscle and NADP-dependent IDH purified from heart were incubated with CoASSCoA or GSH dimer (GSSG) and their enzymatic activities assayed spectrophotometrically. The activity of recombinant PDK2 purified from HEK293 cells was assayed radiometrically using PDH as the substrate. Data shown are mean ± SEM of 3 (**A**, **C** and **D**) or 5 (**B**) independent measurements. Differences between groups were evaluated by a two-way repeated measures ANOVA matching both factors followed by a Tukey *post hoc* test to correct for multiple comparisons when assessing simple effects or Sidak test when assessing the 'reducing agent' effect. *$P < 0.05$. ns, not significant. (**E**) Cellular functions of CoA. In addition to its well-established role as an essential metabolic cofactor, CoA may also function as an antioxidant in cellular response to oxidative or metabolic stress via protein CoAlation.

Side 4 A: Coenzym A

ABCC1 ATP binding cassette subfamily C member 1 [*Homo sapiens* (human)]

Gene ID: 4363, updated on 5-Feb-2017

Genet er hypermethyleret i Vega 2014 og Vega 2017 -studierne.

Summary

Official Symbol	ABCC1 provided by HGNC
Official Full Name	ATP binding cassette subfamily C member 1 provided by HGNC
Primary source	HGNC:HGNC:51
See related	Ensembl:ENSG00000103222 MIM:158343; Vega:OTTHUMG00000048267
Gene type	protein coding
RefSeq status	REVIEWED
Organism	Homo sapiens
Lineage	Eukaryota; Metazoa; Chordata; Craniata; Vertebrata; Euteleostomi; Mammalia; Eutheria; Euarchontoglires; Primates; Haplorrhini; Catarrhini; Hominidae; Homo
Also known as	MRP; ABCC; GS-X; MRP1; ABC29
Summary	The protein encoded by this gene is a member of the superfamily of ATP-binding cassette (ABC) transporters. ABC proteins transport various molecules across extra-and intra-cellular membranes. ABC genes are divided into seven distinct subfamilies (ABC1, MDR/TAP, MRP, ALD, OABP, GCN20, White). This full transporter is a member of the MRP subfamily which is involved in multi-drug resistance. This protein functions as a multispecific organic anion transporter, with oxidized glutatione, cysteinyl leukotrienes, and activated aflatoxin B1 as substrates. This protein also transports glucuronides and sulfate conjugates of steroid hormones and bile salts. Alternatively spliced variants of this gene have been described but their full-length nature is unknown. [provided by RefSeq, Apr 2012]
Orthologs	mouse all

Genomic context

Galdesyre niveauerne er påvirke hos ME-patienter.

Glutatione er også påvirket.

See ABCC1 in Genome Data Viewer Map Viewer

Location: 16p13.11

Exon count: 34

Annotation release	Status	Assembly	Chr	Location
106	current	GRCh38.p7 (GCF_000001405.33)	16	NC_000016.10 (15949577..16143074)
105	previous assembly	GRCh37.p13 (GCF_000001405.25)	16	NC_000016.9 (16043434..16236931)

Chromosome 16 - NC_000016.10

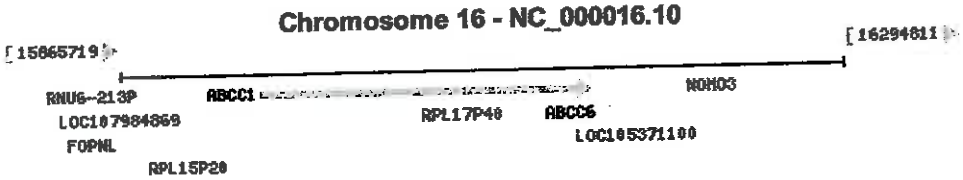

Genomic regions, transcripts, and products

Go to reference sequence details

Genomic Sequence: NC_000016.10 Chromosome 16 Reference GRCh38.p7 Primary Assembly ▼

Go to nucleotide: Graphics FASTA GenBank

ACACA acetyl-CoA carboxylase alpha [*Homo sapiens* (human)]

Gene ID: 31, updated on 19-Jan-2017

Genet er hypermethylert i begge vega studier

↑ Vega 2014 + 2017

Summary

Official Symbol	ACACA provided by HGNC
Official Full Name	acetyl-CoA carboxylase alpha provided by HGNC
Primary source	HGNC:HGNC:84
See related	Ensembl:ENSG00000278540 MIM:200350; Vega:OTTHUMG00000182463
Gene type	protein coding
RefSeq status	REVIEWED
Organism	Homo sapiens
Lineage	Eukaryota; Metazoa; Chordata; Craniata; Vertebrata; Euteleostomi; Mammalia; Eutheria; Euarchontoglires; Primates; Haplorrhini; Catarrhini; Hominidae; Homo
Also known as	ACC; ACAC; ACC1; ACCA; ACACAD
Summary	Acetyl-CoA carboxylase (ACC) is a complex multifunctional enzyme system. ACC is a biotin-containing enzyme which catalyzes the carboxylation of acetyl-CoA to malonyl-CoA, the rate-limiting step in fatty acid synthesis. There are two ACC forms, alpha and beta, encoded by two different genes. ACC-alpha is highly enriched in lipogenic tissues. The enzyme is under long term control at the transcriptional and translational levels and under short term regulation by the phosphorylation/dephosphorylation of targeted serine residues and by allosteric transformation by citrate or palmitoyl-CoA. Multiple alternatively spliced transcript variants divergent in the 5' sequence and encoding distinct isoforms have been found for this gene. [provided by RefSeq, Jul 2008]
Orthologs	mouse all

Genomic context

See ACACA in Genome Data Viewer Map Viewer

Location: 17q12

Exon count: 63

Annotation release	Status	Assembly	Chr	Location
108	current	GRCh38.p7 (GCF_000001405.33)	17	NC_000017.11 (37084992..37406822, complement)
105	previous assembly	GRCh37.p13 (GCF_000001405.25)	17	NC_000017.10 (35441927..35766902, complement)

Chromosome 17 - NC_000017.11

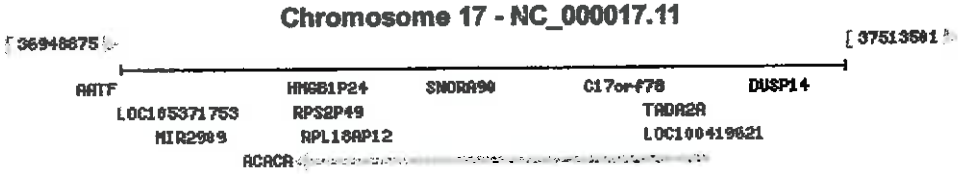

Genomic regions, transcripts, and products

Go to reference sequence details

Genomic Sequence: NC_000017.11 Chromosome 17 Reference GRCh38.p7 Primary Assembly

Go to nucleotide: Graphics FASTA GenBank

PubMed ▼ ACACA

Format: Abstract

Full text links

HighWire

Biochem J. 2017 Nov 6;474(22):3783-3797. doi: 10.1042/BCJ20170416.

A conserved mammalian mitochondrial isoform of acetyl-CoA carboxylase ACC1 provides the malonyl-CoA essential for mitochondrial biogenesis in tandem with ACSF3.

Monteuuis G, Suomi F, Kerätär JM[1], Masud AJ[1], Kastaniotis AJ[2].

Author information

Abstract

Mitochondrial fatty acid synthesis (mtFAS) is a highly conserved pathway essential for mitochondrial biogenesis. The mtFAS process is required for mitochondrial respiratory chain assembly and function, synthesis of the lipoic acid cofactor indispensable for the function of several mitochondrial enzyme complexes and essential for embryonic development in mice. Mutations in human mtFAS have been reported to lead to neurodegenerative disease. The source of malonyl-CoA for mtFAS in mammals has remained unclear. We report the identification of a conserved vertebrate mitochondrial isoform of ACC1 expressed from an ACACA transcript splicing variant. A specific knockdown (KD) of the corresponding transcript in mouse cells, or CRISPR/Cas9-mediated inactivation of the putative mitochondrial targeting sequence in human cells, leads to decreased lipoylation and mitochondrial fragmentation. Simultaneous KD of **ACSF3**, encoding a mitochondrial malonyl-CoA synthetase previously implicated in the mtFAS process, resulted in almost complete ablation of protein lipoylation, indicating that these enzymes have a redundant function in mtFAS. The discovery of a mitochondrial isoform of ACC1 required for lipoic acid synthesis has intriguing consequences for our understanding of mitochondrial disorders, metabolic regulation of mitochondrial biogenesis and cancer.

KEYWORDS: ACC1; **ACSF3**; acetyl-CoA carboxylase; malonyl-CoA; mitochondrial biogenesis; mitochondrial fatty acid synthesis

PMID: 28986507 DOI: 10.1042/BCJ20170416

[Indexed for MEDLINE]

Publication type, MeSH terms, Substances

LinkOut - more resources

ACACA side2

ACAD8 acyl-CoA dehydrogenase family member 8 [*Homo sapiens* (human)]

Gene ID: 27034, updated on 21-Dec-2016

Genet er hypermethyleret i begge Vega studier

Summary

Official Symbol	ACAD8 provided by HGNC
Official Full Name	acyl-CoA dehydrogenase family member 8 provided by HGNC
Primary source	HGNC:HGNC:87
See related	Ensembl:ENSG00000151498 MIM:604773; Vega:OTTHUMG00000167177
Gene type	protein coding
RefSeq status	REVIEWED
Organism	Homo sapiens
Lineage	Eukaryota; Metazoa; Chordata; Craniata; Vertebrata; Euteleostomi; Mammalia; Eutheria; Euarchontoglires; Primates; Haplorrhini; Catarrhini; Hominidae; Homo
Also known as	ARC42; ACAD-8
Summary	This gene encodes a member of the acyl-CoA dehydrogenase family of enzymes that catalyze the dehydrogenation of acyl-CoA derivatives in the metabolism of fatty acids or branch chained amino acids. The encoded protein is a mitochondrial enzyme that functions in catabolism of the branched-chain amino acid valine. Defects in this gene are the cause of isobutyryl-CoA dehydrogenase deficiency.[provided by RefSeq, Nov 2009]
Orthologs	mouse; all

Genomic context

See ACAD8 in Genome Data Viewer Map Viewer

Location: 11q25

Exon count: 14

Annotation release	Status	Assembly	Chr	Location
105	current	GRCh38.p7 (GCF_000001405.33)	11	NC_000011.10 (134253532..134265858)
105	previous assembly	GRCh37.p13 (GCF_000001405.25)	11	NC_000011.9 (134123428..134135749)

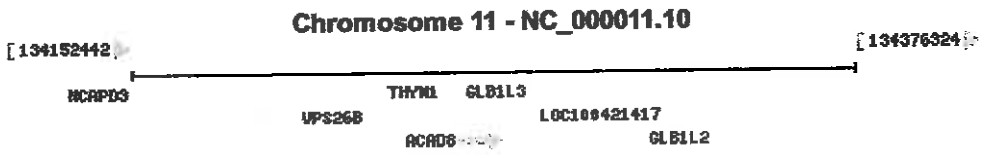

Genomic regions, transcripts, and products

Go to reference sequence details

Genomic Sequence: NC_000011.10 Chromosome 11 Reference GRCh38.p7 Primary Assembly

Go to nucleotide: Graphics FASTA GenBank

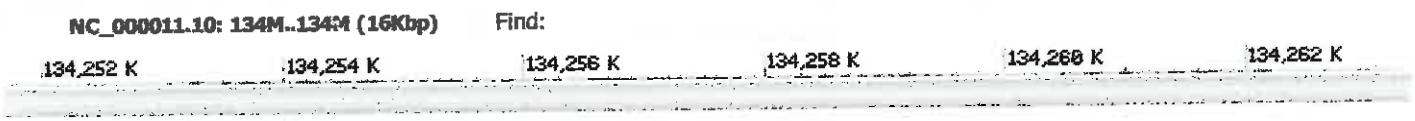

ACAD8

Am. J. Hum. Genet. 67:1095–1103, 2000

Isolated 2-Methylbutyrylglycinuria Caused by Short/Branched-Chain Acyl-CoA Dehydrogenase Deficiency: Identification of a New Enzyme Defect, Resolution of Its Molecular Basis, and Evidence for Distinct Acyl-CoA Dehydrogenases in Isoleucine And Valine Metabolism

Brage Storstein Andresen,[1,2] Ernst Christensen,[3] Thomas J. Corydon,[2] Peter Bross,[1] Bente Pilgaard,[5] Ronald J. A. Wanders,[6] Jos P. N. Ruiter,[6] Henrik Simonsen,[4] Vibeke Winter,[1] Inga Knudsen,[1] Lisbeth Dahl Schroeder,[1,2] Niels Gregersen,[1] and Flemming Skovby[3]

[1]Research Unit for Molecular Medicine, Aarhus University Hospital, and Faculty of Health Science, Skejby Sygehus, and [2]Institute of Human Genetics, Aarhus University, Aarhus; [3]Department of Clinical Genetics, Rigshospitalet, and [4]Statens Serum Institut, Copenhagen; [5]Department of Pediatrics, Roskilde Amtssygehus, Roskilde, Denmark; and [6]Department of Pediatrics, Emma Children's Hospital, and Department of Clinical Chemistry, Academic Medical Center, University of Amsterdam, Amsterdam

Acyl-CoA dehydrogenase (ACAD) defects in isoleucine and valine catabolism have been proposed in clinically diverse patients with an abnormal pattern of metabolites in their urine, but they have not been proved enzymatically or genetically, and it is unknown whether one or two ACADs are involved. We investigated a patient with isolated 2-methylbutyrylglycinuria, suggestive of a defect in isoleucine catabolism. Enzyme assay of the patient's fibroblasts, using 2-methylbutyryl-CoA as substrate, confirmed the defect. Sequence analysis of candidate ACADs revealed heterozygosity for the common short-chain ACAD A625 variant allele and no mutations in ACAD-8 but a 100-bp deletion in short/branched-chain ACAD (SBCAD) cDNA from the patient. Our identification of the *SBCAD* gene structure (11 exons; >20 kb) enabled analysis of genomic DNA. This showed that the deletion was caused by skipping of exon 10, because of homozygosity for a 1228G→A mutation in the patient. This mutation was not present in 118 control chromosomes. In vitro transcription/translation experiments and overexpression in COS cells confirmed the disease-causing nature of the mutant SBCAD protein and showed that ACAD-8 is an isobutyryl-CoA dehydrogenase and that both wild-type proteins are imported into mitochondria and form tetramers. In conclusion, we report the first mutation in the *SBCAD* gene, show that it results in an isolated defect in isoleucine catabolism, and indicate that ACAD-8 is a mitochondrial enzyme that functions in valine catabolism.

Introduction

The individual role of the different acyl-CoA dehydrogenases (ACADs) in isoleucine and valine catabolism is at present unclear, and the underlying enzymatic defects causing accumulation of metabolites derived from isobutyryl-CoA and 2-methylbutyryl-CoA are poorly understood. In 1994, a cDNA encoding a human homologue of rat 2-methyl–branched-chain ACAD was cloned and characterized (Rozen et al. 1994). The enzyme was named "short/branched-chain ACAD" (SBCAD), because it differed from its rat homologue in that it exhibited highest activity with butyryl-CoA and 2-methylbutyryl-CoA and low or no activity (Rozen et al. 1994; Binzak et al. 1999) with isobutyryl-CoA, suggesting a primary role in isoleucine catabolism and, perhaps, also in the catabolism of (short-chain) fatty acids, but not in valine catabolism. So far, none of the ACADs have been demonstrated to have significant enzyme activity with isobutyryl-CoA as substrate. However, the recently identified ACAD-8 (Telford et al. 1999), with unknown substrate specificity, exhibits the highest degree of sequence similarity to SBCAD and to short-chain ACAD (SCAD). Therefore, it is a candidate enzyme for branched-chain amino acid catabolism.

In the present study, we characterize the human *SBCAD* gene structure and describe the identification and characterization of the first mutation in the human *SBCAD* gene from a patient with 2-methylbutyrylglycinuria. Moreover, we investigate the mitochondrial import, processing, and enzyme activities of overexpressed human SBCAD and ACAD-8.

Received May 19, 2000; accepted for publication September 6, 2000; electronically published September 29, 2000.

Address for correspondence and reprints: Dr. Brage Storstein Andresen, Research Unit for Molecular Medicine, Skejby Sygehus, DK 8200 Århus N, Denmark. E-mail: brage@biobase.dk

0002-9297/2000/6705-0007$02.00

Patient and Methods

Case History

This 3-year-old boy is the second of three children of a marriage between first cousins from Pakistan. Preg-

ACAD8 Side2

ACOT7 acyl-CoA thioesterase 7 [*Homo sapiens* (human)]

Gene ID: 11332, updated on 11-Mar-2018

hypermethylerat Vega 2017, 57

Summary
enome Browsers
enome Data Viewer
ap Viewer
riation Viewer (GRCh37.p13)
riation Viewer (GRCh38)
00 Genomes Browser (GRCh37.p13)
nsembl
CSC

Official Symbol	ACOT7 provided by HGNC
Official Full Name	acyl-CoA thioesterase 7 provided by HGNC
Primary source	HGNC:HGNC:24157
See related	Ensembl:ENSG00000097021 MIM:602587; Vega:OTTHUMG00000001285
Gene type	protein coding
RefSeq status	REVIEWED
Organism	Homo sapiens
Lineage	Eukaryota; Metazoa; Chordata; Craniata; Vertebrata; Euteleostomi; Mammalia; Eutheria; Euarchontoglires; Primates; Haplorrhini; Catarrhini; Hominidae; Homo
Also known as	ACT; ACH1; BACH; LACH; LACH1; hBACH; CTE-II
Summary	This gene encodes a member of the acyl coenzyme family. The encoded protein hydrolyzes the CoA thioester of palmitoyl-CoA and other long-chain fatty acids. Decreased expression of this gene may be associated with mesial temporal lobe epilepsy. Alternatively spliced transcript variants encoding distinct isoforms with different subcellular locations have been characterized. [provided by RefSeq, Jul 2008]
Expression	Broad expression in brain (RPKM 26.5), kidney (RPKM 21.3) and 22 other tissues See more
Orthologs	mouse all

Genomic context

See ACOT7 in Genome Data Viewer Map Viewer

Location: 1p36.31

Exon count: 12

Annotation release	Status	Assembly	Chr	Location
108	current	GRCh38.p7 (GCF_000001405.33)	1	NC_000001.11 (6264272..6393766, complement)
105	previous assembly	GRCh37.p13 (GCF_000001405.25)	1	NC_000001.10 (6324332..6453826, complement)

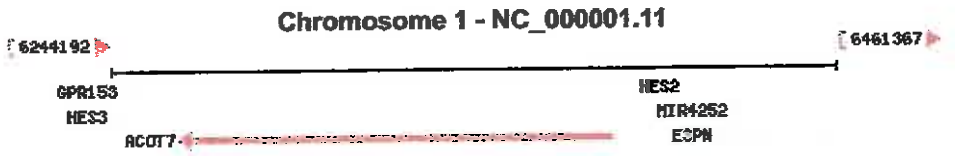

Genomic regions, transcripts, and products

Go to reference sequence details

Genomic Sequence: NC_000001.11 Chromosome 1 Reference GRCh38.p7 Primary Assembly ▼

Go to nucleotide: Graphics FASTA GenBank

ACOT11 acyl-CoA thioesterase 11 [*Homo sapiens* (human)] =BFIT= STARD14

Gene ID: 26027, updated on 11-Mar-2018 hyper ↑ i begge Vegn

Summary
enome Browsers
enome Data Viewer
ap Viewer
riation Viewer (GRCh37.p13)
riation Viewer (GRCh38)
00 Genomes Browser (GRCh37.p13)
nsembl
CSC

Official Symbol	ACOT11 provided by HGNC
Official Full Name	acyl-CoA thioesterase 11 provided by HGNC
Primary source	HGNC:HGNC:18156
See related	Ensembl:ENSG00000182390 MIM:606803; Vega:OTTHUMG00000009891
Gene type	protein coding
RefSeq status	REVIEWED
Organism	Homo sapiens
Lineage	Eukaryota; Metazoa; Chordata; Craniata; Vertebrata; Euteleostomi; Mammalia; Eutheria; Euarchontoglires; Primates; Haplorrhini; Catarrhini; Hominidae; Homo
Also known as	BFIT; THEA; THEM1; STARD14
Summary	This gene encodes a member of the acyl-CoA thioesterase family which catalyse the conversion of activated fatty acids to the corresponding non-esterified fatty acid and coenzyme A. Expression of a mouse homolog in brown adipose tissue is induced by low temperatures and repressed by warm temperatures. Higher levels of expression of the mouse homolog has been found in obesity-resistant mice compared with obesity-prone mice, suggesting a role of acyl-CoA thioesterase 11 in obesity. Alternative splicing results in transcript variants. [provided by RefSeq, Nov 2010]
Expression	Biased expression in kidney (RPKM 35.3), small intestine (RPKM 20.0) and 9 other tissues See more
Orthologs	mouse all

Genomic context (Husk nardilysin fra proteomstudiet)

See ACOT11 in Genome Data Viewer Map Viewer

Location: 1p32.3

Exon count: 18

Annotation release	Status	Assembly	Chr	Location
108	current	GRCh38.p7 (GCF_000001405.33)	1	NC_000001.11 (54548134..54634744)
105	previous assembly	GRCh37.p13 (GCF_000001405.25)	1	NC_000001.10 (55007930..55100417)

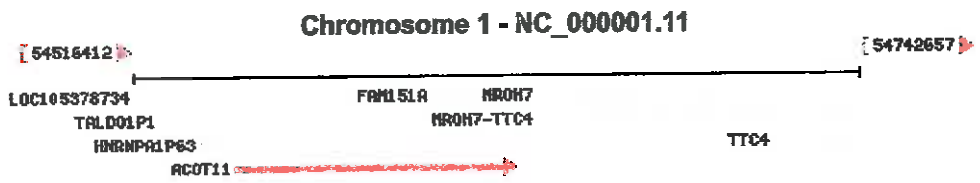

Genomic regions, transcripts, and products

Go to reference sequence details

Genomic Sequence: NC_000001.11 Chromosome 1 Reference GRCh38.p7 Primary Assembly ▼

Go to nucleotide: Graphics FASTA GenBank

BFIT = ACOT11 hypermethyleret
bygge Vega studier

Biochem. J. (2001) 360, 135–142 (Printed in Great Britain)

BFIT, a unique acyl-CoA thioesterase induced in thermogenic brown adipose tissue: cloning, organization of the human gene and assessment of a potential link to obesity

Sean H. ADAMS*[1], Clarissa CHUI†, Sarah L. SCHILBACH†, Xing Xian YU*, Audrey D. GODDARD†, J. Christopher GRIMALDI†, James LEE†, Patrick DOWD†, Steven COLMAN‡ and David A. LEWIN‡

*Department of Endocrinology, Genentech, Inc., South San Francisco, CA 94080, U.S.A., †Department of Molecular Biology, Genentech, Inc., South San Francisco, CA 94080, U.S.A., and †Department of Collaborative Research, CuraGen Corporation, New Haven, CT 06511, U.S.A.

We hypothesized that certain proteins encoded by temperature-responsive genes in brown adipose tissue (BAT) contribute to the remarkable metabolic shifts observed in this tissue, thus prompting a differential mRNA expression analysis to identify candidates involved in this process in mouse BAT. An mRNA species corresponding to a novel partial-length gene was found to be induced 2–3-fold above the control following cold exposure (4 °C), and repressed ≈ 70 % by warm acclimation (33 °C, 3 weeks) compared with controls (22 °C). The gene displayed robust BAT expression (i.e. ≈ 7–100-fold higher than other tissues in controls). The full-length murine gene encodes a 594 amino acid (≈ 67 kDa) open reading frame with significant homology to the human hypothetical acyl-CoA thioesterase KIAA0707. Based on cold-inducibility of the gene and the presence of two acyl-CoA thioesterase domains, we termed the protein brown-fat-inducible thioesterase (BFIT). Subsequent analyses and cloning efforts revealed the presence of a novel splice variant in humans (termed hBFIT2), encoding the orthologue to the murine BAT gene. BFIT was mapped to syntenic regions of chromosomes 1 (human) and 4 (mouse) associated with body fatness and diet-induced obesity, potentially linking a deficit of BFIT activity with exacerbation of these traits. Consistent with this notion, BFIT mRNA was significantly higher (≈ 1.6–2-fold) in the BAT of obesity-resistant compared with obesity-prone mice fed a high-fat diet, and was 2.5-fold higher in controls compared with *ob/ob* mice. Its strong, cold-inducible BAT expression in mice suggests that BFIT supports the transition of this tissue towards increased metabolic activity, probably through alteration of intracellular fatty acyl-CoA concentration.

Key words: fatty acids, hydrolase, metabolic rate.

INTRODUCTION

Remarkable shifts in the energetic profile of brown adipose tissue (BAT) occur upon exposure of rodents to certain environmental challenges (reviewed in [1,2]). Notably, non-shivering thermogenesis and a concomitant increase in fuel uptake and combustion are triggered in BAT upon exposure to a cold environment, thus providing a source of metabolic heat in defence of body temperature. A major catalyst of these events is uncoupling protein 1 (UCP1), which increases mitochondrial membrane proton permeability and thus accelerates flux of fuel-derived reducing equivalents in the electron transport chain. Sympathetic outflow to BAT increases in the cold, eliciting rapid biochemical changes supporting thermogenesis (i.e. stimulation of lipolysis). Such rapid changes are augmented by genetic regulation critical for the full manifestation of non-shivering thermogenesis in BAT. For example, expression of BAT UCP1 is rapidly and dramatically up-regulated following cold exposure in rodents [3], and its loss in UCP1 knockouts renders mice cold-intolerant [4]. Cold-induced proliferation and differentiation of BAT are more chronic events which, by definition, require changes at the level of gene regulation. Generally similar patterns of rodent BAT thermogenic activation may also occur in response to palatable high-fat diets [5,6], probably as a means to combat excessive weight gain under these conditions.

A more complete understanding of the molecular pathways underlying metabolic regulation will ultimately lead to optimal therapeutic regimens to treat obesity, diabetes and other disorders. Due to its metabolic malleability in response to thermoregulatory and nutritional cues, BAT is an attractive venue for studying the molecular basis of energy expenditure and fuel partitioning. BAT genes induced by cold exposure, but repressed in response to a warm environment, are likely to encode proteins involved in the transition of this tissue towards a more thermogenic state. Indeed, cold-induction of the recently described peroxisome proliferator-activated receptor-γ (PPARγ) co-activator-1 (PGC-1) fits this pattern, and this BAT-abundant transcription regulator probably plays a central role in sparking changes important to the regulation of metabolism in a variety of tissues [7,8].

The experiment described herein was based on the premise that metabolically relevant proteins will be discovered through analysis of genes expressed differentially in BAT derived from mice exposed to a variety of environmental temperatures. In particular, proteins encoded by genes upregulated at least 2-fold after cold exposure (4 °C, 48 h) were evaluated as potential candidates for their involvement in thermogenesis or intermediary metabolic regulation, based on their domain structures, homologies to known metabolic proteins and tissue-expression patterns. A gene encoding a BAT-abundant, novel murine acyl-CoA thioesterase termed brown-fat-inducible thioesterase (BFIT) was discovered, and found to be induced or repressed by cold and warm exposure, respectively. Murine BFIT (mBFIT) is homologous to a marginally characterized putative human

→ available CoA

p.140 : "... acceleration of fatty acid flux, may place a strain on

Abbreviations used: BAT, brown adipose tissue; UCP1, uncoupling protein 1; BFIT, brown-fat-inducible thioesterase; mBFIT, murine BFIT; hBFIT, human BFIT; WAT, white adipose tissue; RT-PCR, reverse transcriptase PCR; QEA, Quantitative Expression Analysis; ORF, open reading frame; NEFA, non-esterified fatty acid.

[1] To whom correspondence should be addressed, at Metabolic and Cardiovascular Disease Pharmacology Department, Novartis Pharmaceuticals Corporation, 556 Morris Avenue, Summit, NJ 07901, U.S.A. (e-mail sean.adams@pharma.novartis.com).

OBS på ref 34 i denne. PPT1 løsner fedt for – ankring af G-proteiner

ACOT11/STAR side2

BFIT2 = ACOT11 The gene is hypermethylated de Vega 2014 + de Vega 2017

Published in final edited form as:
Biochemistry. 2012 September 4; 51(35): 6990–6999. doi:10.1021/bi3008824.

Human Brown Fat Inducible Thioesterase *Variant* 2 (BFIT2) Cellular Localization and Catalytic Function#

Danqi Chen‡, John Latham‡, Hong Zhao‡, Marco Bisoffi§, Jeremiah Farelli+, and Debra Dunaway-Mariano‡,*

‡Department of Chemistry and Chemical Biology University of New Mexico, Albuquerque, New Mexico

§Department of Biochemistry and Molecular Biology, University of New Mexico Health Sciences Center, Albuquerque, New Mexico

+Department of Chemistry, Boston University, Boston, Massachusetts, USA 02215.

Abstract

The mammalian brown fat inducible thioesterase variant 2 (BFIT2), also known as ACOT11, is a multi-modular protein containing two consecutive hotdog-fold domains and a C-terminal steroidogenic acute regulatory protein related lipid transfer (START) domain (StarD14). In this study, we demonstrate that the N-terminal region of human BFIT2 (hBFIT2) constitutes a mitochondrial location signal sequence, which undergoes mitochondria-dependent posttranslational cleavage. The mature hBFIT2 is shown to be located in the mitochondrial matrix whereas the paralog "cytoplasmic acetyl-CoA hydrolase" (CACH, also known as ACOT12) was found in the cytoplam. *In-vitro* activity analysis of full-length hBFIT2 isolated from stably transfected HEK293 cells demonstrates selective thioesterase activity directed towards long chain fatty acyl-CoA thioesters, thus distinguishing BFIT2 catalytic function from that of CACH. The results from a protein-lipid overlay test indicate that the hBFIT2 StarD14 domain binds phosphatidylinositol 4-phosphate.

StarD14

Keywords

thioesterase; mitochondria; START domain; hotdog-fold; thioester hydrolysis; lipid metabolism; ACOT11; ACOT12; BFIT; CACH; StarD14; StarD15; fatty acid

Body heat production triggered by low temperature or a high fat diet is known as adaptive thermogenesis (1-4). In brown fat adipose tissue (BAT),[1] thermogenesis is associated with the decoupling of energy metabolism and ATP synthesis *via* the action of the mitochondrial transmembrane protein UCP1 (5-9). UCP1 allows the protons that have been pumped into

#Supported by NIH Grant GM28688

*Corresponding Author: Debra Dunaway-Mariano MSC03 2060; 1 University of New Mexico Albuquerque, New Mexico 87131. Tel.: 505.277.3383; Fax: 505.277.2609; dd39@unm.edu.

SUPPORTING INFORMATION
Detailed experimental protocol and tables and figures reporting experimental results or protein graphics are available free of charge via the Internet at http://pubs.acs.org

page 2: ... "BFIT may perform a more generalized function as a regulator of energy homeostasis."

ACOT11/STAR side 3

phosphatidyl inositol-4-phosphate must be first carried out to measure the binding curve and thereby determine the actual binding constant.

Conclusions

The assignment of the biological functions of the human thioesterases presents a challenge that must be met in order to better understand the regulation of lipid metabolism and its role in lipid-related diseases. The majority of the human thioesterases belong to the hotdog-fold family. Our earlier focus on the structure-function relationships among bacterial hotdog-fold thioesterases has provided us with a platform for tackling the complexities associated with human thioesterase function assignment. Based on our own work, and the work of numerous other investigators, it has become clear that the hotdog-fold thioesterases are limited to CoA or holo-acyl carrier proteins (ACP) thioester substrates because of the topology of the substrate binding site that is set by the conserved fold. Briefly, this fold accommodates the nucleotide or ACP unit on the protein surface at the entrance of a long, narrow tunnel that ultimately leads to the catalytic site. The pantetheine arm threads through the tunnel wherein a combination of desolvation and electrostatic interactions provide a signification fraction of the substrate binding energy. Consequently, some thioesterases are able to hydrolyze both CoA and *holo*ACP thioesters. The pantetheine binding tunnel opens to the catalytic site, which can be enclosed for specific substrate targeting (55) or open to allow substrates with varying sized acyl or aroyl groups to bind (21, 30). In the present study, we showed that hBFIT2 catalyzes the *in-vitro* hydrolysis of fatty acyl-CoA thioesters with a preference for long chains (C14-C16) over shorter chains.

The demonstration of hBFIT2 fatty acyl-CoA thioesterase activity and its localization to the mitochondrial matrix is only the first step in assigning biological function. Notably, hBFIT2 is not the only thioesterase present in the matrix (56-57). The presence of the StarD14 domain in hBFIT suggests that the thioesterase activity is subject to a unique form of regulation, or alternatively that hBFIT performs a biochemical function that extends beyond that of a thioesterase.

Supplementary Material

Refer to Web version on PubMed Central for supplementary material.

References

1. Lowell BB, Spiegelman BM. Towards a molecular understanding of adaptive thermogenesis. Nature. 2000; 404:652–660. [PubMed: 10766252]
2. Butow RA, Bahassi EM. Adaptive thermogenesis: orchestrating mitochondrial biogenesis. Curr Biol. 1999; 9:R767–769. [PubMed: 10531019]
3. Lowell BB. Adaptive thermogenesis: turning on the heat. Curr Biol. 1998; 8:R517–520. [PubMed: 9705924]
4. Puigserver P, Wu Z, Park CW. Graves R, Wright M, Spiegelman BM. A cold-inducible coactivator of nuclear receptors linked to adaptive thermogenesis. Cell. 1998; 92:829–839. [PubMed: 9529258]
5. Nedergaard J, Golozoubova V, Matthias A, Asadi A, Jacobsson A, Cannon B. UCP1: the only protein able to mediate adaptive non-shivering thermogenesis and metabolic inefficiency. Biochim Biophys Acta. 2001; 1504:82–106. [PubMed: 11239487]

ACOT11/ STAR side 4

OPEN ACCESS Freely available online

PLoS one

Comparative Structural Analysis of Lipid Binding START Domains

Ann-Gerd Thorsell[1], Wen Hwa Lee[2], Camilla Persson[1], Marina I. Siponen[1], Martina Nilsson[1], Robert D. Busam[1], Tetyana Kotenyova[1], Herwig Schüler[1]*, Lari Lehtiö[1,3]*

1 Department of Medical Biochemistry and Biophysics, Structural Genomics Consortium, Karolinska Institutet, Stockholm, Sweden, 2 Structural Genomics Consortium, University of Oxford, Headington, Oxford, United Kingdom, 3 Department of Biosciences, Pharmaceutical Sciences, Åbo Akademi University, Turku, Finland

Abstract

Background: Steroidogenic acute regulatory (StAR) protein related lipid transfer (START) domains are small globular modules that form a cavity where lipids and lipid hormones bind. These domains can transport ligands to facilitate lipid exchange between biological membranes, and they have been postulated to modulate the activity of other domains of the protein in response to ligand binding. More than a dozen human genes encode START domains, and several of them are implicated in a disease.

Principal Findings: We report crystal structures of the human STARD1, STARD5, STARD13 and STARD14 lipid transfer domains. These represent four of the six functional classes of START domains.

Significance: Sequence alignments based on these and previously reported crystal structures define the structural determinants of human START domains, both those related to structural framework and those involved in ligand specificity.

Enhanced version: **This article can also be viewed as an enhanced version (http://plosone.org/enhanced/pone.0019521/) in which the text of the article is integrated with interactive 3D representations and animated transitions. Please note that a web plugin is required to access this enhanced functionality. Instructions for the installation and use of the web plugin are available in Text S1.**

Citation: Thorsell A-G, Lee WH, Persson C, Siponen MI, Nilsson M, et al. (2011) Comparative Structural Analysis of Lipid Binding START Domains. PLoS ONE 6(6): e19521. doi:10.1371/journal.pone.0019521

Editor: Nick Gay, University of Cambridge, United Kingdom

Received January 31, 2011; **Accepted** March 31, 2011; **Published** June 30, 2011

Funding: The Structural Genomics Consortium is a registered charity (number 1097737) that receives funds from the Canadian Institutes for Health Research, the Canadian Foundation for Innovation, Genome Canada through the Ontario Genomics Institute, GlaxoSmithKline, Karolinska Institutet, the Knut and Alice Wallenberg Foundation, the Ontario Innovation Trust, the Ontario Ministry for Research and Innovation, Merck & Co., Inc., the Novartis Research Foundation, the Swedish Agency for Innovation Systems, the Swedish Foundation for Strategic Research and the Wellcome Trust. LL was also supported by the Academy of Finland Grant 128322. The funders had no role in study design, data collection and analysis, decision to publish, or preparation of the manuscript.

Competing Interests: The authors have received funding from the following commercial sources: GlaxoSmithkline, Merck & Co., Inc. and Novartis. This does not alter the authors' adherence to all the PLoS ONE policies on sharing data and materials.

* E-mail: lari.lehtio@abo.fi(LL); herwig.schuler@ki.se (HS)

Introduction

The START domain is a ubiquitous conserved module for binding and transporting lipids [1]. Although the functions of most START domain containing proteins remain unknown, some regulate steroidogenesis and some are known to transfer lipids between membranes. There are approximately 40 proteins containing domains with START homology encoded in the human genome. The most well-characterized START domain containing proteins have been divided into 6 groups based on their phylogenetic relationships [2,3], but additional members can be assigned to most of these groups. Group 1 contains the name-giving family member, steroidogenic acute regulatory protein (StAR/STARD1), and STARD3. Both are cholesterol carriers, and mutations in STARD1 cause congenital lipoid adrenal hyperplasia. Group 2 consist of proteins containing only a START domain; group 3 proteins are capable of binding different ligands, such as phosphatidyl choline (STARD2/PCTP) and ceramides (STARD11); group 4 proteins (DLC, or deleted in cancerous liver cells) are frequently de-regulated in cancer and contain Rho-GTPase activating domains; group 5 proteins contain two thioesterase domains; and group 6 consists of only STARD9, a 4614-residue protein with unknown function, that contains a kinesin motor domain at its N-terminus. Mitochondria contain at least the group 2 phosphatidylcholine transfer protein STARD7, and also the Coenzyme Q binding protein Coq10, which was recently identified to contain a divergent START domain [4].

Structural analyses of START domains from groups 1–3 have provided detailed insights into how these proteins sequester specific lipids [5–9] (summarized in Table 1). The ~210 residue globular START module is a curved β-sheet gripped by two α-helices. The concave face of the β-sheet and the C-terminal α-helix enclose a hydrophobic cavity that can accommodate lipid molecules. Here we present crystal structures of four human START domains, those of STARD1, STARD5, STARD13 and STARD14/ACOT11. These structures extend our knowledge onto group 4 and 5 START domains, and enable a family-wide comparison of their lipid binding cavities. This structural

ACOT 11/Star sids

Thorsell et al: Comparative Structural Analysis of Lipid Binding START domains.

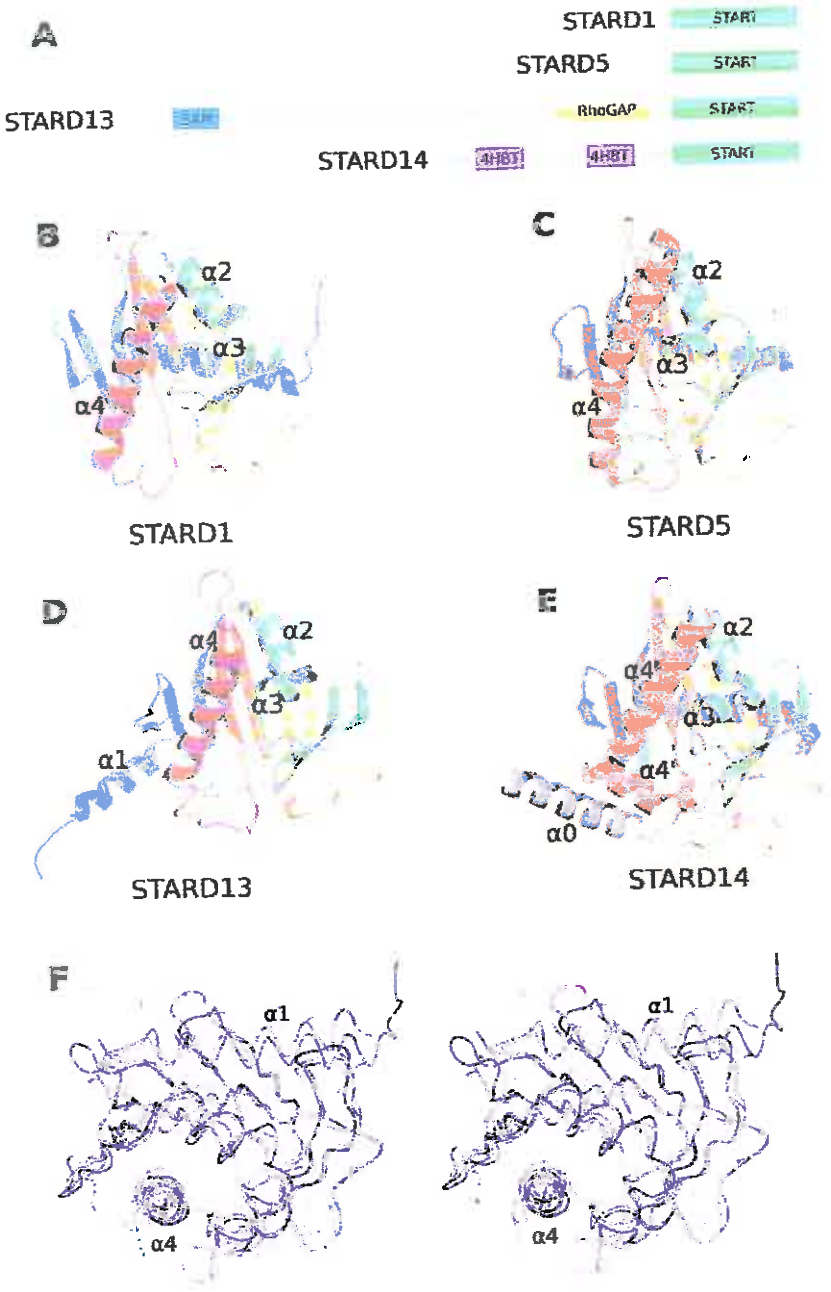

STARD13 hyper-methylated (Vega 2017)

ACOT11= STARD14 hyper-methylated (Vega 2014 and Vega 2017)

Page 9: "Based on our structural analysis we propose charged lipids as ligands for STARD13 and fatty acids as ligands for STARD14."

Figure 2. Overview of the crystal structures reported in this study. (A) Cartoon of the START domains studied here in context of the respective full-length proteins (drawn approximately to scale). (B–E) Side-by-side comparison of human STARD1, -5, -13, and -14 in a similar orientation. All START domain structures are colored from the N-terminus (blue) to the C-terminus (red) and the linker to the N-terminal thioesterase domain of STARD14 (panel E) is shown in grey. (F) Stereo view of a superposition of the backbone traces of the four crystal structures shown in panels B through E (blue, STARD1; red, STARD5; cyan, STARD13; yellow, STARD14). The view is that of panels B–E with an approximately 90° rotation downward toward the viewer.

doi:10.1371/journal.pone.0019521.g002

around this residue has been proposed to stabilize the C-terminal helix in a closed conformation [14]. Conservation of this structural feature across the domain family indicates that a lipid binding mechanism via local unfolding or a significant conformational change in the C-terminal helix could be a family wide phenomenon. Mutation in the adjacent, highly conserved residue Asn148 has been observed in congenital lipoid adrenal hyperplasia (lipoid CAH) [15], which add further evidence to the functional importance of this region (Fig. 4B).

Lipoid CAH is linked also to other mutations in the STARD1 encoding gene. Some of these mutations lead to premature stop codons, while others change the protein activities and lipid binding

ACOT11/StarD6

Remember: GRAMD1A the most hypermethylated gene associated with quality of life in ME

Article

TRANSPARENT PROCESS

THE EMBO JOURNAL

Molecular basis for sterol transport by StART-like lipid transfer domains (Vega 2017)

Florian A Horenkamp[1,†], Diana P Valverde[1,†], Jodi Nunnari[2] & Karin M Reinisch[1,*]

Abstract

Lipid transport proteins at membrane contact sites, where two organelles are closely apposed, play key roles in trafficking lipids between cellular compartments while distinct membrane compositions for each organelle are maintained. Understanding the mechanisms underlying non-vesicular lipid trafficking requires characterization of the lipid transporters residing at contact sites. Here, we show that the mammalian proteins in the lipid transfer proteins anchored at a membrane contact site (LAM) family, called GRAMD1a-c, transfer sterols with similar efficiency as the yeast orthologues, which have known roles in sterol transport. Moreover, we have determined the structure of a lipid transfer domain of the yeast LAM protein Ysp2p, both in its apo-bound and sterol-bound forms, at 2.0 Å resolution. It folds into a truncated version of the steroidogenic acute regulatory protein-related lipid transfer (StART) domain, resembling a lidded cup in overall shape. Ergosterol binds within the cup, with its 3-hydroxy group interacting with protein indirectly via a water network at the cup bottom. This ligand binding mode likely is conserved for the other LAM proteins and for StART domains transferring sterols.

Keywords cholesterol; endoplasmic reticulum; lipid transport protein; membrane contact sites; StART domain
Subject Categories Membrane & Intracellular Transport; Structural Biology
DOI 10.15252/embj.201798002 | Received 14 August 2017 | Revised 2 February 2018 | Accepted 5 February 2018
The EMBO Journal (2018) e98002

Introduction

Lipids, which are synthesized primarily in the endoplasmic reticulum (ER), become redistributed to other compartments asymmetrically. As a result, organelles differ in the composition of their lipid bilayers, imparting different biochemical and biophysical characteristics and helping to define organelle identity (Bigay & Antonny, 2012). Membrane contact sites, where two organelles are closely apposed, and the lipid transfer proteins enriched at such sites play critical roles in lipid redistribution (Lahiri *et al*, 2015; Drin *et al*, 2016; Kentala *et al*, 2016; Reinisch & De Camilli, 2016; Saheki *et al*, 2016). By definition, lipid transport proteins include lipid binding modules which function by solubilizing lipids during transit across the cytosol between two organelle membranes. Some transport proteins additionally serve as tethers, helping to maintain the architecture of contact sites. Identification and characterization of lipid transporters at membrane contact sites are an area of ongoing research critical in unraveling the mechanisms that underlie lipid homeostasis (Schauder *et al*, 2014; Lahiri *et al*, 2015; Drin *et al*, 2016; Kentala *et al*, 2016; Reinisch & De Camilli, 2016; Saheki *et al*, 2016; Lees *et al*, 2017).

The lipid transfer proteins anchored at a membrane contact site (LAM) or lipid transfer at contact site (Ltc) family of lipid transporters was discovered on the basis of distant sequence homology and structural alignment with proteins containing a steroidogenic acute regulatory protein-related lipid transfer (StART) domain (Gatta *et al*, 2015; Murley *et al*, 2015). A number of StART proteins transfer sterol, whereas others are involved in the transport of other lipids such as ceramide, phosphatidylcholine, or bile acids (Clark, 2012; Alpy & Tomasetto, 2014; Letourneau *et al*, 2015). Proteins in the LAM/Ltc family all feature an unstructured N-terminus, followed by a pleckstrin homology-like domain known as a GRAM domain, one or two StART-like domains, a transmembrane segment anchored to the ER, and a short ER-luminal stretch (Gatta *et al*, 2015; Murley *et al*, 2015; Fig 1A). Although there are no known StART domain proteins in *S. cerevisiae*, there are six LAM/Ltc proteins with StART-like domains, which localize to contacts between the ER and the plasma membrane (PM; Ysp2p/Lam2p/Ltc4p, Lam4p/Ltc3p, Ysp1p/Lam1p, Sip3p/Lam3p; Gatta *et al*, 2015) or either ER–mitochondrial or ER–vacuolar contacts (Lam5p/Ltc2p, Lam6p/Ltc1p) (Elbaz-Alon *et al*, 2015; Murley *et al*, 2015). Characterized yeast LAM/Ltc proteins all bind and/or transport sterol (Gatta *et al*, 2015; Murley *et al*, 2015) and have been implicated in coordinating sterol homeostasis with cellular stress responses (Murley *et al*, 2017). We show here that the three mammalian LAM/Ltc proteins, called GramD1a-c, all efficiently transport sterols *in vitro* and so are also likely to function in sterol transport, perhaps with similar roles in stress response as in fungi. How the LAM/Ltc proteins, or related proteins in the StART family, interact with sterol has so far been unknown.

To address how StART and StART-like proteins bind sterol, we determined the crystal structure of a StART-like domain of

1 Department of Cell Biology, Yale University School of Medicine, New Haven, CT, USA
2 Department of Molecular and Cellular Biology, University of California, Davis, Davis, CA, USA
*Corresponding author. Tel: +1 203 785 6469; E-mail: karin.reinisch@yale.edu
†These authors contributed equally to this work

ACOT11 / star side 7

StaRT-like

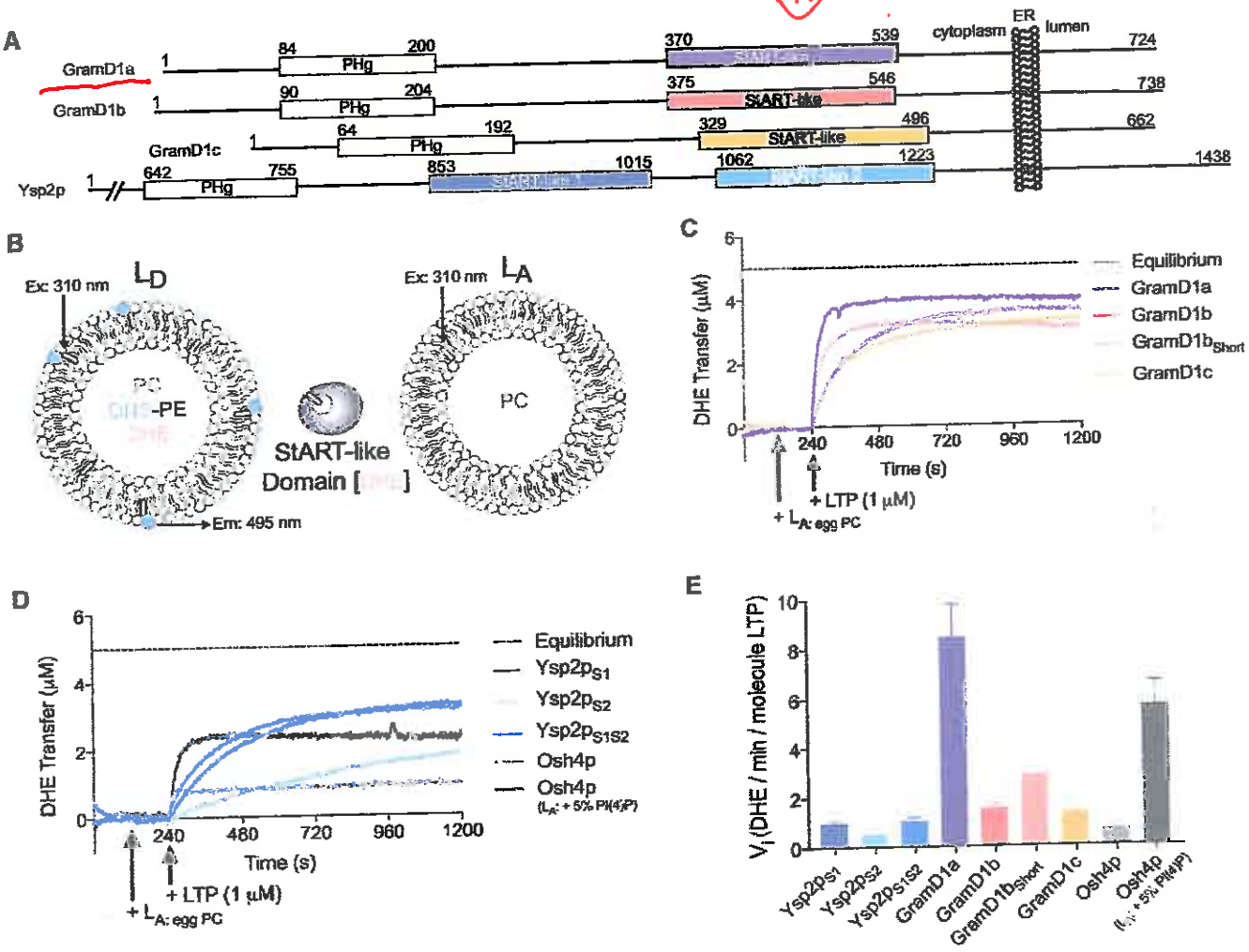

Figure 1. StART-like domains of Ysp2p and GramD1a-c transfer DHE between membranes.

A Domain architecture of Ysp2p and GramD1a-c.

B Schematic of the DHE transport assay. Donor liposomes L_D (92.5/5/2.5 mol% egg PC/DHE/DNS-PE, 200 μM total lipid) were incubated with acceptor liposomes L_A (egg PC, 200 μM total lipid). Transfer of DHE by lipid transfer proteins between L_D and L_A liposomes results in the loss of FRET between DHE and DNS-PE. For reference, the signal of a sample with DHE in equilibrium between L_D (95/2.5/2.5 mol% egg PC/DHE/DNS-PE, 200 μM total lipid) and L_A (97.5/2.5 mol% egg PC/DHE, 200 μM total lipid) was measured. After subtraction of the buffer reaction, the signal was normalized to the amount of DHE present in L_A based on the signal of the equilibrium sample.

C DHE transfer by 1 μM of the StART-like domain of GramD1a (residues 363–565, purple), GramD1b (residues 372–572, red), GramD1b$_{Short}$ (residues 372–550, salmon), and GramD1c (residues 323–521, orange). Mean of three independent experiments. For mean ± SD, see Fig EV1A. The dashed black line represents DHE equilibrium between L_D and L_A.

D DHE transfer by 1 μM of the first (residues 851–1,017, blue), second (residues 1,027–1,244, light blue), or a construct comprising both (residues 851–1,244, steel blue) StART-like domains of Ysp2p or Osh4p (light gray). Addition of 5 mol% PI(4)P to the acceptor liposomes increases Osh4p sterol transfer activity (Osh4p L_A + 5% PI(4)P, dark gray). Mean of three independent experiments. For mean ± SD, see Fig EV1B. The dashed black line represents DHE equilibrium between L_D and L_A.

E Initial DHE transfer rates (V_i, mean ± SD, $n = 3$).

25–40× (~40 DHE/min/molecule LTP) over those initially measured for sterol transfer by Ysp2p$_{S1}$ and GramD1b with liposomes composed of egg PC (Fig 1E).

To assess whether the StART-like domains preferentially transport sterol, we examined their ability to transfer other lipids, namely phosphatidylethanolamine (PE) and PS. We monitored the transfer of radiolabeled PE (14C) (and cholesterol (3H) as a positive control) between "heavy" and "light" liposomes, containing 0.75 M or no sucrose, respectively, by scintillation counting after separating the liposomes by centrifugation. We used another established FRET-based assay to follow PS transfer (Moser von Filseck *et al*, 2015a; Fig 3A). The transfer reaction was carried out in the presence of NBD-labeled PS sensor (NBD-C2$_{Lact}$), with donor liposomes containing 5 mol% brain PS and 2 mol% 1,2-dioleoyl-*sn*-glycero-3-phosphoethanolamine-N-(lissamine rhodamine B sulfonyl) (Rhod-PE). The fluorescence of NBD-C2$_{Lact}$ is quenched by Rhod-PE in the

ACOT11 / Star side 8

ACSF3 acyl-CoA synthetase family member 3 [*Homo sapiens* (human)]

Gene ID: 197322, updated on 3-Apr-2018

hypermethyleret (beta-diff: 0,0755), Body
p = 3,45E-05, FDR = 0,008164, Vega 2017, Label S1

Summary
enome Browsers
enome Data Viewer
ap Viewer
riation Viewer (GRCh37.p13)
riation Viewer (GRCh38)
00 Genomes Browser (GRCh37.p13)
nsembl
CSC

Official Symbol	ACSF3 provided by HGNC
Official Full Name	acyl-CoA synthetase family member 3 provided by HGNC
Primary source	HGNC:HGNC:27288
See related	Ensembl:ENSG00000176715 MIM:614245; Vega:OTTHUMG00000138044
Gene type	protein coding
RefSeq status	REVIEWED
Organism	Homo sapiens
Lineage	Eukaryota; Metazoa; Chordata; Craniata; Vertebrata; Euteleostomi; Mammalia; Eutheria; Euarchontoglires; Primates; Haplorrhini; Catarrhini; Hominidae; Homo
Summary	This gene encodes a member of the acyl-CoA synthetase family of enzymes that activate fatty acids by catalyzing the formation of a thioester linkage between fatty acids and coenzyme A. The encoded protein is localized to mitochondria, has high specificity for malonate and methylmalonate and possesses malonyl-CoA synthetase activity. Mutations in this gene are a cause of combined malonic and methylmalonic aciduria. Alternatively spliced transcript variants have been observed for this gene. [provided by RefSeq, Sep 2013]
Expression	Ubiquitous expression in duodenum (RPKM 1.5), lymph node (RPKM 1.5) and 25 other tissues See more
Orthologs	mouse all

Domæne: MCS og calc (involveret i lipid transport)

Også kaldet malonyl-CoA synthetase (MCS)

Functions navner:
acid-ligase activity
very long-chain fatty acid CoA ligase activity

Genomic context

See ACSF3 in Genome Data Viewer Map Viewer

Location: 16q24.3

Exon count: 19

Annotation release	Status	Assembly	Chr	Location
109	current	GRCh38.p12 (GCF_000001405.38)	16	NC_000016.10 (89093809..89160556)
105	previous assembly	GRCh37.p13 (GCF_000001405.25)	16	NC_000016.9 (89160217..89222171)

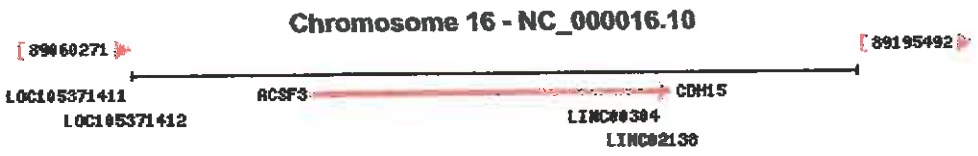

Genomic regions, transcripts, and products

Go to reference sequence details

Genomic Sequence: NC_000016.10 Chromosome 16 Reference GRCh38.p12 Primary Assembly ▼

Go to nucleotide: Graphics FASTA GenBank

ACSF3 side 1

Published in final edited form as:
Nat Genet. ; 43(9): 883–886. doi:10.1038/ng.908.

Exome sequencing identifies *ACSF3* as the cause of Combined Malonic and Methylmalonic Aciduria

Jennifer L. Sloan[1,*], Jennifer J. Johnston[2,*], Irini Manoli[1,&], Randy J. Chandler[1,3,&], Caitlin Krause[2], Nuria Carrillo-Carrasco[1], Suma D. Chandrasekaran[1], Justin R. Sysol[1], Kevin O'Brien[4], Natalie S. Hauser[1], Julie C. Sapp[2], Heidi M. Dorward[4], Marjan Huizing[4], NIH Intramural Sequencing Center Group[5], Bruce A. Barshop[6], Susan A. Berry[7], Philip M. James[8], Neena L. Champaigne[9], Pascale de Lonlay[10], Vassilli Valayannopoulos[10], Michael D. Geschwind[11], Dimitar K. Gavrilov[12], William L. Nyhan[6], Leslie G. Biesecker[2,#], and Charles P. Venditti[1]

[1]Genetics and Molecular Biology Branch, National Human Genome Research Institute, National Institutes of Health, Bethesda, MD, USA

[2]Genetic Disease Research Branch, National Human Genome Research Institute, National Institutes of Health, Bethesda, MD, USA

[3]Department of Pharmacology, Institute for Biomedical Sciences, The George Washington University, Washington, DC

[4]Medical Genetics Branch, National Human Genome Research Institute, National Institutes of Health, Bethesda, MD USA

#Corresponding Author: Leslie G. Biesecker, MD, Genetic Disease Research Branch, National Human Genome Research Institute, National Institutes of Health, 49 Convent Drive Room 4A56, Bethesda, MD 20892-4472, Tel: 301-402-2041; Fax: 301-402-2170; lesljeb@helix.nih.gov.
*, &These authors contributed equally to this work

Author contributions
J.C.S. and L.G.B. developed the exome sequencing protocol, J.L.S., I.M., J.C.S., L.G.B., and C.P.V. designed clinical research studies, NISC performed exome sequencing, J.J.J., J.L.S., I.M., R.J.C., L.G.B. and C.P.V. performed bioinformatic analyses, J.J.J. and C.K. performed mutational analysis and genotyping, R.J.C., N.C.C., S.D.C. and J.R.S. performed cell culture studies and Western blot analyses, R.J.C. created viral vectors and performed cellular complementation studies, J.L.S., M.H., and H.M.D. performed immunofluorecense experiments, J.L.S., J.R.S. and I.M. performed enzymatic assays, J.L.S., I.M., N.S.H., K.O., J.C.S., B.A.B., S.A.B., P.M.J., N.L.C., P.D., V.V., M.D.G., W.L.N., L.G.B. and C.P.V. contributed to clinical evaluations and the delineation of the patient phenotypes, D.K.G. performed organic acid measurements, J.L.S., J.J.J., L.G.B. and C.P.V. prepared manuscript, L.G.B. and C.P.V. conceived and supervised the study.

Competing financial interest
The authors declare no competing financial interests. LGB is an uncompensated advisor to the Illumina Corporation.

URLs
GeneReviews, http://www.ncbi.nlm.nih.gov/bookshelf/NBK1231/
ClinicalTrials, http://clinicaltrials.gov
Phrap assembler, http://www.phrap.org
Homologene, http://www.ncbi.nlm.nih.gov/homologene
MitoProtII, http://ihg.gsf.de/ihg/mitoprot.html

Accession numbers
Canine *ACSF3*, JF907588.1; Human *ACSF3*, NM_174917.2. The accession numbers for *ACSF3* orthologues and ACS homologues are listed in Online Methods.

ACSF3 side2

PubMed ▼

ormat: Abstract

Biomed Mass Spectrom. 1982 Jan;9(1):1-5.

The identification of (E)-2-methylglutaconic acid, a new isoleucine metabolite, in the urine of patients with beta-ketothiolase deficiency, propionic acidaemia and methylmalonic acidaemia.

Duran M, Bruinvis L, Ketting D, Kamerling JP, Wadman SK, Schutgens RB.

Abstract

The identification of (E)-2-methylglutaconic acid, a 'new' metabolite of isoleucine, is described. The substance was detected in urine samples from patients with propionic acidaemia, methylmalonic acidaemia and so-called beta-ketothiolase deficiency; in the majority of cases together with N-tiglylglycine. (E)-2-Methylglutaconic acid is thought to be the end product of the 3-methylcrotonyl-CoA carboxylase-catalysed carboxylation of tiglyl-CoA. Prerequisites for the quantitative gas chromatographic analysis of the unstable 2- (and 3-) methyl-glutaconic acid ditrimethylsilyl ester are given.

PMID: 7059658 DOI: 10.1002/bms.1200090102

[PubMed - indexed for MEDLINE]

2-methylglutaconic acid var ned reguleret i plasma fra ME patienter

MeSH Terms, Substances

LinkOut - more resources

PubMed Commons

0 comments

(Germain's studie)

PubMed Commons home

How to join PubMed Commons

Se også under BCKDDK

ACSF 3 side 3

Cell Chem Biol. 2017 Jun 22;24(6):673-684.e4. doi: 10.1016/j.chembiol.2017.04.009. Epub 2017 May 4.

The Mammalian Malonyl-CoA Synthetase ACSF3 Is Required for Mitochondrial Protein Malonylation and Metabolic Efficiency.

Bowman CE[1], Rodriguez S[2], Selen Alpergin ES[1], Acoba MG[3], Zhao L[4], Hartung T[5], Claypool SM[3], Watkins PA[6], Wolfgang MJ[7].

Author information

Abstract

Malonyl-coenzyme A (malonyl-CoA) is a central metabolite in mammalian fatty acid biochemistry generated and utilized in the cytoplasm; however, little is known about noncanonical organelle-specific malonyl-CoA metabolism. Intramitochondrial malonyl-CoA is generated by a malonyl-CoA synthetase, ACSF3, which produces malonyl-CoA from malonate, an endogenous competitive inhibitor of succinate dehydrogenase. To determine the metabolic requirement for mitochondrial malonyl-CoA, ACSF3 knockout (KO) cells were generated by CRISPR/Cas-mediated genome editing. ACSF3 KO cells exhibited elevated malonate and impaired mitochondrial metabolism. Unbiased and targeted metabolomics analysis of KO and control cells in the presence or absence of exogenous malonate revealed metabolic changes dependent on either malonate or malonyl-CoA. While ACSF3 was required for the metabolism and therefore detoxification of malonate, ACSF3-derived malonyl-CoA was specifically required for lysine malonylation of mitochondrial proteins. Together, these data describe an essential role for ACSF3 in dictating the metabolic fate of mitochondrial malonate and malonyl-CoA in mammalian metabolism.

KEYWORDS: ACSF3; CRISPR/Cas; SIRT5; acetyl-CoA; malonate; malonyl-CoA synthetase; malonylation; metabolomics; mitochondrial metabolism; succinylation

PMID: 28479296 PMCID: PMC5482780 [Available on 2018-06-22] DOI: 10.1016/j.chembiol.2017.04.009

[Indexed for MEDLINE]

ACSF3 side 4

PubMed

Format: Abstract

Full text links

Hum Mol Genet. 2017 Jul 15;26(14):2803-2811. doi: 10.1093/hmg/ddx177.

Epigenome-wide association study of rheumatoid arthritis identifies differentially methylated loci in B cells.

Julià A[1], Absher D[2], López-Lasanta M[1], Palau N[1], Pluma A[1], Waite Jones L[2], Glossop JR[3], Farrell WE[3], Myers RM[4], Marsal S[1].

Author information

Abstract

Epigenetic regulation of immune cell types could be critical for the development and maintenance of autoimmune diseases like rheumatoid arthritis (RA). B cells are highly relevant in RA, since patients express autoantibodies and depleting this cell type is a successful therapeutic approach. Epigenetic variation, such as DNA methylation, may mediate the pathogenic activity of B cells. In this study, we performed an epigenome-wide association study (EWAS) for RA with three different replication cohorts, to identify disease-specific alterations in DNA methylation in B cells. CpG methylation in isolated B lymphocytes was assayed on the Illumina HumanMethylation450 BeadChip in a discovery cohort of RA patients (N = 50) and controls (N = 75). Differential methylation was observed in 64 CpG sites ($q < 0.05$). Six biological pathways were also differentially methylated in RA B cells. Analysis in an independent cohort of patients (N = 15) and controls (N = 15) validated the association of 10 CpG sites located on 8 genes CD1C, TNFSF10, PARVG, NID1, DHRS12, ITPK1, **ACSF3** and TNFRSF13C, and 2 intergenic regions. Differential methylation at the CBL signaling pathway was replicated. Using an additional case-control cohort (N = 24), the association between RA risk and CpGs cg18972751 at CD1C ($P = 2.26 \times 10\text{-}9$) and cg03055671 at TNFSF10 ($P = 1.67 \times 10\text{-}8$) genes was further validated. Differential methylation at genes CD1C, TNFSF10, PARVG, NID1, DHRS12, ITPK1, **ACSF3**, TNFRSF13C and intergenic region chr10p12.31 was replicated in a cohort of systemic lupus erythematosus (SLE) patients (N = 47) and controls (N = 56). Our results highlight genes that may drive the pathogenic activity of B cells in RA and suggest shared methylation patterns with SLE.

PMID: 28475762 DOI: 10.1093/hmg/ddx177

[Indexed for MEDLINE]

ACSF3 hyper Vega 2017

ITPK1 hyper -"-

PARVG hyper Vega2014 +2017

Publication type, MeSH terms

LinkOut - more resources

→ Søg efter resten

ACSF3 side 5

page 342 in this article: ACSF3 is specifically expressed at high levels in normal B-cells, indicating a specific role in B-cell development. The possible role of this protein in B-cell malignancies remains to be investigated

GENES, CHROMOSOMES & CANCER 51:338–343 (2012)

The CBFA2T3/ACSF3 Locus Is Recurrently Involved in IGH Chromosomal Translocation t(14;16)(q32;q24) in Pediatric B-Cell Lymphoma with Germinal Center Phenotype

Itziar Salaverria,[1†] Takashi Akasaka,[2†] Stefan Gesk,[1] Monika Szczepanowski,[3] Birgit Burkhardt,[4] Lana Harder,[1] Christine Damm-Welk,[4] Ilske Oschlies,[3] Wolfram Klapper,[3] Martin J. S. Dyer,[2] and Reiner Siebert[1*]

[1]Institute of Human Genetics, University Hospital Schleswig-Holstein Campus Kiel/Christian-Albrechts University, Kiel, Germany
[2]MRC Toxicology Unit, University of Leicester, Leicester, UK
[3]Department of Pathology, Hematopathology Section and Lymph Node, University Hospital Schleswig-Holstein Campus Kiel/Christian-Albrechts University, Kiel, Germany
[4]Department of Pediatric Hematology and Oncology, Justus-Liebig University, Giessen, Germany

Translocations involving immunoglobulin (*IG*) loci are the hallmarks of several subtypes of B-cell lymphoma. Common to these translocations is that cellular proto-oncogenes come under the influence of *IG* regulatory elements leading to deregulated expression. In case of a breakpoint in the *IGH* switch region, oncogene activation can take place on both derivative chromosomes, which means that in principle one translocation can result in concurrent activation of two genes. By fluorescence in situ hybridization (FISH), we identified a case of leukemic B-cell lymphoma in a child with an *IGH* break and unknown partner. Subsequent long-distance inverse PCR revealed fusion of *IGH* Sμ in 14q32 and the 5′ region of *CBFA2T3* in 16q24.3, suggesting presence of the t(14;16)(q32;q24.3). Candidate oncogenes targeted through this translocation are *CBFA2T3* and *ACSF3*, which could be activated on der(16) and der(14), respectively. FISH screening of a population-based cohort of B-cell lymphomas from a prospective trial for the treatment of lymphoma in childhood (BFM-NHL) identified additionally a follicular lymphoma Grade 3/diffuse large B-cell lymphoma with *IGH-CBFA2T3/ACSF3* juxtaposition. Both lymphomas shared expression of CD10 and CD20 in the absence of TdT, suggesting a germinal center (GC) B-cell origin. Our data indicate that the *CBFA2T3/ACSF3* locus is a novel recurrent oncogenic target of *IGH* translocations, which might contribute to the pathogenesis of pediatric GC-derived B-cell lymphoma.

INTRODUCTION

Chromosomal translocation to the immunoglobulin heavy (*IGH*) or light (*IGL* or *IGK*) chain loci is a well-known mechanism of oncogene activation in B-cell neoplasms. Such *IG* translocations are the hallmarks of several subtypes of B-cell lymphoma such as the t(8;14)(q24;q32) in Burkitt lymphoma (BL) or t(11;14)(q13;q32) in mantle cell lymphoma (Willis and Dyer, 2000; Siebert et al., 2001). Thus, detection of *IG* translocations, which are assumed to be primary transforming events in many B-cell malignancies, aids to the classification of B-cell lymphomas. The oncogene activation in *IGH* translocations due to erroneous *VDJ* recombination usually takes place on the der(14), whereas in case of switch-associated translocations—such as in t(4;14) in multiple myeloma—oncogene activation can take place on both derivative chromosomes due to translocation of one of the enhancers to the derivative partner chromosome (Chesi et al., 1998; Willis and Dyer, 2000).

The two most common lymphoma subtypes in Western countries are diffuse large B-cell lymphoma (DLBCL) and follicular lymphoma (FL), which account for up to 36 and 32% of all lymphomas, respectively (Anderson et al., 1998). Both subtypes are thought to originate from germinal center (GC)-derived B-cells. Roughly, 85% of FL carry the chromosomal translocation t(14;18)(q32;q21) as primary oncogenic event.

Supported by: Deutsche Krebshilfe (Molecular Mechanisms in Malignant Lymphomas Network), Grant number: 70-3173-Tr3; UK Medical Research Council; Kinderkrebsinitative Buchholz, Holm-Seppensen; and Alexander von Humboldt Foundation (Fellowship).

†These authors contributed equally to this work.

*Correspondence to: Reiner Siebert, Institute of Human Genetics, University Hospital Schleswig-Holstein, Campus Kiel, Schwanenweg 24, D-24105 Kiel, Germany.
E-mail: rsiebert@medgen.uni-kiel.de

Received 16 August 2011; Accepted 2 November 2011
DOI 10.1002/gcc.21919
Published online 22 December 2011 in Wiley Online Library (wileyonlinelibrary.com).

CBFA2T3 hypermethylated Vega 2017

ACSF3 side 6

ACSL1 acyl-CoA synthetase long chain family member 1 [*Homo sapiens* (human)]

genekspression opreguleret Nguyen2017 p=0,0397

Gene ID: 2180, updated on 29-Mar-2018

enome Browsers
Summary
enome Data Viewer
ap Viewer
riation Viewer (GRCh37.p13)
riation Viewer (GRCh38)
00 Genomes Browser (GRCh37.p13)
nsembl
CSC

Official Symbol	ACSL1 provided by HGNC
Official Full Name	acyl-CoA synthetase long chain family member 1 provided by HGNC
Primary source	HGNC:HGNC:3569
See related	Ensembl:ENSG00000151726 MIM:152425; Vega:OTTHUMG00000160547
Gene type	protein coding
RefSeq status	REVIEWED
Organism	Homo sapiens
Lineage	Eukaryota; Metazoa; Chordata; Craniata; Vertebrata; Euteleostomi; Mammalia; Eutheria; Euarchontoglires; Primates; Haplorrhini; Catarrhini; Hominidae; Homo
Also known as	ACS1; LACS; FACL1; FACL2; LACS1; LACS2
Summary	The protein encoded by this gene is an isozyme of the long-chain fatty-acid-coenzyme A ligase family. Although differing in substrate specificity, subcellular localization, and tissue distribution, all isozymes of this family convert free long-chain fatty acids into fatty acyl-CoA esters, and thereby play a key role in lipid biosynthesis and fatty acid degradation. Several transcript variants encoding different isoforms have been found for this gene. [provided by RefSeq, Nov 2013]
Expression	Biased expression in fat (RPKM 357.3), liver (RPKM 217.4) and 10 other tissues See more
Orthologs	mouse all

Genomic context

Husk at nogle processer er først opregulerede hos ME patienter og senenhen nedregulerede. Lige nu samler vi viden for at se hvordan metabolismen er påvirket.

Location: 4q35.1

Exon count: 28

See ACSL1 in Genome Data Viewer Map Viewer

Annotation release	Status	Assembly	Chr	Location
109	current	GRCh38.p12 (GCF_000001405.38)	4	NC_000004.12 (184755595..184826593, complement)
105	previous assembly	GRCh37.p13 (GCF_000001405.25)	4	NC_000004.11 (185676749..185747215, complement)

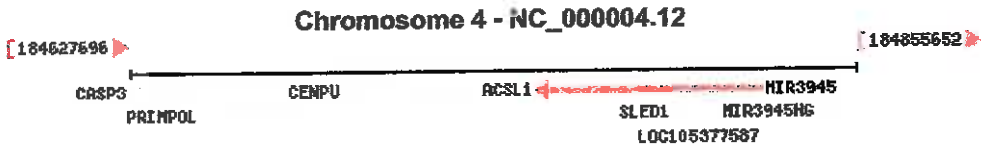

Genomic regions, transcripts, and products

Go to reference sequence details

Genomic Sequence: NC_000004.12 Chromosome 4 Reference GRCh38.p12 Primary Assembly ▼

Go to nucleotide: Graphics FASTA GenBank

NC_000004.12 Find: Tools

Genekspression af AGXT2L2 er opreguleret hos ME/CFS patienter i Nguyens studie 2017 (adolescents)

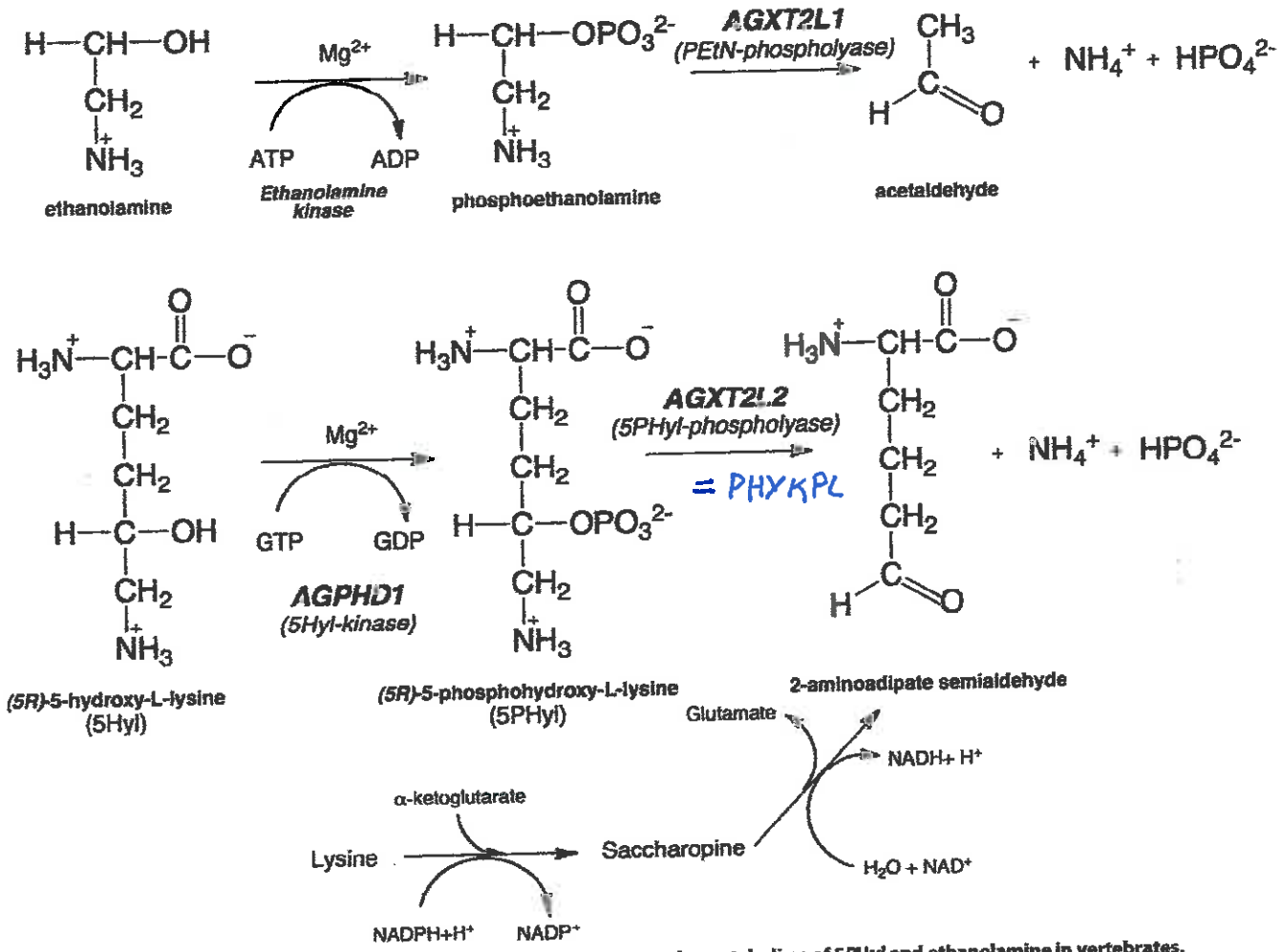

FIGURE 5. **Contribution of AGPHD1, AGXT2L2, and AGXT2L1 to the metabolism of 5PHyl and ethanolamine in vertebrates.**

(40). This enzyme is bound to the cell membrane and cleaves extracellular substrates such as PLP, inorganic pyrophosphate, and PEtN. Thus, AGXT2L1 deficiency is likely to lead to ethanolaminuria rather than phosphoethanolaminuria. Ethanolaminuria is likely to be caused also by ethanolamine kinase deficiency. There are few reports of ethanolaminuria (41–44), and its significance is not known. The variability in the associated symptoms (often including neurological symptoms) and in the amount of ethanolamine excreted in urine suggests that different genetic defects may be involved.

In addition to this, several studies suggest that AGXT2L1 may be involved in psychiatric disorders. AGXT2L1 was reported to be among the most up-regulated brain-specific genes in bipolar disorder and schizophrenia (45). AGXT2L1 was down-regulated in suicide completers (46) and in 72% of major depressive disorder: suicide cases compared with age-matched controls (47). A genome-wide association analysis indicated the association of schizophrenia with SNPs in the region of the COL25A1 gene, near the AGXT2L1 gene, on chromosome 4q25 (48). AGXT2L1 was the most up-regulated gene in a genome-wide expression study following 2 weeks of lithium administration to mice (49). With the identification of AGXT2L1 as the PEtN catabolic enzyme (and not as a transaminase participating in glutamate catabolism [50]), these findings suggest that the pathophysiology of schizophrenia and bipolar disorder may involve a perturbation in PEtN metabolism. Although it is difficult to formulate a coherent hypothesis at this stage, this conclusion is consistent with the finding that the PEtN and glycerophosphorylethanolamine levels, as determined by ^{31}P magnetic resonance spectroscopy, are increased in the brain of chronic, medicated schizophrenic compared with matched controls (39).

Function of Bacterial Homologues of Vertebrate AGPHD1 and AGXT2L1/2—The role of the bacterial homologues of AGXT2L1/2 and AGPHD1 is unclear at this stage. *E. carotovora* (*P. atrosepticum* in Fig. 2) has two different loci comprising each an AGXT2L1/2 homologue and an AGPHD1 homologue. It is likely that one or both of these pairs of enzymes are involved in the conversion of ethanolamine to acetaldehyde that has been reported previously (12). However, the fact that ethanolamine metabolism did not proceed further than its conversion to acetaldehyde because of the lack of acetaldehyde dehydrogenase suggests that the physiological function of these enzymes in this bacterium must be in the metabolism of a compound different from ethanolamine. The absence of an aminoadipate semialdehyde dehydrogenase orthologue from the *E.*

AMACR alpha-methylacyl-CoA racemase [*Homo sapiens* (human)]

Gene ID: 23600, updated on 4-Mar-2018

↑hyper vega2017 ↓ hypo ; CD4+ T-celler P=0,015920 (Brenu 2014)

↑ i PBMCs FDR= 0,0084 (Vega 2017 Tabel S1)

Summary

enome Browsers
enome Data Viewer
ap Viewer
ariation Viewer (GRCh37.p13)
ariation Viewer (GRCh38)
00 Genomes Browser (GRCh37.p13)
ssembl
SSC

Official Symbol	AMACR provided by HGNC
Official Full Name	alpha-methylacyl-CoA racemase provided by HGNC
Primary source	HGNC:HGNC:451
See related	Ensembl:ENSG00000242110 MIM:604489; Vega:OTTHUMG00000000734
Gene type	protein coding
RefSeq status	REVIEWED
Organism	Homo sapiens
Lineage	Eukaryota; Metazoa; Chordata; Craniata; Vertebrata; Euteleostomi; Mammalia; Eutheria; Euarchontoglires; Primates; Haplorrhini; Catarrhini; Hominidae; Homo
Also known as	RM; RACE; CBAS4; P504S; AMACRD
Summary	This gene encodes a racemase. The encoded enzyme interconverts pristanoyl-CoA and C27-bile acylCoAs between their (R)- and (S)-stereoisomers. The conversion to the (S)-stereoisomers is necessary for degradation of these substrates by peroxisomal beta-oxidation. Encoded proteins from this locus localize to both mitochondria and peroxisomes. Mutations in this gene may be associated with adult-onset sensorimotor neuropathy, pigmentary retinopathy, and adrenomyeloneuropathy due to defects in bile acid synthesis. Alternatively spliced transcript variants have been described. Read-through transcription also exists between this gene and the upstream neighboring C1QTNF3 (C1q and tumor necrosis factor related protein 3) gene. [provided by RefSeq, Mar 2011]
Expression	Broad expression in kidney (RPKM 38.3), liver (RPKM 31.1) and 22 other tissues See more
Orthologs	mouse all

Genomic context

Proces: beta-oxidation of pristanoyl-coA
Bile acid metabolism

See AMACR in Genome Data Viewer Map Viewer

Location: 5p13.2

Exon count: 5

Interaction: FKBP5, PEX5, PSMG3+4, CEP152...

Annotation release	Status	Assembly	Chr	Location
108	current	GRCh38.p7 (GCF_000001405.33)	5	NC_000005.10 (33986986..34008115, complement)
105	previous assembly	GRCh37.p13 (GCF_000001405.25)	5	NC_000005.9 (33987091..34008220, complement)

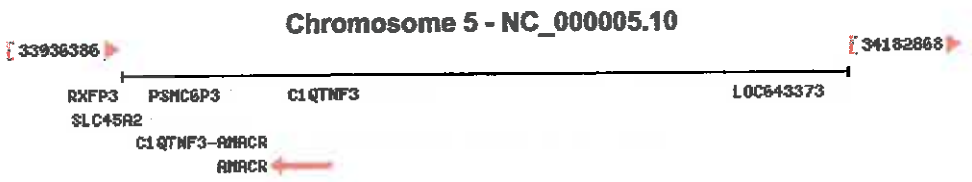

Genomic regions, transcripts, and products

Go to reference sequence details

Genomic Sequence: NC_000005.10 Chromosome 5 Reference GRCh38.p7 Primary Assembly

Uddrag af additional file2, Table S1 Vega 2017
(12.608 signifikant methylerede loci)

Probe	P-Value	FDR	Beta-Differer	Mean (ME/Cl	Mean (Contr	UCSC RefGene Name	UCSC RefGene Accession Number	Genic Location	Closest CpG Island	Relation to CpG Island
cg03591753	0,00051024	0,00881453	0,08028787	0,68957864	0,60929077	FKBP5	NM_001145775	5'UTR	chr6:35655607-3565	S_Shelf
cg05098551	0,00026697	0,00817622	0,05384496	0,679627	0,62578204	FKBP7;FKBP7;PLEKHA3	NM_001135212;NM_181342;NM_01!	TSS1500;TSS150(	chr2:179344852-179	N_Shore
cg12405639	0,00016459	0,00816422	-0,0572086	0,73212444	0,78933301	FKBP6;FKBP6	NM_001135211;NM_003602	Body;Body	chr7:72741804-7274	S_Shelf
cg15929276	0,00019065	0,00816422	0,05153261	0,25831984	0,20678723	FKBP5	NM_001145775	5'UTR	NA	NA
cg18397975	0,00040643	0,00842707	0,10536688	0,8072428	0,70187592	AMACR;AMACR;AMAC	NM_001167595;NM_001167597;NM_	Body;Body;Body;	NA	NA
cg24560920	0,0003076	0,00823207	0,06673043	0,87297155	0,80624113	FKBP7;FKBP7;PLEKHA3	NM_001135212;NM_181342;NM_01!	TSS1500;TSS150(	chr2:179344852-179	N_Shore

AMACR er hypermethyleret

Gene gov databasen oplyser, at der er interaktion mellem AMACR og FKBP5. FKBP5 er ligeledes hypermethyleret.

AMACR side2

Basisviden om AMACR - sebortfra prostata

Published in final edited form as:
Prostate. 2015 February ; 75(2): 200–210. doi:10.1002/pros.22905.

Dietary Influences on Tissue Concentrations of Phytanic Acid and AMACR Expression in the Benign Human Prostate

Yachana Kataria[1], **Margaret Wright**[2], **Ryan J. Deaton**[1], **Erika Enk Rueter**[1], **Benjamin A. Rybicki**[3], **Ann B. Moser**[4], **Vijayalakshmi Ananthanrayanan**[5], and **Peter H. Gann**[1,*]

[1]Department of Pathology, University of Illinois at Chicago, Chicago, Illinois [2]American Academy of Pediatrics, Elk Grove, Illinois [3]Department of Public Health Sciences, Henry Ford Health Systems, Detroit, Michigan [4]Peroxisomal Diseases Lab, Hugo W. Moser Research Institute at Kennedy Krieger, Baltimore, Maryland [5]Department of Pathology, University of Chicago, Chicago, Illinois

Abstract

BACKGROUND—Alpha-methylacyl-CoA racemase (AMACR) is an enzyme involved in fatty acid metabolism that is markedly over-expressed in virtually all prostate cancers (PCa), relative to benign tissue. One of AMACR's primary substrates, phytanic acid, is derived predominately from red meat and dairy product consumption. Epidemiological evidence suggests links between dairy/red meat intake, as well as phytanic acid levels, and elevated PCa risk. This study investigates the relationships among dietary intake, serum and tissue concentrations of phytanic acid, and AMACR expression (mRNA and protein) in the histologically benign human prostate.

METHODS—Men undergoing radical prostatectomy for the treatment of localized disease provided a food frequency questionnaire (n = 68), fasting blood (n = 35), benign fresh frozen prostate tissue (n = 26), and formalin-fixed paraffin-embedded (FFPE) sections (n = 67). Serum and tissue phytanic acid concentrations were obtained by gas chromatography–mass spectrometry. We extracted RNA from epithelial cells using laser capture microdissection and quantified mRNA expression of AMACR and other genes involved in the peroxisomal phytanic acid metabolism pathway via qRT-PCR. Immunohistochemistry for AMACR was performed on FFPE sections and subsequently quantified via digital image analysis. Associations between diet, serum, and tissue phytanic acid levels, as well as AMACR and other gene expression levels were assessed by partial Spearman correlation coefficients.

RESULTS—High-fat dairy intake was the strongest predictor of circulating phytanic acid concentrations ($r = 0.35$, $P = 0.04$). Tissue phytanic acid concentrations were not associated with any dietary sources and were only weakly correlated with serum levels ($r = 0.29$, $P = 0.15$). AMACR gene expression was not associated with serum phytanic acid ($r = 0.13$, $P = 0.47$), prostatic phytanic acid concentrations ($r = 0.03$, $P = 0.88$), or AMACR protein expression ($r = -0.16$, $P = 0.20$).

*Correspondence to: Peter H. Gann, MD, ScD, Department of Pathology (MC 847), College of Medicine, 840 S. Wood Street, Chicago, IL 60612. pgann@uic.edu.

Conflict of interest: The authors declare no conflict of interest.

AMACR side3

The present study, which to our knowledge is the first to measure phytanic acid concentrations in prostate tissue, benefited from LCM to collect a homogeneous histologically normal epithelial cell population for gene expression analysis. Additionally, quantitative image analysis is an accurate and reproducible way to evaluate IHC in these RP specimens. However, certain limitations of this study are acknowledged, including a relatively small sample size that limits power and the ability to control for potential confounders. Additionally, the FFQs utilized did not allow us to discriminate between fatty and non-fatty fish while only the former is a source of phytanic acid [14]. Of further concern is the high CV (18%) for tissue phytanic acid concentration, which suggests poor reproducibility. However, this could be attributed to the heterogeneity of the prostate tissue, because repeat samples were not taken from precisely the same tissue location and hence were not strictly identical.

Although the reason for AMACR overexpression in prostate cancer, and its potential link to the etiology of this disease, remains unresolved, we believe there are promising avenues for future research. It is conceivable that AMACR participates in a broad program altering fatty acid metabolism in prostate cancer, a program designed to meet increased demands for energy production and biosynthesis. Most cancer cells rely on glycolysis as a primary source of energy for proliferation and growth, however, prostate cancer utilizes fatty acid oxidation as its predominant source of bioenergy [35]. Due to AMACR upregulation, branched chain fatty acids such as phytanic acid—and possibly other yet unidentified dietary substrates as well—are oxidized to acetyl-CoA, which then can be used either to produce ATP via the Krebs cycle, or as building blocks for lipid synthesis [36]. Indeed, our data showed that RNA expression in benign tissue for AMACR and fatty acid synthase (FASN) were moderately to strongly correlated ($r = 0.59$, $P < 0.01$), suggesting that they are coordinately regulated in high-risk tissue. AMACR is known to be pleotropic with respect to its substrates; for example, it also plays an important in role in the metabolism of bile acids and nonsteroidal anti-inflammatory drugs, such as ibuprofen [37]. Enhanced peroxisomal β-oxidation, as reflected by AMACR upregulation, might confer a growth advantage on prostate cancer cells, not only from catabolism of branched chain fatty acid substrates, but also from its involvement in initial oxidation of very long chain fatty acids and fatty acid derivatives that cannot be metabolized in mitochondria [38]. Therefore, manipulation of AMACR expression in cultured benign and malignant prostate cells could reveal important new substrates that are linked to cell growth and also clarify AMACR's role in metabolic adaptation during carcinogenesis.

CONCLUSION

In conclusion, we found that there is no simple chain of association linking dairy intake to phytanic acid concentrations in the prostate and to AMACR expression in benign tissue, despite evidence that dairy intake and serum levels are linked and in vitro data indicating upregulation of AMACR expression when phytanic acid is added to cultured PCa cells [15]. These results do not support a direct relationship between local prostatic phytanic acid concentration and AMACR expression. Studies that examine temporality and distribution of phytanic acid concentration in the prostate are warranted, as are studies examining the effects of manipulating AMACR expression in both benign and malignant cultured cells.

AMACR side 4

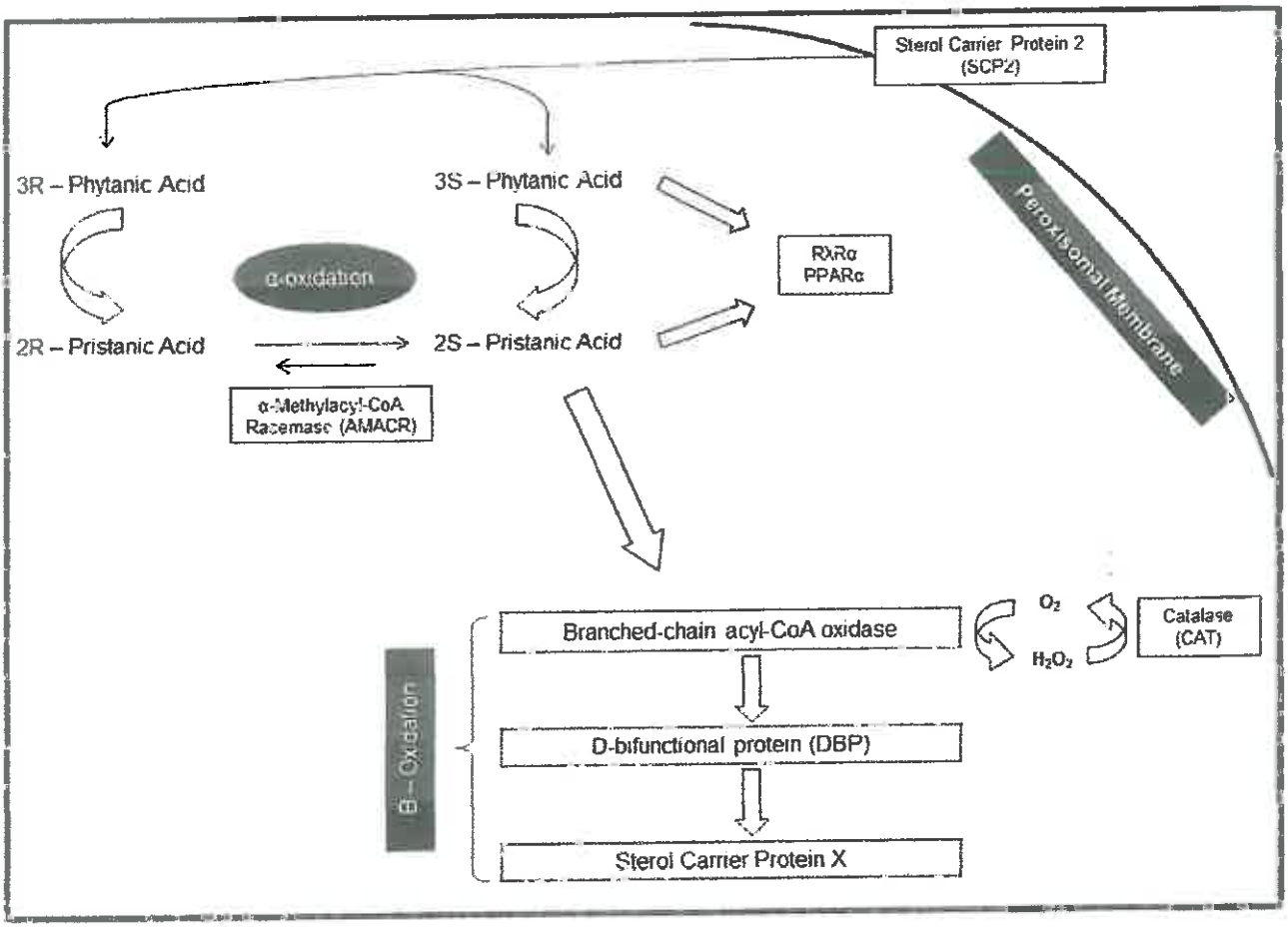

Fig. 1.
Role of AMACR in the metabolism of phytanic acid.

pristanic acid plasma niveau højere hos ME patienter end hos kontrol (Germain)

AMACR sidst

Mol Neurobiol
DOI 10.1007/s12035-016-0334-0

AMACR, (EFTB, PFKFB3)

Humoral Immunity Profiling of Subjects with Myalgic Encephalomyelitis Using a Random Peptide Microarray Differentiates Cases from Controls with High Specificity and Sensitivity

Sahajpreet Singh[1] · Phillip Stafford[2] · Karen A. Schlauch[3,4] · Richard R. Tillett[4] · Martin Gollery[5] · Stephen Albert Johnston[2] · Svetlana F. Khaiboullina[1,6] · Kenny L. De Meirleir[1] · Shanti Rawat[1] · Tatjana Mijatovic[7] · Krishnamurthy Subramanian[1] · András Palotás[6,8] · Vincent C. Lombardi[1,9]

Received: 3 June 2016 / Accepted: 29 November 2016

Abstract Myalgic encephalomyelitis (ME) is a complex, heterogeneous illness of unknown etiology. The search for biomarkers that can delineate cases from controls is one of the most active areas of ME research; however, little progress has been made in achieving this goal. In contrast to identifying biomarkers that are directly involved in the pathological process, an immunosignature identifies antibodies raised to proteins expressed during, and potentially involved in, the pathological process. Although these proteins might be unknown, it is possible to detect antibodies that react to these proteins using random peptide arrays. In the present study, we probe a custom 125,000 random 12-mer peptide microarray with sera from 21 ME cases and 21 controls from the USA and Europe and used these data to develop a diagnostic signature. We further used these peptide sequences to potentially uncover the naturally occurring candidate antigens to which these antibodies may specifically react with in vivo. Our analysis revealed a subset of 25 peptides that distinguished cases and controls with high specificity and sensitivity. Additionally, Basic Local Alignment Search Tool (BLAST) searches suggest that these peptides primarily represent human self-antigens and endogenous retroviral sequences and, to a minor extent, viral and bacterial pathogens.

Keywords Antibody · Chronic fatigue syndrome · Immunosignature · Myalgic encephalomyelitis · Peptide array

Introduction

Myalgic encephalomyelitis (ME), also commonly referred to as chronic fatigue syndrome or ME/CFS, is a heterogeneous illness characterized by a number of physical symptoms and comorbid conditions including neurocognitive dysfunction,

Sahajpreet Singh and Phillip Stafford contributed equally to this work.

✉ András Palotás
palotas@asklepios-med.eu

✉ Vincent C. Lombardi
vclombardi@nvcbr.org

1 Nevada Center for Biomedical Research, 1664 N Virginia St. MS 0552, Reno, NV 89557-0552, USA

2 The Biodesign Institute Center for Innovations in Medicine at Arizona State University, Tempe, AZ, USA

3 Department of Biochemistry and Molecular Biology, University of Nevada, Reno, NV, USA

4 Nevada INBRE Bioinformatics Core, University of Nevada, Reno, NV, USA

5 Tahoe Bioinformatics, Incline Village, Reno, NV, USA

6 Kazan Federal University, Kazan, Russian Federation

7 R.E.D. Laboratories, Zellik, Belgium

8 Asklepios-Med (private medical practice and research center), Kossuth Lajos sgt. 23, Szeged 6722, Hungary

9 Department of Pharmacology, University of Nevada, Reno, School of Medicine, Reno, NV, USA

Published online: 15 December 2016

AMACR side6

Table 2 Number of peptides homologous to a respective human protein sequences

Peptides	Accession	Symbol	Description	Length	Adj.
4	Q8NAP1	GATS	Stromal antigen 3 opposite strand	163	40.8
13	NP_033173	SEC23A	Sec23 homolog A	765	58.8
10	AKI70819	ETFDH	Electron transfer flavoprotein Dehydrogenase	617	61.7
9	NP_073150	EBF2	Early B-cell factor 2	575	63.9
5	AAH27322	SLC25A40	Solute carrier family 25 Member 40	338	67.6
5	EAX02872	ARMCX4	Armadillo repeat containing, X-linked 4	360	72
4	EAW58763	CD274	CD274 molecule	290	72.5
7	NP_056530	PLA2G3	Phospholipase A2 group III	509	72.7
7	Q6PJ69	TRIM65	Tripartite motif containing 65	517	73.9
4	NP_001103408	C6orf136	Chromosome 6 open reading frame 136	315	78.75
4	CAG46638	HMOX2	Heme oxygenase 2	316	79
7	NP_004877	APBA3	Amyloid beta precursor Protein binding family A member 3	575	82.1
9	P19835	CEL	Carboxyl ester lipase	753	83.7
7	NP_001171517	MX1	MX dynamin-like GTPase 1	662	94.6
4	ABQ59031	AMACR	Alpha-methylacyl-CoA racemase	382	95.5
4	NP_003140	STAC	SH3 and cysteine-rich domain	402	100.5
6	NP_001307526	DDX5	DEAD-box helicase 5	614	102.3
4	NP_060708	AGK	Acylglycerol kinase	422	105.5
5	NP_001086	ASIC1	Acid sensing ion Channel subunit 1	528	105.6
7	NP_758441	CTAGE1	Cutaneous T-cell Lymphoma-associated antigen 1	745	106.4
5	CAG33352	CCT2	Chaperonin containing TCP1 subunit 2	535	107
4	CAG33687	LGMN	Legumain	433	108.3
10	NP_006217	PLCL1	Phospholipase C-like 1	1095	109.5
5	NP_000449	HNF1B	HNF1 homeobox B	557	111.4
4	NP_068712	GABRB3	Gamma-aminobutyric acid type A receptor Beta3 subunit	473	118.25
6	P20592	MX2	MX dynamin-like GTPase 2	715	119.7
7	NP_060868	CACNA2D3	Calcium voltage-gated channel auxiliary subunit alpha2delta 3	1091	121.2
5	P30825	SLC7A1	Solute carrier family 7 member 1	629	125.8
4	NP_004557	PFKFB3	6-Phosphofructo-2-kinase/fructose-2,6-biphosphatase 3	520	130
4	XP_011509718	ACOXL	Acyl-CoA oxidase-like	547	136.8

Numerous other human pathogens were identified that contained homologous sequences to our random peptides but were excluded because of our adjusting metric (data not shown).

Table 3 Number of peptides homologous to respective human endogenous retroviral sequences

Peptides	Accession	Symbol	Description	Length	Adj.
7	NP_001138567	HHLA1	HERV-H LTR-associating protein 1 precursor	531	75.8
3	P61566	ERVK-24	Endogenous retrovirus group K member 24	588	196
3	AAY87455	ERVK-6	Env type 1, partial	603	201
4	AAM81188	HRV-5	Pol protein, partial	863	215.7
3	P61570	ERVK-25	Endogenous retrovirus group K member 25	661	220.3
3	P61565	ERVK-21	Endogenous retrovirus group K member 21	698	232.6
2	P60507	ERVFC1	Endogenous retrovirus group FC1 env polyprotein	584	292
2	Q14264	ERV3–1	Endogenous retrovirus Group 3 member 1	604	302
2	ABB52637	ERVPABLB-1	Endogenous retrovirus group PABLB member 1	665	332.5

AMACR side 7

AMPK

Houten et al

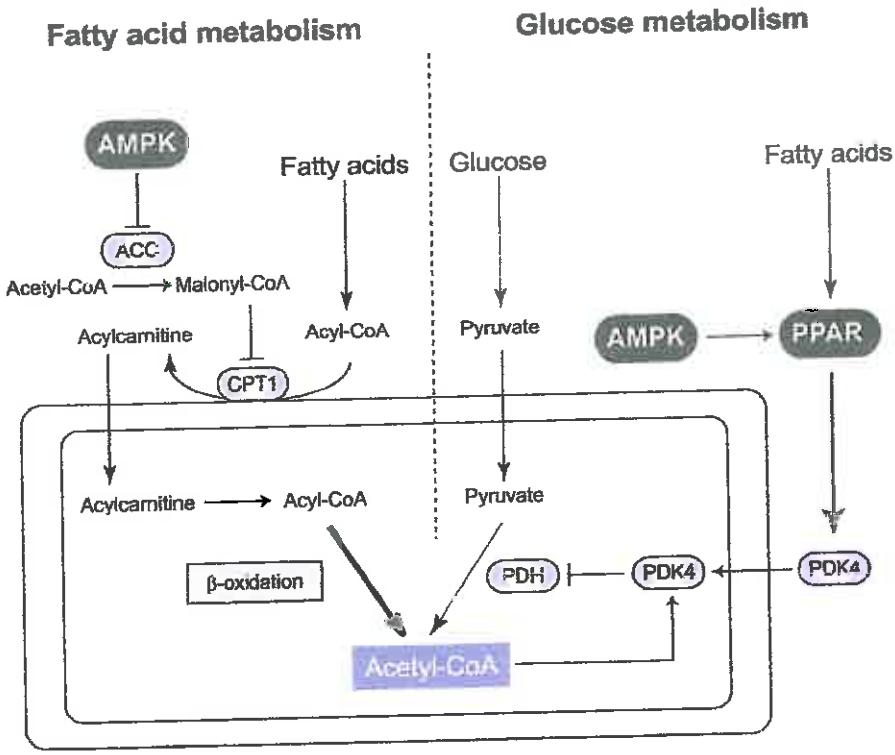

Figure 6. A scheme depicting major metabolic effects of AMPK activation and fatty acids. AMPK activation relieves repression of CPT1 by malonyl-CoA by phosphorylation and inactivation of ACC. At the same time, fatty acids and AMPK decrease glucose oxidation by a synergistic effect on the expression levels of PDK4.

effects of AICAR. AICAR is able to inhibit glucose phosphorylation and oxidative phosphorylation in hepatocytes [27, 28]. Our data, however, strongly suggest that fatty acids synergize with AMPK to decrease glucose oxidation.

Discussion

AMPK activation has a wide impact on cellular metabolism. One of the best-characterized effects is the decrease in the activity of cellular biosynthetic pathways. Principal targets for phosphorylation by AMPK are 3-hydroxy-3-methylglutaryl-CoA reductase and ACC, which leads to a decrease in the biosynthesis of sterols and fatty acids, respectively. More importantly, the decreased activity of ACC also leads to a decrease in cellular malonyl-CoA levels. Malonyl-CoA is an inhibitor of CPT1, the first enzyme in the carnitine shuttle that is necessary for the import of acyl-CoAs into mitochondria (Fig. 6). CPT1 catalyzes the rate-limiting step in the FAO pathway [29]. Therefore, the lower malonyl-CoA levels resulting from activated AMPK signaling promote increased FAO aimed to restore cellular energy status.

PPARs are other important mediators in tissue fuel selection. PPARs include PPARα (NR1C1), PPARβ/δ (NR1C2) and PPARγ (NR1C3) and belong to the nuclear receptor family of transcription factors. PPARs function as ligand-activated transcription factors, which are activated by (dietary) fatty acids such as oleate. PPARα controls the expression of many enzymes of the FAO pathway and mediates the response to fasting [30, 31]. Many studies have shown that PDK4 is also a PPAR target gene. For example, PDK4 expression is upregulated by natural (fatty acids [9, 32]) and synthetic PPAR ligands (PPARα, Wy-14643 [9] and PPARβ/δ, GW501516 [33]). Importantly, the Wy-14643- and fasting-induced increase in PDK4 expression was absent in PPARα$^{-/-}$ mice [34] and the GW501516-mediated increase was absent in PPARβ$^{-/-}$ primary muscle cells [35]. More recently, a potential PPRE in the PDK4 promoter was characterized [36]. PDK4 is able to phosphorylate and inactivate PDH and therefore decrease glucose oxidation, which allows increased FAO. We now provide evidence that PDK4 expression is synergistically induced by AMPK and fatty acids (Fig. 6). AMPK activation by hypoxia or AICAR has no effect on PDK4 expression by itself, but increases the ligand-dependent activation of PDK4 by fatty acids (oleate but also octanoate, Fig. 1E).

We used a PPAR luciferase reporter assay to provide further evidence for a role for PPAR and AMPK. In this system, AICAR increased the ligand-dependent activation by the natural PPAR ligand oleate and by the synthetic PPAR agonists bezafibrate and Wy-14643. GW501516, a synthetic PPARβ agonist did not

ATP5A1 ATP synthase, H+ transporting, mitochondrial F1 complex, alpha subunit 1, cardiac muscle [*Homo sapiens* (human)]

Gene ID: 498, updated on 12-Mar-2017

Summary ATP5A1 hypermethylert i Vega 2014 (har ikke slået den op i Vega 31, 2017) måske er den øget?

Official Symbol	ATP5A1 provided by HGNC
Official Full Name	ATP synthase, H+ transporting, mitochondrial F1 complex, alpha subunit 1, cardiac muscle provided by HGNC
Primary source	HGNC:HGNC:823
See related	Ensembl:ENSG00000152234 MIM:164360; Vega:OTTHUMG00000132637
Gene type	protein coding
RefSeq status	REVIEWED
Organism	Homo sapiens
Lineage	Eukaryota; Metazoa; Chordata; Craniata; Vertebrata; Euteleostomi; Mammalia; Eutheria; Euarchontoglires; Primates; Haplorrhini; Catarrhini; Hominidae; Homo
Also known as	OMR; ORM; ATPM; MOM2; ATP5A; hATP1; MC5DN4; ATP5AL2; COXPD22; HEL-S-123m
Summary	This gene encodes a subunit of mitochondrial ATP synthase. Mitochondrial ATP synthase catalyzes ATP synthesis, using an electrochemical gradient of protons across the inner membrane during oxidative phosphorylation. ATP synthase is composed of two linked multi-subunit complexes: the soluble catalytic core, F1, and the membrane-spanning component, Fo, comprising the proton channel. The catalytic portion of mitochondrial ATP synthase consists of 5 different subunits (alpha, beta, gamma, delta, and epsilon) assembled with a stoichiometry of 3 alpha, 3 beta, and a single representative of the other 3. The proton channel consists of three main subunits (a, b, c). This gene encodes the alpha subunit of the catalytic core. Alternatively spliced transcript variants encoding the different isoforms have been identified. Pseudogenes of this gene are located on chromosomes 9, 2, and 16. [provided by RefSeq, Mar 2012]
Orthologs	mouse all

Genomic context ATP5A1 precursor kunne ikke påvises i spinalvæske fra ME patienter. Normalværdi: 2 Schutzer proteom-studie

See ATP5A1 in Genome Data Viewer Map Viewer

Location: 18q21.1

Exon count: 13

Annotation release	Status	Assembly	Chr	Location
108	current	GRCh38.p7 (GCF_000001405.33)	18	NC_000018.10 (46084144..46104233, complement)
105	previous assembly	GRCh37.p13 (GCF_000001405.25)	18	NC_000018.9 (43664110..43684199, complement)

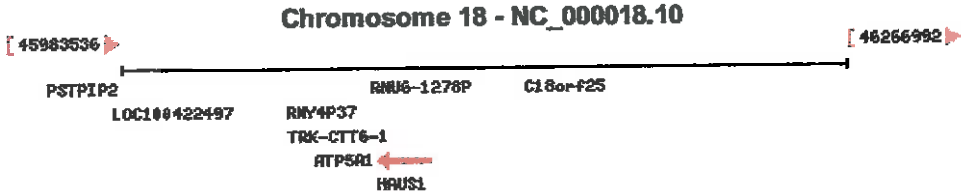

ATP10A ATPase phospholipid transporting 10A (putative) [*Homo sapiens* (human)

hypermethylated TSS1500, Body
Vega 2017.57

Gene ID: 57194, updated on 29-Mar-2018

enome Browsers
enome Data Viewer
ap Viewer
riation Viewer (GRCh37.p13)
riation Viewer (GRCh38)
00 Genomes Browser (GRCh37.p13)
sembl
CSC

Summary

Official Symbol	ATP10A provided by HGNC
Official Full Name	ATPase phospholipid transporting 10A (putative) provided by HGNC
Primary source	HGNC:HGNC:13542
See related	Ensembl:ENSG00000206190 MIM:605855; Vega:OTTHUMG00000171703
Gene type	protein coding
RefSeq status	REVIEWED
Organism	Homo sapiens
Lineage	Eukaryota; Metazoa; Chordata; Craniata; Vertebrata; Euteleostomi; Mammalia; Eutheria; Euarchontoglires; Primates; Haplorrhini; Catarrhini; Hominidae; Homo
Also known as	ATPVA; ATPVC; ATP10C
Summary	The protein encoded by this gene belongs to the family of P-type cation transport ATPases, and to the subfamily of aminophospholipid-transporting ATPases. The aminophospholipid translocases transport phosphatidylserine and phosphatidylethanolamine from one side of a bilayer to another. This gene is maternally expressed. It maps within the most common interval of deletion responsible for Angelman syndrome, also known as 'happy puppet syndrome'. [provided by RefSeq, Jul 2008]
Expression	Ubiquitous expression in adrenal (RPKM 2.8), lung (RPKM 2.6) and 23 other tissues See more
Orthologs	mouse all

Genomic context

ATP10A involved in Plasma Membrane Dynamics

See ATP10A in Genome Data Viewer Map Viewer

Location: 15q12

Exon count: 28

Annotation release	Status	Assembly	Chr	Location
109	current	GRCh38.p12 (GCF_000001405.38)	15	NC_000015.10 (25672241..25865144, complement)
105	previous assembly	GRCh37.p13 (GCF_000001405.25)	15	NC_000015.9 (25923859..26110304, complement)

Chromosome 15 - NC_000015.10

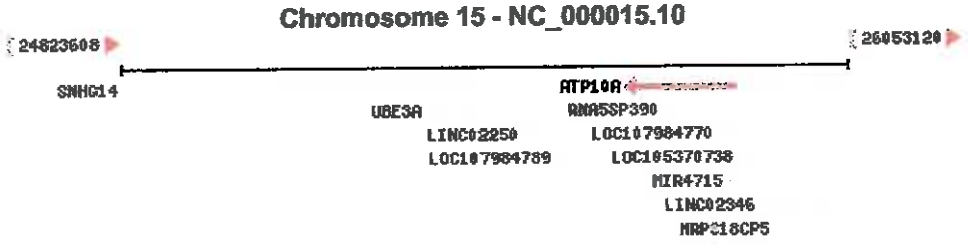

Genomic regions, transcripts, and products

Go to reference sequence details

BCKDK branched chain ketoacid dehydrogenase kinase [*Homo sapiens* (human)]

Gene ID: 10295, updated on 1-Apr-2018 hypomethylect [illegible] T 551500, Vega2017,57

Summary
enome Browsers
enome Data Viewer
ap Viewer
riation Viewer (GRCh37.p13)
riation Viewer (GRCh38)
00 Genomes Browser (GRCh37.p13)
nsembl
CSC

Official Symbol	BCKDK provided by HGNC
Official Full Name	branched chain ketoacid dehydrogenase kinase provided by HGNC
Primary source	HGNC:HGNC:16902
See related	Ensembl:ENSG00000103507 MIM:614901; Vega:OTTHUMG00000047356
Gene type	protein coding
RefSeq status	REVIEWED
Organism	Homo sapiens
Lineage	Eukaryota; Metazoa; Chordata; Craniata; Vertebrata; Euteleostomi; Mammalia; Eutheria; Euarchontoglires; Primates; Haplorrhini; Catarrhini; Hominidae; Homo
Also known as	BDK; BCKDKD
Summary	The branched-chain alpha-ketoacid dehydrogenase complex (BCKD) is an important regulator of the valine, leucine, and isoleucine catabolic pathways. The protein encoded by this gene is found in the mitochondrion, where it phosphorylates and inactivates BCKD. Several transcript variants encoding different isoforms have been found for this gene. [provided by RefSeq, Dec 2012]
Expression	Ubiquitous expression in kidney (RPKM 12.8), heart (RPKM 12.4) and 25 other tissues See more
Orthologs	mouse all

component: mitochondrial alpha-ketoglutarate dehydrogenase complex also known as: 3-methyl-2-oxobutanoate dehydrogenase [lipoamide]-kinase

Genomic context

See BCKDK in Genome Data Viewer Map Viewer

Location: 16p11.2

Exon count: 12

Annotation release	Status	Assembly	Chr	Location
109	current	GRCh38.p12 (GCF_000001405.38)	16	NC_000016.10 (31108294..31117651)
105	previous assembly	GRCh37.p13 (GCF_000001405.25)	16	NC_000016.9 (31119615..31124112)

Chromosome 16 - NC_000016.10

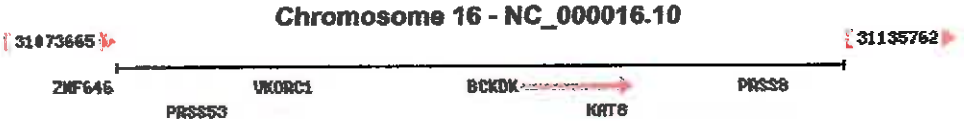

Genomic regions, transcripts, and products

Go to reference sequence details

Genomic Sequence: NC_000016.10 Chromosome 16 Reference GRCh38.p12 Primary Assembly ▼

Go to nucleotide: Graphics FASTA GenBank

NC_000016.10 Find: Tools

31,107 K | 31,108 K | 31,109 K | 31,110 K | 31,111 K | 31,112 K | 31,113 K | 31,114 K | 31,115 K | 31,116 K

Genes NCBI Homo sapiens Annotation Release 109 2018-

STK17a hypo Vega 2014

BLVRA biliverdin reductase A [*Homo sapiens* (human)]

Gene ID: 644, updated on 21-Dec-2017

hyper Vega 2017

Hide sidebar >>

Summary
enome Browsers
enome Data Viewer
ap Viewer
riation Viewer (GRCh37.p13)
riation Viewer (GRCh38)
00 Genomes Browser (GRCh37.p13)
nsembl
CSC

Official Symbol	BLVRA provided by HGNC
Official Full Name	biliverdin reductase A provided by HGNC
Primary source	HGNC:HGNC:1062
See related	Ensembl:ENSG00000106605 MIM:109750; Vega:OTTHUMG00000128953
Gene type	protein coding
RefSeq status	REVIEWED
Organism	Homo sapiens
Lineage	Eukaryota; Metazoa; Chordata; Craniata; Vertebrata; Euteleostomi; Mammalia; Eutheria; Euarchontoglires; Primates; Haplorrhini; Catarrhini; Hominidae; Homo
Also known as	BVR; BLVR; BVRA
Summary	The protein encoded by this gene belongs to the biliverdin reductase family, members of which catalyze the conversion of biliverdin to bilirubin in the presence of NADPH or NADH. Mutations in this gene are associated with hyperbiliverdinemia. Alternatively spliced transcript variants have been found for this gene. [provided by RefSeq, Dec 2011]
Expression	Ubiquitous expression in spleen (RPKM 33.2), lung (RPKM 23.1) and 25 other tissues See more
Orthologs	mouse all

Genomic context

Kolesterol, galdesyrer og bilirubin omsætning er påvirket i ME

See BLVRA in Genome Data Viewer Map Viewer

Location: 7p13

Exon count: 11

Annotation release	Status	Assembly	Chr	Location
108	current	GRCh38.p7 (GCF_000001405.33)	7	NC_000007.14 (43758153..43807342)
105	previous assembly	GRCh37.p13 (GCF_000001405.25)	7	NC_000007.13 (43798272..43846941)

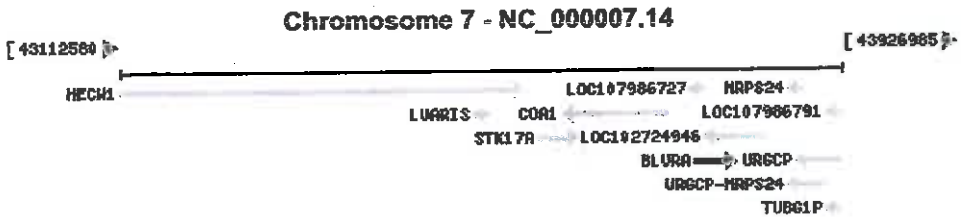

Genomic regions, transcripts, and products

Go to reference sequence details

Genomic Sequence: NC_000007.14 Chromosome 7 Reference GRCh38.p7 Primary Assembly

Go to nucleotide: Graphics FASTA GenBank

NC_000007.14 | Find:

.750 K | 43.755 K | 43.760 K | 43.765 K | 43.770 K | 43.775 K | 43.780 K | 43.785 K | 43.790 K

CAB39L calcium binding protein 39 like [*Homo sapiens* (human)]

Gene ID: 81617, updated on 3-Apr-2018

hypermethylated 5'UTR, 1st Exon Vega 2017,57

Summary
enome Browsers
enome Data Viewer
ap Viewer
riation Viewer (GRCh37.p13)
riation Viewer (GRCh38)
00 Genomes Browser (GRCh37.p13)
nsembl
CSC

Official Symbol	CAB39L provided by HGNC
Official Full Name	calcium binding protein 39 like provided by HGNC
Primary source	HGNC:HGNC:20290
See related	Ensembl:ENSG00000102547 MIM:612175; Vega:OTTHUMG00000016914
Gene type	protein coding
RefSeq status	VALIDATED
Organism	Homo sapiens
Lineage	Eukaryota; Metazoa; Chordata; Craniata; Vertebrata; Euteleostomi; Mammalia; Eutheria; Euarchontoglires; Primates; Haplorrhini; Catarrhini; Hominidae; Homo
Also known as	MO2L; MO25-BETA; bA103J18.3
Expression	Broad expression in prostate (RPKM 17.8), adrenal (RPKM 15.4) and 23 other tissues See more
Orthologs	mouse all

Genomic context

Interagerer med: ACOT7, BCKDK, CAB39, DCXR, MLH1, STK11 STRADA

pathway: LKB1 → AMPK → TOR

Location: 13q14.2

Exon count: 16

See CAB39L in Genome Data Viewer Map Viewer

Annotation release	Status	Assembly	Chr	Location
109	current	GRCh38.p12 (GCF_000001405.38)	13	NC_000013.11 (49308650..49444851, complement)
105	previous assembly	GRCh37.p13 (GCF_000001405.25)	13	NC_000013.10 (49882786..50018221, complement)

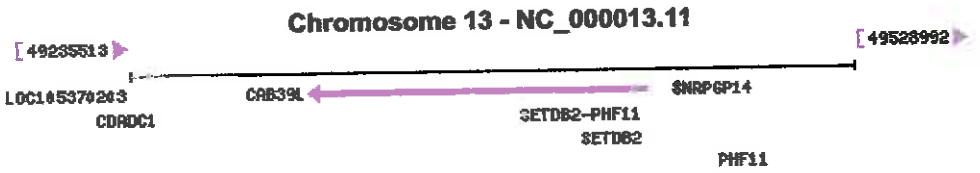

Genomic regions, transcripts, and products

Go to reference sequence details

Genomic Sequence: NC_000013.11 Chromosome 13 Reference GRCh38.p12 Primary Assembly ▼

Go to nucleotide: Graphics FASTA GenBank

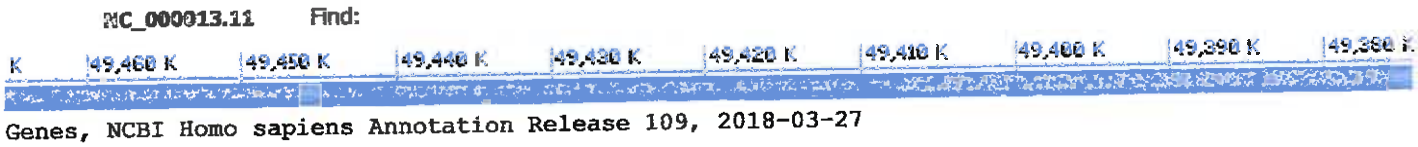

CBFA2T2 CBFA2/RUNX1 translocation partner 2 [*Homo sapiens* (human)]

Gene ID: 9139, updated on 29-Mar-2018

hypermethylent Vega 2014
cerospinal fluid (normal-CFS-postLyme):
novalue - 2 -no value
Schutzer 2011

Summary

Official Symbol	CBFA2T2 provided by HGNC
Official Full Name	CBFA2/RUNX1 translocation partner 2 provided by HGNC
Primary source	HGNC:HGNC:1536
See related	Ensembl:ENSG00000078699 MIM:603672; Vega:OTTHUMG00000032261
Gene type	protein coding
RefSeq status	REVIEWED
Organism	Homo sapiens
Lineage	Eukaryota; Metazoa; Chordata; Craniata; Vertebrata; Euteleostomi; Mammalia; Eutheria; Euarchontoglires; Primates; Haplorrhini; Catarrhini; Hominidae; Homo
Also known as	EHT; p85; MTGR1; ZMYND3
Summary	In acute myeloid leukemia, especially in the M2 subtype, the t(8;21)(q22;q22) translocation is one of the most frequent karyotypic abnormalities. The translocation produces a chimeric gene made up of the 5'-region of the RUNX1 (AML1) gene fused to the 3'-region of the CBFA2T1 (MTG8) gene. The chimeric protein is thought to associate with the nuclear corepressor/histone deacetylase complex to block hematopoietic differentiation. The protein encoded by this gene binds to the AML1-MTG8 complex and may be important in promoting leukemogenesis. Several transcript variants are thought to exist for this gene, but the full-length natures of only three have been described. [provided by RefSeq, Jul 2008]
Expression	Ubiquitous expression in prostate (RPKM 6.7), testis (RPKM 4.3) and 25 other tissues See more
Orthologs	mouse all

Genomic context

See CBFA2T2 in Genome Data Viewer Map Viewer

Location: 20q11.21-q11.22

Exon count: 18

Annotation release	Status	Assembly	Chr	Location
109	current	GRCh38.p12 (GCF_000001405.38)	20	NC_000020.11 (33490070..33650031)
105	previous assembly	GRCh37.p13 (GCF_000001405.25)	20	NC_000020.10 (32077928..32237837)

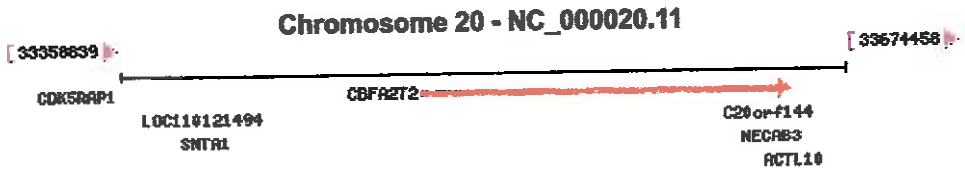

Genomic regions, transcripts, and products

Go to reference sequence details

Genomic Sequence: NC_000020.11 Chromosome 20 Reference GRCh38.p12 Primary Assembly ▼

CBFA2T3 CBFA2/RUNX1 translocation partner 3 [*Homo sapiens* (human)]

Gene ID: 863, updated on 3-Apr-2018

hypermethyleret TSS200, 5'UTR Vega2017,S7

Summary
enome Browsers
enome Data Viewer
ap Viewer
riation Viewer (GRCh37.p13)
riation Viewer (GRCh38)
00 Genomes Browser (GRCh37.p13)
nsembl
CSC

Official Symbol	CBFA2T3 provided by HGNC
Official Full Name	CBFA2/RUNX1 translocation partner 3 provided by HGNC
Primary source	HGNC:HGNC:1537
See related	Ensembl:ENSG00000129993 MIM:603870; Vega:OTTHUMG00000137864
Gene type	protein coding
RefSeq status	REVIEWED
Organism	Homo sapiens
Lineage	Eukaryota; Metazoa; Chordata; Craniata; Vertebrata; Euteleostomi; Mammalia; Eutheria; Euarchontoglires; Primates; Haplorrhini; Catarrhini; Hominidae; Homo
Also known as	ETO2; MTG16; MTGR2; ZMYND4; RUNX1T3
Summary	This gene encodes a member of the myeloid translocation gene family which interact with DNA-bound transcription factors and recruit a range of corepressors to facilitate transcriptional repression. The t(16;21)(q24;q22) translocation is one of the less common karyotypic abnormalities in acute myeloid leukemia. The translocation produces a chimeric gene made up of the 5'-region of the runt-related transcription factor 1 gene fused to the 3'-region of this gene. This gene is also a putative breast tumor suppressor. Alternative splicing results in transcript variants. [provided by RefSeq, Nov 2010]
Expression	Broad expression in spleen (RPKM 6.2), lymph node (RPKM 3.7) and 24 other tissues See more
Orthologs	mouse all

RUNX2 ↑ Vega2017,S7
RUNX3 ↓ Vega2017,S7 + Vega2014

Genomic context

See CBFA2T3 in Genome Data Viewer Map Viewer

Location: 16q24.3

Exon count: 15

Interagerer med følgende hypermethylerede gener: LDB1 TAL1 TCF3

Annotation release	Status	Assembly	Chr	Location
109	current	GRCh38.p12 (GCF_000001405.38)	16	NC_000016.10 (88874855..88977149, complement)
105	previous assembly	GRCh37.p13 (GCF_000001405.25)	16	NC_000016.9 (88941263..89043568, complement)

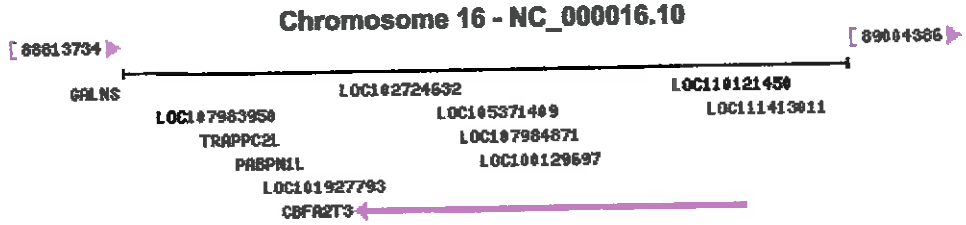

Genomic regions, transcripts, and products

Go to reference sequence details

Genomic Sequence: NC_000016.10 Chromosome 16 Reference GRCh38.p12 Primary Assembly ▼

CLYBL = citrate lyase beta like

Table 2 (continued)

Chromosome	SNP ID	Gene/expressed sequence tag Genome Build 36.3EST	Genotype	Frequency, n		p value	
				controls	CFS subjects	genotype	allele
13	rs7994531	BG220650	TT	0 (0.0)	6 (17.1)	0.0004	0.0001
			TC	6 (17.1)	16 (45.7)		
			CC	29 (82.9)	13 (37.1)		
	rs1931035	unknown	AA	0 (0.0)	6 (15.8)	0.0025	0.0001
			AG	4 (10.0)	9 (23.7)		
			GG	36 (90.0)	23 (60.5)		
	rs1359536	unknown	TT	38 (95.0)	27 (69.2)	0.0045	0.0005
			TC	2 (5.0)	7 (18.0)		
			CC	0 (0.0)	5 (12.8)		
	rs547571	*HS6ST3*	AA	0 (0.0)	1 (2.50)	0.0003	0.0002
			AG	3 (7.50)	16 (40.0)		
			GG	37 (61.7)	23 (57.5)		
	rs1555589	*CLYBL*	AA	24 (77.4)	18 (45.0)	0.0123	0.0004
			AG	6 (19.4)	13 (32.5)		
			GG	1 (3.23)	9 (22.5)		
	rs7325773	CA425896	CC	31 (79.5)	18 (45.0)	0.0012	0.0006
			CG	8 (20.5)	17 (42.5)		
			GG	0 (0.0)	5 (12.5)		
	rs10507556	unknown	AA	2 (5.3)	0 (0.0)	0.0051	0.001
			AG	8 (21.1)	1 (2.6)		
			GG	28 (73.7)	38 (97.4)		
14	rs2372200	unknown	GG	0 (0.0)	5 (13.5)	0.0026	0.0004
			GA	7 (20.0)	16 (43.2)		
			AA	28 (80.0)	16 (43.2)		
	rs3759688	*SIX6*	GG	28 (77.8)	39 (100.0)	0.0015	0.0008
			GT	7 (19.4)	0 (0.0)		
			TT	1 (2.8)	0 (0.0)		
17	rs6503623	*KRTHA3A*	AA	27 (69.2)	38 (97.4)	0.0017	0.0004
			AG	9 (23.1)	1 (2.56)		
			GG	3 (7.69)	0 (0.0)		
19	rs400322	*LILRB4*	AA	0 (0.0)	6 (16.2)	0.0032	0.0001
			AG	5 (13.9)	11 (29.7)		
			GG	31 (86.1)	20 (54.1)		
	rs10500321	*NLRP11*	CC	0 (0.0)	2 (5.1)	0.0021	0.0008
			CT	4 (10.0)	14 (35.9)		
			TT	36 (90.0)	23 (59.0)		
	rs2059152	*NLRP11*	AA	0 (0.0)	2 (5.1)	0.0028	0.001
			AG	4 (10.0)	14 (35.9)		
			GG	36 (90.0)	23 (59.0)		
	rs382958	*NLRP13*	CC	3 (7.89)	13 (37.1)	0.0051	0.0002
			CT	11 (29.0)	10 (28.6)		
			TT	24 (63.2)	12 (34.3)		
21	rs1399592	*KCNJ6*	GG	6 (16.2)	15 (40.5)	0.0038	0.0004
			GT	15 (40.5)	18 (48.7)		
			TT	16 (43.2)	4 (10.8)		

Mapping of SNPs to respective chromosomes, genes or expressed sequence tags was accomplished with NCBI Genome Build 36.3. Values in parentheses represent percentages.

Jra Smith et al: Convergent Genomic Studies Identify Association of GRIK2 and NPAS2 with CFS.

CLYBL side 1

CLYBL er hypermethyleret, body, kromosom 13
FDR = 0,008, Vega 2017, tabel S1.

Human Molecular Genetics, 2014, Vol. 23, No. 9 2313–2323
doi:10.1093/hmg/ddt624
Advance Access published on December 11, 2013

CLYBL is a polymorphic human enzyme with malate synthase and β-methylmalate synthase activity

Laura Strittmatter[1,2,4], Yang Li[1,5], Nathan J. Nakatsuka[1,3], Sarah E. Calvo[1,2,4], Zenon Grabarek[1,4], and Vamsi K. Mootha[1,2,4,*]

[1]Department of Molecular Biology, Howard Hughes Medical Institute, Massachusetts General Hospital, Boston, MA 02114, USA [2]Department of Systems Biology, [3]Harvard-MIT Division of Health Sciences and Technology, Harvard Medical School, Boston, MA 02115, USA [4]Broad Institute of Harvard and Massachusetts Institute of Technology, Cambridge, MA 02141, USA [5]Department of Statistics, Harvard University, Cambridge, MA 02138, USA

Received September 30, 2013; Revised November 15, 2013; Accepted December 9, 2013

CLYBL is a human mitochondrial enzyme of unknown function that is found in multiple eukaryotic taxa and conserved to bacteria. The protein is expressed in the mitochondria of all mammalian organs, with highest expression in brown fat and kidney. Approximately 5% of all humans harbor a premature stop polymorphism in CLYBL that has been associated with reduced levels of circulating vitamin B12. Using comparative genomics, we now show that CLYBL is strongly co-expressed with and co-evolved specifically with other components of the mitochondrial B12 pathway. We confirm that the premature stop polymorphism in CLYBL leads to a loss of protein expression. To elucidate the molecular function of CLYBL, we used comparative operon analysis, structural modeling and enzyme kinetics. We report that CLYBL encodes a malate/β-methylmalate synthase, converting glyoxylate and acetyl-CoA to malate, or glyoxylate and propionyl-CoA to β-methylmalate. Malate synthases are best known for their established role in the glyoxylate shunt of plants and lower organisms and are traditionally described as not occurring in humans. The broader role of a malate/β-methylmalate synthase in human physiology and its mechanistic link to vitamin B12 metabolism remain unknown.

INTRODUCTION

Vitamin B12, or cobalamin, is an essential cofactor required for the activity of two human enzymes: mitochondrial methylmalonyl-CoA mutase (MUT) and cytoplasmic methionine synthase (MTR). Humans obtain cobalamin from diet or supplements, and once absorbed, the vitamin is further processed to its active forms—adenosylcobalamin for MUT and methylcobalamin for MTR. Vitamin B12 metabolism and utilization have been extensively studied, and with the exception of the mitochondrial transporter, the molecular identities of all proteins necessary for B12 maturation have been identified (1,2).

Two recent human genetic association studies have begun to define the genetic loci that control B12 levels (3,4). Of the 12 non-intergenic loci collectively identified by these two studies, 11 lie near genes with established or purported roles in vitamin B12 biology, including B12 absorption (*MS4A3, FUT2, FUT6, TCN1, TCN2, CUBN, CD320*), B12 maturation (*ABCD4, MMAA, MMACHC*) and B12-dependent catalysis (*MUT*). The 12th locus corresponds to a stop polymorphism within CLYBL, an uncharacterized protein. The B12-associated polymorphism (rs41281112) changes Arg259 to a stop codon, predicted to produce a truncated CLYBL protein. Notably, this polymorphism had the largest effect on B12 levels of all the SNPs reported: Chinese men homozygous for the premature stop had 3-fold reduced concentrations of circulating B12, with heterozygotes exhibiting an intermediate phenotype (3).

Although CLYBL appears to be a metabolic enzyme, its activity remains entirely unknown. CLYBL is annotated as 'citrate lyase beta like' because it shows sequence similarity to citE, a component of an enzymatic complex (citE/citD/citF) found in bacteria that cleaves citrate to oxaloacetate and acetyl-CoA (ACoA) (5,6). All three subunits are necessary for complete lyase activity and often co-occur in the same operon (6,7). Humans, as well as other eukaryotes and certain bacteria and archea, possess homologs of citE but not of citD or citF, hinting at an alternate function for this gene (7). Moreover, citrate cleavage in humans is mediated by the cytosolic, ATP-dependent ATP

*To whom correspondence should be addressed at: Department of Molecular Biology, Massachusetts General Hospital, 185 Cambridge Street 6th Floor, Boston, MA 02114, USA. Tel: +1 6176439710; Email: vamsi@hms.harvard.edu

CLYBL side2

CLYBL og methyl malonyl-CoA

With the structural model in hand, we sought to further confirm that CLYBL had malate synthase and β-methylmalate synthase activities by mutating specific residues predicted to be critical for various aspects of catalysis. Based on homology modeling and evolutionary conservation, we mutated residues Glu75 and Glu171, predicted to be important for coordinating a magnesium-binding water molecule and directly binding magnesium, respectively, to Gly and found that these mutants had no malate synthase or β-methylmalate synthase activity in our DTNB-linked assay (data not shown). We also mutated Asp250 to Gly to evaluate the effect of a charge mutation at a residue that is conserved but distal to the active site, and found that this mutation reduced but did not eliminate these activities (data not shown). We also attempted to express and purify the Arg259Stop LOF variant (Fig. 1A,C–E) identified from the 1000 Genomes data and associated with low circulating B12 levels, but the expressed protein was insoluble, suggesting that the human mutant may be improperly folded if it is expressed at all, consistent with what we observed in cell lines from individuals with the premature stop polymorphism (Fig. 1E).

DISCUSSION

Our computational, enzymatic and structural homology analyses demonstrate that purified recombinant CLYBL possesses malate synthase and β-methylmalate synthase activities, which, to our knowledge, is the first time that such activities have been ascribed to a human protein. Malate synthase is traditionally described as operating in alternative carbon assimilation pathways such as the glyoxylate shunt. At present, the link between CLYBL and circulating B12 levels remains unclear, but it is notable that the newly identified substrates and products of CLYBL, as well as gene products strongly co-expressed with and co-evolving with CLYBL (Fig. 2), lie in close proximity to the mitochondrial B12 pathway (Fig. 6).

It is important to consider the kinetic parameters of CLYBL in the context of previously reported malate synthases. Previously studied malate synthase enzymes vary widely in their affinity for glyoxylate, ranging from a K_m of 2 mM in *Ricinus communis* (32) to 21 μM in *E. coli* (24). The 3.6 mM K_m reported here is at the high end of this spectrum, but it is similar to the 3.1 mM K_m reported for Mcl1 in *R. sphaeroides* (Table 1; Supplementary Material, Table S1) (21). Mcl1 is not a complete malate synthase, but rather condenses glyoxylate and ACoA to malyl-CoA before malyl-CoA is cleaved by the paralogous Mcl2. It is also notable that Mcl1 can catalyze condensation of both ACoA and PCoA with glyoxylate with similar kinetics to those observed for CLYBL (21). It is important to note that in our assays CLYBL is relatively inefficient, with low specific activity, but it could be the case that CLYBL requires an additional protein partner or post-translational modification *in vivo* to enhance its activity. When we screened possible substrate pairs, we noted that CLYBL had low activity with pyruvate and ACoA too, suggesting that it has low citramalate synthase activity. It is possible that CLYBL has additional enzymatic activities with greater catalytic efficiency that have not been tested here.

We note in our structural modeling that CLYBL is missing a large C-terminal domain present in malate synthase enzymes. Critically, CLYBL is missing a conserved aspartate (Asp633 in *M. tuberculosis* malate synthase G) predicted to work as a catalytic base that abstracts a proton from ACoA to initiate the malate synthase reaction (25,26). An Asp residue in a structurally equivalent position is absolutely conserved in all G form (~730 amino acids) malate synthases as well as in their shorter analogs: the A form (~530 amino acids), e.g. the *E. coli* and *B. anthracis* malate synthases (31) and the H form (~430 amino acids), e.g. *H. volcanii* (26). Substitution of this critical Asp with Asn in the *E. coli* G malate synthase was shown to render the protein inactive (24). Thus, a question arises which, if any, part of CLYBL could substitute for the missing catalytic Asp. A comparison of our model of CLYBL with the template *H. volcanii* malate synthase indicates that the C-terminal 50 amino acid segment of the polypeptide chain, which we were unable to model due to the low sequence similarity, is too short to fold into a stable structure required for positioning the critical Asp close to the bound substrate within the same monomer. We hypothesize that this critical contribution must be provided by intermolecular interactions within an oligomeric structure. Strong support for this prediction comes from the structure of the putative citrate lyase beta subunit from *B. xenovorans* (PDB 3r4i). The 339 amino acid polypeptide chain of this protein folds into a TIM barrel structure like CLYBL, but also contains a small flexible C-terminal domain, which extends into the catalytic domain of the neighboring

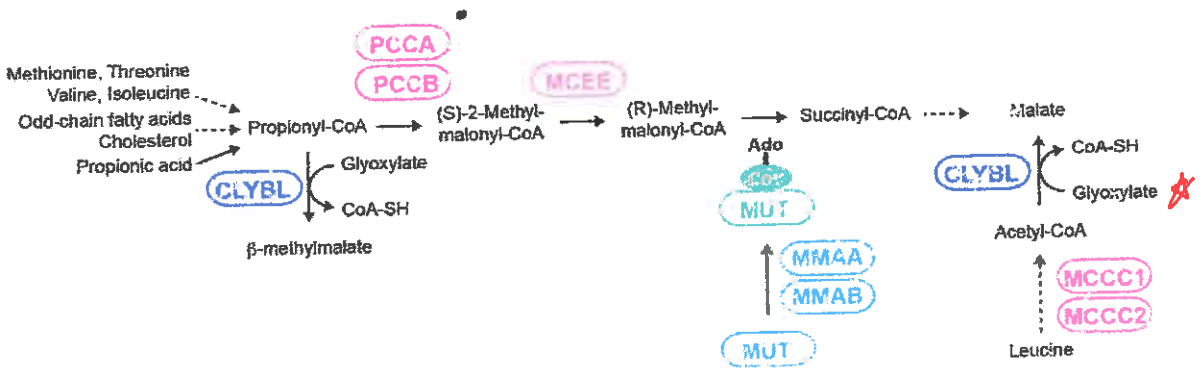

Figure 6. Newly identified enzymatic activities of CLYBL in the context of mitochondrial B12 metabolism. Genes in light blue encode enzymes in the mitochondrial B12 pathway. Genes in magenta encode transcripts and proteins that are highly co-expressed with CLYBL. Solid lines indicate one-step reactions and dashed lines represent multiple enzymatic steps.

• PCCA = propionyl Coenzyme A carboxylase, alpha polypeptide
Genet er hypermethyleret i både Vega 2014 og 2017, tabel S7.
* Lavere plasmaniveau af metabolitten glyoxylate i Germain et al (2017) metabolomic studie. (også lavere niveau af succinylcarnitine)

CLYBL side 3

COX10 COX10, heme A:farnesyltransferase cytochrome c oxidase assembly factor [*Homo sapiens* (human)]

Gene ID: 1352, updated on 29-Mar-2018 hypermethylated Vega 2014+2017

enome Browsers
enome Data Viewer
ap Viewer
ariation Viewer (GRCh37.p13)
ariation Viewer (GRCh38)
00 Genomes Browser (GRCh37.p13)
ısembl
CSC

Summary

Official Symbol	COX10 provided by HGNC
Official Full Name	COX10, heme A:farnesyltransferase cytochrome c oxidase assembly factor provided by HGNC
Primary source	HGNC:HGNC:2260
See related	Ensembl:ENSG00000006695 MIM:602125; Vega:OTTHUMG00000058814
Gene type	protein coding
RefSeq status	REVIEWED
Organism	Homo sapiens
Lineage	Eukaryota; Metazoa; Chordata; Craniata; Vertebrata; Euteleostomi; Mammalia; Eutheria; Euarchontoglires; Primates; Haplorrhini; Catarrhini; Hominidae; Homo
Summary	Cytochrome c oxidase (COX), the terminal component of the mitochondrial respiratory chain, catalyzes the electron transfer from reduced cytochrome c to oxygen. This component is a heteromeric complex consisting of 3 catalytic subunits encoded by mitochondrial genes and multiple structural subunits encoded by nuclear genes. The mitochondrially-encoded subunits function in electron transfer, and the nuclear-encoded subunits may function in the regulation and assembly of the complex. This nuclear gene encodes heme A:farnesyltransferase, which is not a structural subunit but required for the expression of functional COX and functions in the maturation of the heme A prosthetic group of COX. This protein is predicted to contain 7-9 transmembrane domains localized in the mitochondrial inner membrane. A gene mutation, which results in the substitution of a lysine for an asparagine (N204K), is identified to be responsible for cytochrome c oxidase deficiency. In addition, this gene is disrupted in patients with CMT1A (Charcot-Marie-Tooth type 1A) duplication and with HNPP (hereditary neuropathy with liability to pressure palsies) deletion. [provided by RefSeq, Jul 2008]
Expression	Broad expression in testis (RPKM 12.8), heart (RPKM 8.8) and 25 other tissues See more
Orthologs	mouse all

Genomic context

See COX10 in Genome Data Viewer Map Viewer

Location: 17p12

Exon count: 7

Annotation release	Status	Assembly	Chr	Location
109	current	GRCh38.p12 (GCF_000001405.38)	17	NC_000017.11 (14069402..14208679)
105	previous assembly	GRCh37.p13 (GCF_000001405.25)	17	NC_000017.10 (13972719..14111996)

Chromosome 17 - NC_000017.11

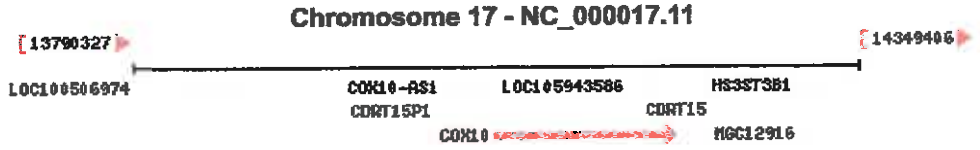

side 5 ↑↑

CYB5R2 cytochrome b5 reductase 2 [*Homo sapiens* (human)]

Gene ID: 51700, updated on 6-Dec-2016

Hide sidebar >>

Summary

hypermethylated Vega 2014 se ogsi PPFIBP2

Official Symbol	CYB5R2 provided by HGNC
Official Full Name	cytochrome b5 reductase 2 provided by HGNC
Primary source	HGNC:HGNC:24376
See related	Ensembl:ENSG00000166394 MIM:608342; Vega:OTTHUMG00000165665
Gene type	protein coding
RefSeq status	REVIEWED
Organism	Homo sapiens
Lineage	Eukaryota; Metazoa; Chordata; Craniata; Vertebrata; Euteleostomi; Mammalia; Eutheria; Euarchontoglires; Primates; Haplorrhini; Catarrhini; Hominidae; Homo
Also known as	B5R.2
Summary	The protein encoded by this gene belongs to the flavoprotein pyridine nucleotide cytochrome reductase family of proteins. Cytochrome b-type NAD(P)H oxidoreductases are implicated in many processes including cholesterol biosynthesis, fatty acid desaturation and elongation, and respiratory burst in neutrophils and macrophages. Cytochrome b5 reductases have soluble and membrane-bound forms that are the product of alternative splicing. In animal cells, the membrane-bound form binds to the endoplasmic reticulum, where it is a member of a fatty acid desaturation complex. Alternative splicing results in multiple transcript variants. [provided by RefSeq, Nov 2014]
Orthologs	mouse all

Genomic context

See CYB5R2 in Genome Data Viewer Map Viewer

Location: 11p15.4

Exon count: 13

Annotation release	Status	Assembly	Chr	Location
108	current	GRCh38.p7 (GCF_000001405.33)	11	NC_000011.10 (7665095..7678568, complement)
105	previous assembly	GRCh37.p13 (GCF_000001405.25)	11	NC_000011.9 (7686326..7695807, complement)

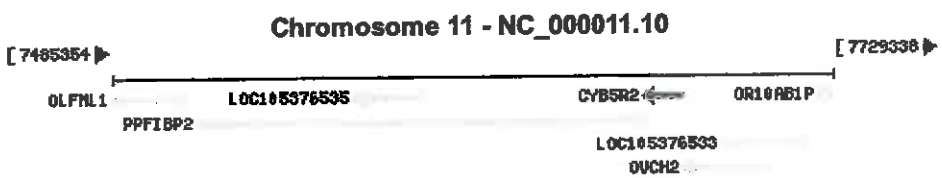

Genomic regions, transcripts, and products

Go to reference sequence details

Genomic Sequence: NC_000011.10 Chromosome 11 Reference GRCh38.p7 Primary Assembly

Go to nucleotide: Graphics FASTA GenBank

NC_000011.10: 7.7M..7.7M (18Kbp) C | Find:

CYB5R3 cytochrome b5 reductase 3 [*Homo sapiens* (human)]

Gene ID: 1727, updated on 11-Mar-2018

hypermethylect Vega 2017, 57

Summary
enome Browsers
enome Data Viewer
ap Viewer
riation Viewer (GRCh37.p13)
riation Viewer (GRCh38)
l00 Genomes Browser (GRCh37.p13)
isembl
CSC

Official Symbol	CYB5R3 provided by HGNC
Official Full Name	cytochrome b5 reductase 3 provided by HGNC
Primary source	HGNC:HGNC:2873
See related	Ensembl:ENSG00000100243 MIM:613213; Vega:OTTHUMG00000150745
Gene type	protein coding
RefSeq status	REVIEWED
Organism	Homo sapiens
Lineage	Eukaryota; Metazoa; Chordata; Craniata; Vertebrata; Euteleostomi; Mammalia; Eutheria; Euarchontoglires; Primates; Haplorrhini; Catarrhini; Hominidae; Homo
Also known as	B5R; DIA1
Summary	*This gene encodes cytochrome b5 reductase, which includes a membrane-bound form in somatic cells (anchored in the endoplasmic reticulum, mitochondrial and other membranes) and a soluble form in erythrocytes. The membrane-bound form exists mainly on the cytoplasmic side of the endoplasmic reticulum and functions in desaturation and elongation of fatty acids, in cholesterol biosynthesis, and in drug metabolism. The erythrocyte form is located in a soluble fraction of circulating erythrocytes and is involved in methemoglobin reduction. The membrane-bound form has both membrane-binding and catalytic domains, while the soluble form has only the catalytic domain. Alternate splicing results in multiple transcript variants. Mutations in this gene cause methemoglobinemias. [provided by RefSeq, Jan 2010]*
Expression	Ubiquitous expression in fat (RPKM 110.9), testis (RPKM 52.5) and 24 other tissues See more
Orthologs	mouse all

Genomic context

Location: 22q13.2

Proces: L-ascorbic acid metabolic proces, cholesterol synthesis xenobiotics

Interagerer: HOXB5, MOV10, ESR1 ↑

Exon count: 12

See CYB5R3 in Genome Data Viewer Map Viewer

Annotation release	Status	Assembly	Chr	Location
108	current	GRCh38.p7 (GCF_000001405.33)	22	NC_000022.11 (42617840..42649399, complement)
105	previous assembly	GRCh37.p13 (GCF_000001405.25)	22	NC_000022.10 (43013846..43045405, complement)

Chromosome 22 - NC_000022.11

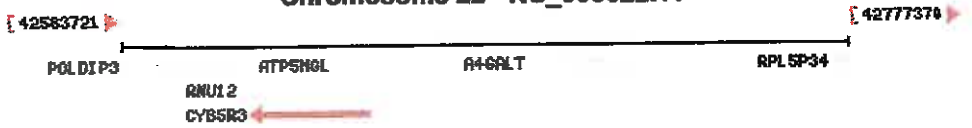

Genomic regions, transcripts, and products

Go to reference sequence details

D2HGDH D-2-hydroxyglutarate dehydrogenase [*Homo sapiens* (human)]

Gene ID: 728294, updated on 5-Nov-2017

Summary

Official Symbol	D2HGDH provided by HGNC
Official Full Name	D-2-hydroxyglutarate dehydrogenase provided by HGNC
Primary source	HGNC:HGNC:28358
See related	Ensembl:ENSG00000180902 MIM:609186; Vega:OTTHUMG00000151474
Gene type	protein coding
RefSeq status	VALIDATED
Organism	Homo sapiens
Lineage	Eukaryota; Metazoa; Chordata; Craniata; Vertebrata; Euteleostomi; Mammalia; Eutheria; Euarchontoglires; Primates; Haplorrhini; Catarrhini; Hominidae; Homo
Also known as	D2HGD
Summary	This gene encodes D-2hydroxyglutarate dehydrogenase, a mitochondrial enzyme belonging to the FAD-binding oxidoreductase/transferase type 4 family. This enzyme, which is most active in liver and kidney but also active in heart and brain, converts D-2-hydroxyglutarate to 2-ketoglutarate. Mutations in this gene are present in D-2-hydroxyglutaric aciduria, a rare recessive neurometabolic disorder causing developmental delay, epilepsy, hypotonia, and dysmorphic features. [provided by RefSeq, Jul 2008]
Expression	Ubiquitous expression in skin (RPKM 9.9), kidney (RPKM 7.5) and 25 other tissues See more
Orthologs	mouse all

Genomic context

See D2HGDH in Genome Data Viewer Map Viewer

Location: 2q37.3

Exon count: 20

Annotation release	Status	Assembly	Chr	Location
108	current	GRCh38.p7 (GCF_000001405.33)	2	NC_000002.12 (241734579..241768816)
105	previous assembly	GRCh37.p13 (GCF_000001405.25)	2	NC_000002.11 (242674030..242708231)

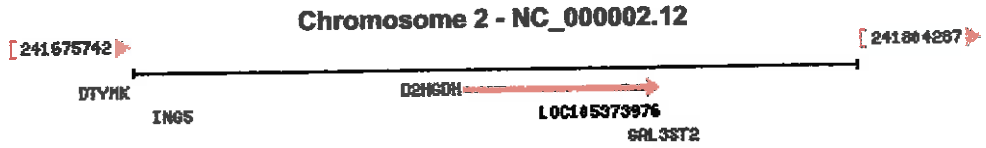

Genomic regions, transcripts, and products

Go to reference sequence details

Genomic Sequence: NC_000002.12 Chromosome 2 Reference GRCh38.p7 Primary Assembly

Go to nucleotide: Graphics FASTA GenBank

NC_000002.12 Find:

Follow ME in Denmark

Thoughts and guesses about research in Myalgic encephalomyelitis/(Chronic Fatigue Syndrome)

torsdag den 18. januar 2018

D2HGDH, PHYKPL and ME

The gene D2HGDH is hypomethylated in ME patients, and this is associated with quality of life (1). Hypomethylation can result in upregulation of gene transcription. In agreement with this, gene expression of D2HGDH was upregulated in whole blood from adolescent ME/CFS patients (2).

D2HGDH encodes D-2-hydroxy-glutarate dehydrogenase, which converts D-2-hydroxyglutarate to alpha-ketoglutarate (alpha - KG). Mutations in D2HGDH are present in D-2-hydroxyglutaric aciduria, a rare neurometabolic disorder.

It is possible that 2-hydroxy glutarate is generated in relation to lysine breakdown. PHYKPL, 5-phosphohydroxy-L-lysine phospholyase, gene expression is upregulated in ME/CFS patients (2).

D2HGDH regulates alpha-KG levels and alpha-KG dependent dioxygenase function by modulating isocitrate dehydrogenase 2 (IDH2) (3).

Some of the enzymes that regulate histone and DNA methylation belong to the family of alpha-KG dependent dioxygenases.

Fx, D2HGHD induces demethylation of histone H3K4me3, so it becomes H3K4. This change is relevant to B cell differentiation (3,4)

D2HGDH is one of the genes that when mutant may promote epigenetic changes in B-cell cancer (3).

Furthermore, alpha-KG metabolism and IDH2 expression are part of the metabolic reprogramming-response in pyruvate dehydrogenase deficient cells (5).

References:

1. Vega et al: Epigenetic modifications and glucocorticoid sensitivity in ME/CFS. BMC Medical Genomics, 2017, 10, 11
2. Nguyen et al: Whole blood gene expression in adolescent CFS: an exploratory crosssectional study suggesting altered B cell differentiation and survival. J Transl Med. 2017,15,102.
3. Lin et al: D2HGDH regulates alpha-ketoglutarate levels and dioxygenase function by modulating IDH2. Nat Comm. 16.jul 2015.
4. Barneda-Zahonero et al: Epigenetic regulation of B lymphocyte differentiation, transdifferentiation and reprogramming. Hindawi, 2012, ID564381
5. Rajagopalan et al. Metabolic plasticity maintains proliferation in pyruvate dehydrogenase deficient cells. Cancer & Metabolism (2015) 3:7

Indsendt af Helle Nielsen kl. 21.50 G+

Ingen kommentarer:

Send en kommentar

Bemærk! Kun medlemmer af denne blog kan sende kommentarer.

Indtast din kommentar...

Kommenter som: Helle Nielsen (

Log ud

Vis eksempe

Underret mig

Start

D2HGDH side2

Follow ME in Denmark

Thoughts and guesses about research in Myalgic encephalomyelitis/(Chronic Fatigue Syndrome)

lørdag den 20. januar 2018

KDM2B, PHYH, P3H2, PLOD3 and ME

Alpha-ketoglutarate dependent dioxygenases are also called 2-oxoglutarate oxygenases. They are a large family of enzymes with most diverse functions (1).

The following examples are relevant for ME research.

KDM2B
KDM2B (lysine demethylase 2B) is one of the 2OG-oxygenases described in ref 1. The gene KDM2B is hypermethylated in ME patients (2). And KDM2B is hypomethylated in $CD4^+$ T cells from ME patients (3). KDM2B is able to regulate histone 3 methylation. KDM2B expression is also known to regulate ribosome biogenesis, and is a positive regulator of glycolysis. KDM2B is an important mediator of hematopoietic cell development.

PHYH
PHYH (phytanoyl-CoA 2-hydroxylase) is a peroxisomal protein that is involved in the alpha-oxidation of 3-methyl branched fatty acids. The gene is hypermethylated in ME patients (2).

P3H2
P3H2 (prolyl 3-hydroxylase 2, also known as LEPREL1) play a critical role in collagen chain assembly, stability and cross-linking by catalyzing post-translational 3-hydroxylation of proline residues. This is important to basement membranes. Interestingly, P3H2 has a FIS1 mitochondriat fission protein1) domain. P3H2 is hypomethylated in ME patients (2).

PLOD3
PLOD3 (procollagen-lysine, 2-oxoglutarate 5-dioxygenase 3) catalyzes the hydroxylation of lysyl residues in collagen-like peptides. PLOD3 is found in the basement membrane. Reduced levels are associated to disease. Spinal fluid PLOD3 levels in ME patients:9 and normal value:14 (4). Interestingly, PLOD3 is located on chromosome 7 besides FIS1 and CLDN15. CLDN15 is hypermethylated in ME patients and this is associated to quality of life (2).CLDN15 (claudin 15) is an integral membrane pretein and component of tight junction strands. CLDN15 has been associated with irritabel bowel syndrome.

References:

1. Loenarz and Schofield: Expanding chemical biology of 2-oxoglutarate oxygenases. Nat Chem Biol, 2008, 4, 3.
2. Vega et al: Epigenetic modifications and glucocorticoid sensitivity in ME/CFS. BMC Medical Genomics, 2017, 10, 11
3. Brenu et al: Methylation profile of CD4+ T cells in CFS/ME. J. Clin Cell Immunol 5, 228
4. Schutzer et al: Distinct Cerebrospinal Fluid Proteomes Differentiate Post- Treatment Lyme Disease from Chronic Fatigue Syndrome. PLOS One February 2011, volume 6, Issue

Knowledge about the genes: www.ncbi.nlm.nih.gov/gene

Helle Nielsen kl. 13:43

Ingen kommentarer:

Send en kommentar

Bemærk! Kun medlemmer af denne blog kan sende kommentarer.

Indtast din kommentar...

Kommenter som: Helle Nielsen (I Log ud

Translate
Select Language

Useful links
- A primer for clinical practitioners
- Anesthesia information
- CFIDS
- CFS Advisory Committee
- Cort Johnson blog
- International Consensus Primer
- Latest research - action for ME
- ME Foreningen
- ME and Rituximab
- Myalgic encephalomyelitis International Consensus Criteria
- Oslo Universitetssygehus - information
- Phoenix Rising
- Research1st

Blog-arkiv
- 2018 (4)
  - januar (4)
    - D2HGDH, PHYKPL and ME
    - DGKZ and ME
    - ATP6V0E2, PRF1, GNLY and ME
    - ACVR1, activiner og ME
- 2017 (19)
- 2016 (11)
- 2015 (14)
- 2014 (35)
- 2013 (59)
- 2012 (25)

Om mig
Helle Nielsen
Følg
Vis hele min profil

Email
followmeindenmark@gmail.com

Twitter
https://twitter.com/followmeindk

Follow by Email
Email address...

D2HGDH side 3

D2HGDH

J Inherit Metab Dis (2012) 35:571–587
DOI 10.1007/s10545-012-9462-5

METABOLIC DISSERTATION

Progress in understanding 2-hydroxyglutaric acidurias

Martijn Kranendijk · Eduard A. Struys · Gajja S. Salomons · Marjo S. Van der Knaap · Cornelis Jakobs

Martijn Kranendijk

Received: 13 December 2011 / Revised: 25 January 2012 / Accepted: 30 January 2012 / Published online: 6 March 2012

Abstract The organic acidurias D-2-hydroxyglutaric aciduria (D-2-HGA), L-2-hydroxyglutaric aciduria (L-2-HGA), and combined D,L-2-hydroxyglutaric aciduria (D,L-2-HGA) cause neurological impairment at young age. Accumulation of D-2-hydroxyglutarate (D-2-HG) and/or L-2-hydroxyglutarate (L-2-HG) in body fluids are the biochemical hallmarks of these disorders. The current review describes the knowledge gathered on 2-hydroxyglutaric acidurias (2-HGA), since the description of the first patients in 1980. We report on the clinical, genetic, enzymatic and metabolic characterization of D-2-HGA type I, D-2-HGA type II, L-2-HGA and D,L-2-HGA, whereas for D-2-HGA type I and type II novel clinical information is presented which was derived from questionnaires.

Abbreviations

2-HG	2-hydroxyglutaric acid (undifferentiated for chiral D- or L-form)
2-HGA	2-hydroxyglutaric aciduria
D-2-HG	D-2-hydroxyglutaric acid
D-2-HGA	D-2-hydroxyglutaric aciduria
D-2-HGDH	D-2-hydroxyglutarate dehydrogenase enzyme
D2HGDH	gene encoding D-2-hydroxyglutarate dehydrogenase
L-2-HG	L-2-hydroxyglutaric acid
L-2-HGA	L-2-hydroxyglutaric aciduria
L-2-HGDH	L-2-hydroxyglutarate dehydrogenase enzyme
L2HGDH	gene encoding L-2-hydroxyglutarate dehydrogenase
D,L-2-HGA	combined D,L-2-hydroxyglutaric aciduria
IDH2	gene encoding isocitrate dehydrogenase 2
2-KG	2-ketoglutaric acid
HOT	hydroxyacid-oxoacid transhydrogenase enzyme
L-malDH	L-malate dehydrogenase enzyme
MIM	Mendelian Inheritance in Man
CSF	cerebrospinal fluid

Communicated by: K. Michael Gibson

Competing interest: None declared.

M. Kranendijk · E. A. Struys · G. S. Salomons · C. Jakobs (✉)
Metabolic Unit - Department of Clinical Chemistry,
VU University Medical Center,
Amsterdam, The Netherlands
e-mail: C.Jakobs@vumc.nl

M. S. Van der Knaap
Paediatric Neurology, VU University Medical Center,
Amsterdam, The Netherlands

Introduction

Gregersen et al (1977) were the first to identify enantiomeric D- and L-2-hydroxyglutaric acids (D-2-HG and L-2-HG) as normal constituents of human urine. Three years later, two novel inborn errors of metabolism were simultaneously reported in the *Journal of Inherited Metabolic Disease*. Chalmers et al (1980) identified a patient with D-2-hydroxyglutaric aciduria (D-2-HGA), while Duran et al (1980) described a case of L-2-hydroxyglutaric aciduria (L-2-HGA), landmark publications that identified the metabolic hallmarks (D- and L-2-HG) in these disorders. Muntau et al (2000) described a third biochemical variant of 2-hydroxyglutaric aciduria (2-HGA) when they reported three

DHGDH side 4

D2HGDH

patients with elevated urinary D- and L-2-HG, denoted by these authors as "combined D,L-2-hydroxyglutaric aciduria" (D,L-2-HGA). Major milestones in research on these disorders came with gene discovery: *D2HGDH* encoding D-2-hydroxyglutarate dehydrogenase (D-2-HGDH)(Achouri et al 2004) and *L2HGDH* encoding L-2-hydroxyglutarate dehydrogenase (L-2-HGDH)(Rzem et al 2004; Topcu et al 2004). In many D-2-HGA, and the majority of L-2-HGA patients, genetic characterization revealed pathogenic mutations in these genes (Struys et al 2005c; Steenweg et al 2010). Nonetheless, in fully one-half of D-2-HGA patients no mutations in *D2HGDH* were detected (Kranendijk et al 2010a). Subsequently, we described gain-of-function mutations in *isocitrate dehydrogenase 2* (*IDH2*) which proved causative for the D-2-HG accumulation in previously unclassified D-2-HGA patients (Kranendijk et al 2010b). In sum, the preceding decade has provided tremendous advances in our understanding of the inborn 2-hydroxyglutaric acidurias, which will undoubtedly provide a solid foundation from which to develop novel and effective treatment strategies.

This *Review* evaluates metabolic, enzymatic, genetic and clinical progress in our understanding of the *rare inborn organic acidurias* D-2-HGA, L-2-HGA and D,L-2-HGA. Future research and therapeutic perspectives are also briefly discussed.

Enantiomeric D,L-2-hydroxyglutaric acid and its origin

The five-carbon dicarboxylic acid 2-hydroxyglutaric acid (2-HG) possesses a hydroxyl group at the second carbon (Fig. 1) which yields a chiral center. Accordingly, two three-dimensional (3D) structures exist, including D-2-HG and L-2-HG, which represent "non-superimposable" mirror images (Fig. 2). Systemic names are (R)-2-hydroxypentanedioic acid and (S)-2-hydroxypentanedioic acid, respectively, for D- and L-2-HG. Whereas enantiomers share identical chemical and physical properties (melting point, mass, solubility and pKa), their differing 3D-structures result in considerable differences in enzymatic and molecular properties.

Pilot studies employing stable isotope labeled [$^{13}C_6$]glucose or [$^{2}H_5$]glutamic acid with D-2-HGA lymphoblast cell cultures revealed that mitochondrial 2-ketoglutarate (2-KG), a tricarboxylic acid (TCA) cycle intermediate, can be metabolized to D-2-HG (Struys et al 2004b). Subsequent studies documented the existence of hydroxyacid-oxoacid

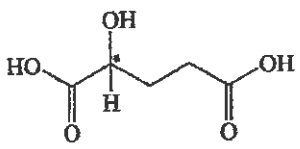

Fig. 1 2-hydroxyglutaric acid with a chiral center at the 2nd carbon (*)

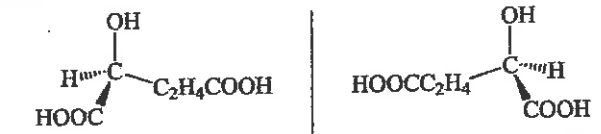

D-2-hydroxyglutaric acid (R)-2-hydroxypentanedioic acid | L-2-hydroxyglutaric acid (S)-2-hydroxypentanedioic acid

Fig. 2 Enantiomers D- and L-2-hydroxyglutaric acid (D-2-HG and L-2-HG, systemic IUPAC names included)

transhydrogenase (HOT) activity in human liver and fibroblasts, representing the first demonstration of a human enzyme whose catalytic function was production of D-2-HG (Struys et al 2005c). HOT catalyzes the conversion of γ-hydroxybutyrate (GHB) to succinic semialdehyde (SSA) with a stoichiometric production of D-2-HG from 2-KG (Fig. 3). Similarly, pilot studies of L-2-HGA lymphoblasts incubated with [$^{13}C_6$]glucose and [$^{2}H_5$]glutamic acid further delineated that mitochondrial 2-KG is the precursor of L-2-HG (Struys et al 2007). Currently, the only enzyme known to generate L-2-HG from 2-KG in human is L-malate dehydrogenase (L-malDH) (Fig. 3), whose primary catalytic function is the interconversion of L-malate to oxaloacetate (Rzem et al 2007).

The diagnosis of 2-hydroxyglutaric aciduria

The differential diagnosis of 2-hydroxyglutaric aciduria begins with the clinical evaluation of a patient with unexplained developmental delay and/or other neurological dysfunction of unknown etiology, raising suspicion for a metabolic disorder. Provisional diagnosis of the disorder is occasionally suggested by abnormal brain MRI findings. Urinary organic acid screening with gas chromatography-mass spectrometry (GC-MS), performed in multiple metabolic centers, can reveal increased 2-HG, but the chiral configuration remains to be determined. Although the clinical presentation often can suggest either D-2-HGA or

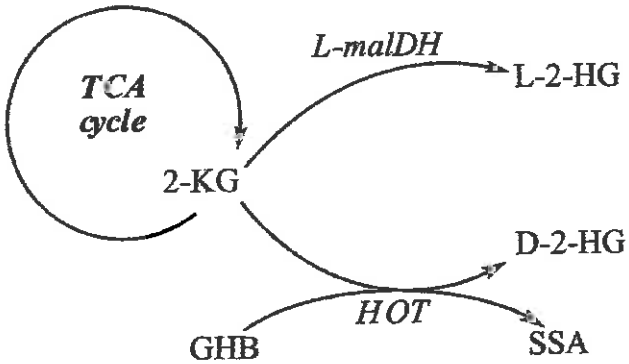

Fig. 3 Enzymes L-malDH and HOT are responsible for production of D-2-HG and L-2-HG from 2-KG

DGHGDH side 5

DECR1 2,4-dienoyl-CoA reductase 1 [*Homo sapiens* (human)]

Gene ID: 1666, updated on 3-Apr-2018

genekspression upreglerad
Nguyen 2017, p = 0,059

Summary
enome Browsers
enome Data Viewer
ap Viewer
riation Viewer (GRCh37.p13)
riation Viewer (GRCh38)
00 Genomes Browser (GRCh37.p13)
nsembl
CSC

Official Symbol	DECR1 provided by HGNC
Official Full Name	2,4-dienoyl-CoA reductase 1 provided by HGNC
Primary source	HGNC:HGNC:2753
See related	Ensembl:ENSG00000104325 MIM:222745; Vega:OTTHUMG00000163829
Gene type	protein coding
RefSeq status	REVIEWED
Organism	Homo sapiens
Lineage	Eukaryota; Metazoa; Chordata; Craniata; Vertebrata; Euteleostomi; Mammalia; Eutheria; Euarchontoglires; Primates; Haplorrhini; Catarrhini; Hominidae; Homo
Also known as	DECR; NADPH; SDR18C1
Summary	This gene encodes an accessory enzyme which participates in the beta-oxidation and metabolism of unsaturated fatty enoyl-CoA esters. [provided by RefSeq, Jul 2008]
Expression	Ubiquitous expression in liver (RPKM 86.6), fat (RPKM 60.8) and 25 other tissues See more
Orthologs	mouse all

Genomic context

See DECR1 in Genome Data Viewer Map Viewer

Location: 8q21.3

Exon count: 13

Annotation release	Status	Assembly	Chr	Location
109	current	GRCh38.p12 (GCF_000001405.38)	8	NC_000008.11 (90001352..90053633)
105	previous assembly	GRCh37.p13 (GCF_000001405.25)	8	NC_000008.10 (91013580..91064232)

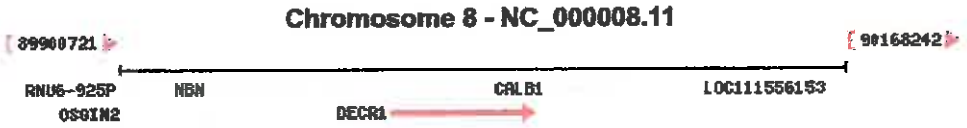

Genomic regions, transcripts, and products

Go to reference sequence details

Genomic Sequence: NC_000008.11 Chromosome 8 Reference GRCh38.p12 Primary Assembly ▼

Go to nucleotide: Graphics FASTA GenBank

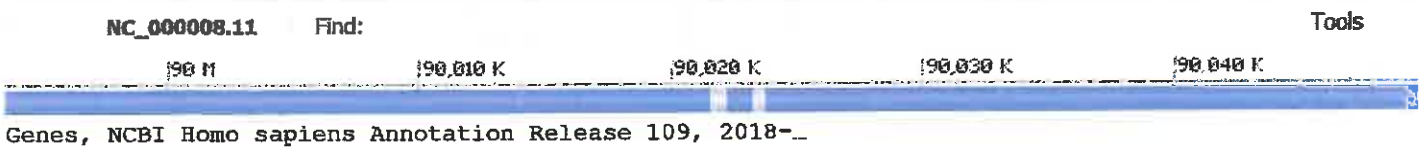

ETFB electron transfer flavoprotein beta subunit [*Homo sapiens* (human)]

Gene ID: 2109, updated on 29-Mar-2018 hypomethylated TSS200, Body, Vega2017,57

Summary
enome Browsers
enome Data Viewer
ap Viewer
riation Viewer (GRCh37.p13)
riation Viewer (GRCh38)
00 Genomes Browser (GRCh37.p13)
nsembl
CSC

Official Symbol	ETFB provided by HGNC
Official Full Name	electron transfer flavoprotein beta subunit provided by HGNC
Primary source	HGNC:HGNC:3482
See related	Ensembl:ENSG00000105379 MIM:130410; Vega:OTTHUMG00000182903
Gene type	protein coding
RefSeq status	REVIEWED
Organism	Homo sapiens
Lineage	Eukaryota; Metazoa; Chordata; Craniata; Vertebrata; Euteleostomi; Mammalia; Eutheria; Euarchontoglires; Primates; Haplorrhini; Catarrhini; Hominidae; Homo
Also known as	MADD; FP585
Summary	This gene encodes electron-transfer-flavoprotein, beta polypeptide, which shuttles electrons between primary flavoprotein dehydrogenases involved in mitochondrial fatty acid and amino acid catabolism and the membrane-bound electron transfer flavoprotein ubiquinone oxidoreductase. The gene deficiencies have been implicated in type II glutaricaciduria. Alternatively spliced transcript variants have been found for this gene. [provided by RefSeq, Jul 2008]
Expression	Ubiquitous expression in liver (RPKM 75.6), fat (RPKM 65.8) and 25 other tissues See more
Orthologs	mouse all

Genomic context

See ETFB in Genome Data Viewer Map Viewer

Location: 19q13.41

Exon count: 7

Annotation release	Status	Assembly	Chr	Location
109	current	GRCh38.p12 (GCF_000001405.38)	19	NC_000019.10 (51345155..51366418, complement)
105	previous assembly	GRCh37.p13 (GCF_000001405.25)	19	NC_000019.9 (51848409..51869672, complement)

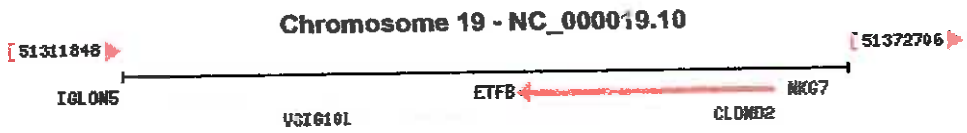

Genomic regions, transcripts, and products

Go to reference sequence details

Genomic Sequence: NC_000019.10 Chromosome 19 Reference GRCh38.p12 Primary Assembly

Go to nucleotide: Graphics FASTA GenBank

NC_000019.10 Find: ETFB side 1 Tools

370 K | 51,365 K | 51,360 K | 51,355 K | 51,350 K

Copos NCBI Homo sapiens Annotation Release 109 2018-

ETF α og β Subunit

THE JOURNAL OF BIOLOGICAL CHEMISTRY VOL. 284, NO. 7, pp. 4222–4229, February 13, 2009

Role of Flavinylation in a Mild Variant of Multiple Acyl-CoA Dehydrogenation Deficiency

A MOLECULAR RATIONALE FOR THE EFFECTS OF RIBOFLAVIN SUPPLEMENTATION*[S]

Received for publication, July 25, 2008, and in revised form, December 11, 2008 Published, JBC Papers in Press, December 16, 2008, DOI 10.1074/jbc.M805719200

Bárbara J. Henriques[‡], João V. Rodrigues[‡], Rikke K. Olsen[§], Peter Bross[§], and Cláudio M. Gomes[‡1]

From the [‡]Instituto Tecnologia Química e Biológica, Universidade Nova de Lisboa, 2780-756 Oeiras, Portugal and the [§]Research Unit for Molecular Medicine, Århus University Hospital, Skejby 8200 Århus N, Denmark

Mutations in the genes encoding the α-subunit and β-subunit of the mitochondrial electron transfer flavoprotein (ETF) and the electron transfer flavoprotein:ubiquinone oxidoreductase (ETF:QO) cause multiple acyl-CoA dehydrogenation deficiency (MADD), a disorder of fatty acid and amino acid metabolism. Point mutations in ETF, which may compromise folding, and/or activity, are associated with both mild and severe forms of MADD. Here we report the investigation on the conformational and stability properties of the disease-causing variant ETFβ-D128N, and our findings on the effect of flavinylation in modulating protein conformational stability and activity. A combination of biochemical and biophysical methods including circular dichroism, visible absorption, flavin, and tryptophan fluorescence emission allowed the analysis of structural changes and of the FAD moiety. The ETFβ-D128N variant retains the overall fold of the wild type, but under stress conditions its flavin becomes less tightly bound. Flavinylation is shown to improve the conformational stability and biological activity of a destabilized D128N variant protein. Moreover, the presence of flavin prevented proteolytic digestion by avoiding protein destabilization. A patient homozygous for the ETFβ-D128N mutation developed severe disease symptoms in association with a viral infection and fever. In agreement, our results suggest that heat inactivation of the mutant may be more relevant at temperatures above 37 °C. To mimic a situation of fever *in vitro*, the flavinylation status was tested at 39 °C. FAD exerts the effect of a pharmacological chaperone, improving ETF conformation, and yielding a more stable and active enzyme. Our results provide a structural and functional framework that could help to elucidate the role that an increased cellular FAD content obtained from riboflavin supplementation may play in the molecular pathogenesis of not only MADD, but genetic disorders of flavoproteins in general.

Multiple acyl-CoA dehydrogenation deficiency (MADD,[2] MIM 231680; also designated glutaric acidemia type II (GAII)) is caused by mutations in either of the genes encoding the two subunits of electron transfer flavoprotein (ETF) or the monomeric enzyme ETF:ubiquinone oxidoreductase (ETF:QO) (1, 2). The flavin adenine dinucleotide (FAD) in ETF receives electrons from at least 12 different mitochondrial FAD-containing dehydrogenases, which are involved in fatty acid β-oxidation and amino acid metabolism (3). ETF is subsequently oxidized by the membrane-bound ETF:QO. This last component, which harbors both a FAD and an [4Fe-4S] cluster, mediates the transfer of reducing equivalents to the respiratory ubiquinone pool, leading to subsequent ATP production (4, 5). As a result of deficient function of either ETF or ETF:QO, the acyl-CoA dehydrogenases are blocked because they cannot transfer the electrons gained in the dehydrogenation reactions, entailing accumulation of various acyl-esters in blood and urine, hence the term MADD (1). The clinical features of patients suffering from MADD are rather heterogeneous. It ranges from lethal cases with neonatal anomalies to mildly affected individuals, presenting in childhood or adulthood with hypoglycemic, encephalopathy, and/or myopathy (1, 6). There is evidence that the severity of the clinical phenotype, to some extent, depends on the location and nature of mutations in the genes encoding ETF or ETF:QO, with null mutations severely affecting mRNA expression, processing and/or stability being associated with lethal disease and missense mutations leaving some residual ETF/ETF:QO enzyme activity being associated with milder clinical forms (6–9). In patients with milder disease variants, symptoms are often intermittent and only become evident during periods of illness and catabolic stress, indicating that in this group of patients, in whom residual ETF/ETF:QO enzyme activity allows modulation of the enzymatic phenotype, the disease severity does not depend only on the nature of the gene defect but also on cellular factors that may modulate the enzymatic phenotype (6). This potential for *in vitro* modulation of the enzymatic phenotype has been established for a large number of disease-causing mutations affecting flavin-containing mitochondrial acyl-CoA dehydrogenases (10). In these cases, missense mutations have been shown to impair folding to the native structure and/or destabilize the native folded structure,

* The work was supported by the Fundação para a Ciência e Tecnologia (FCT/MCTES, Portugal): Research Grant PTDC/SAU-GMG/70033/2006 (to C. M. G.), and Fellowships SFRH/BD/29200/2006 (to B. J. H.) and SFRH/BPD/34763/2007 (to J. V. R.). The costs of publication of this article were defrayed in part by the payment of page charges. This article must therefore be hereby marked "*advertisement*" in accordance with 18 U.S.C. Section 1734 solely to indicate this fact.

[S] The on-line version of this article (available at http://www.jbc.org) contains supplemental Figs. S1 and S2.

[1] To whom correspondence should be addressed: ITQB/UNL. Av. República 127, 2780-756 Oeiras, Portugal. Tel.: 351-214469332; Fax: 351-214411277; E-mail: gomes@itqb.unl.pt.

[2] The abbreviations used are: MADD, multiple acyl-CoA dehydrogenation deficiency; WT, wild type; ETF, electron transfer flavoprotein; PDB, Protein Data Bank; CD, circular dichroism; C_m, denaturant midpoint transition concentration.

ETFB side 2

EFTB

(ACSF2)

Published in final edited form as:
Mol Cell. 2016 August 18; 63(4): 621–632. doi:10.1016/j.molcel.2016.06.033.

Mitochondrial protein interaction mapping identifies new regulators of respiratory chain function

Brendan J. Floyd[1,2,10], **Emily M. Wilkerson**[3,10], **Mike T. Veling**[1,2,10], **Catie E. Minogue**[3,10], **Chuanwu Xia**[4], **Emily T. Beebe**[2], **Russell L. Wrobel**[2], **Holly Cho**[1,2], **Laura S. Kremer**[5,6], **Charlotte L. Alston**[7], **Katarzyna A. Gromek**[2], **Brendan K. Dolan**[2], **Arne Ulbrich**[3], **Jonathan A. Stefely**[1,2], **Sarah L. Bohl**[1,2], **Kelly M. Werner**[2], **Adam Jochem**[1], **Michael S. Westphall**[9], **Jarred W. Rensvold**[1], **Robert W. Taylor**[7], **Holger Prokisch**[5,6], **Jung-Ja P. Kim**[4], **Joshua J. Coon**[3,8,9], and **David J. Pagliarini**[1,2,*]

[1]Morgridge Institute for Research, Madison, WI 53715, USA

[2]Department of Biochemistry, University of Wisconsin–Madison, Madison, WI 53706, USA

[3]Department of Chemistry, University of Wisconsin–Madison, Madison, WI 53706, USA

[4]Department of Biochemistry, Medical College of Wisconsin, Milwaukee, WI 53226, USA

[5]Institute of Human Genetics, Technische Universität München, 81675 München, Germany

[6]Institute of Human Genetics, Helmholtz Zentrum München, 85764 Neuherberg, Germany

[7]Wellcome Trust Centre for Mitochondrial Research, Institute of Neuroscience, The Medical School, Newcastle University, Newcastle upon Tyne NE2 4HH, UK

[8]Department of Biomolecular Chemistry, University of Wisconsin–Madison, Madison, WI 53706, USA

[9]Genome Center of Wisconsin, University of Wisconsin–Madison, Madison, WI 53706, USA

SUMMARY

Mitochondria are essential for numerous cellular processes, yet hundreds of their proteins lack robust functional annotation. To reveal new functions for these proteins (termed MXPs) we assessed condition-specific protein-protein interactions for 50 select MXPs using affinity enrichment mass spectrometry. Our data connect MXPs to diverse mitochondrial processes, including multiple aspects of respiratory chain function. Building upon these observations, we validated C17orf89 as a complex I (CI) assembly factor. Disruption of C17orf89 markedly reduced

*Correspondence: dpagliarini@morgridge.org.
[10]Co-first author

AUTHOR CONTRIBUTIONS

B.J.F. and D.J.P. conceived of the project and its design. B.J.F, C.E.M., E.M.W., M.T.V., C.X., E.T.B., H.C., L.S.K., C.L.A., K.A.G., B.K.D., A.U., J.A.S., S.L.B., K.M.W., C.E.W., J.W.R., R.W.T., H.P., J.J.K., J.J.C., D.J.P., performed experiments and data analysis. R.L.W., A.J., M.S.W., J.W.R., R.W.T., H.P., J.J.K., J.J.C., D.J.P., provided key experimental resources and/or aided in experimental design. B.J.F. and D.J.P. wrote the manuscript.

ETFB side3

EFTB

LYRM4 hypermethylect
vega 2017 57

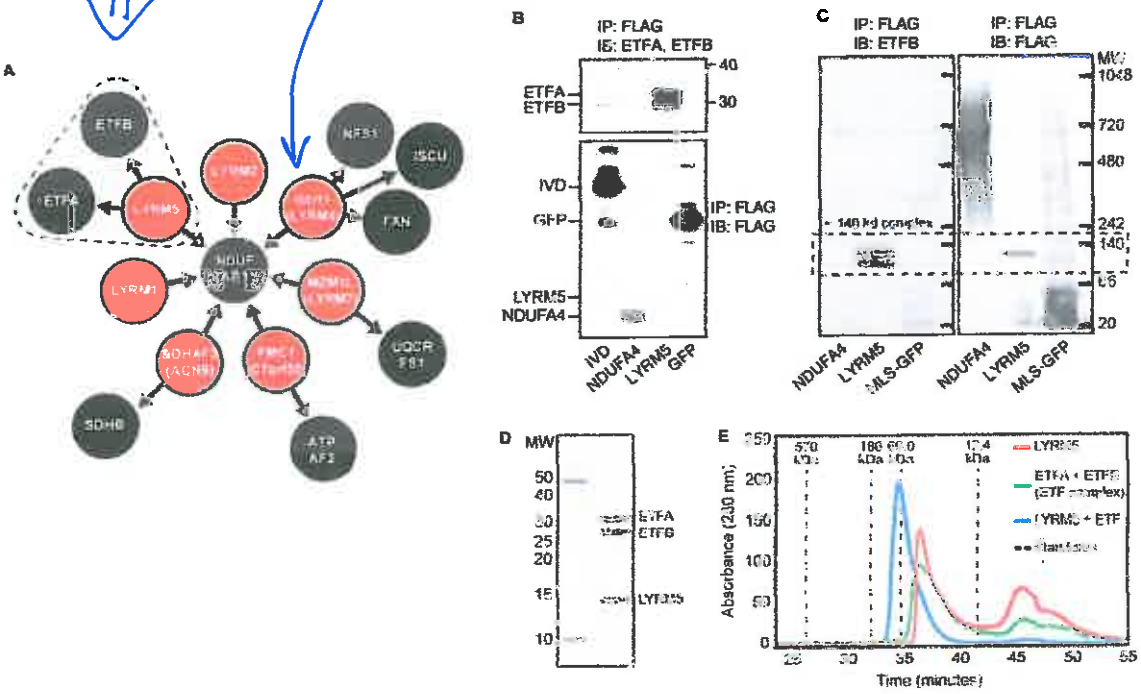

Figure 5. LYRM5 forms a complex with ETF

(A) Schematic of top-scoring LYRM PPIs. LYRM5-ETF interactions are shaded.

(B) Validation of the interaction between LYRM5 and both ETFA and ETFB. C-terminally FLAG-tagged GFP, IVD, NDUFA4, and LYRM5 were immunoprecipitated (IP) from HEK cells and immunoblotted (IB) with anti-ETFA and anti-ETFB (upper) or anti-FLAG (lower). LYRM5 enriched for both ETF proteins more efficiently than IVD, a known ETF interactor.

(C) IP of LYRM5-FLAG or MLS-GFP-FLAG from HEK293 cells analyzed by Blue Native-PAGE analysis and IB. The same membrane was blotted for ETFB (left) and then FLAG (right) (see also Figure S5).

(D) Recombinant N-terminally His-tagged LYRM5 and untagged ETFA/B were co-expressed in *E. coli*. Purification of LYRM5 by metal affinity chromatography led to the co-purification of ETFA/B.

(E) LYRM5 and ETF form a stable complex. Size exclusion chromatography of LYRM5 alone (red), ETF alone (green), or the co-purified LYRM5-ETF complex (blue) noted in (D).

ETFB side 4

Expression

ACSF2 / ETFB

HPA RNA-seq normal tissues

See details

- Project title: HPA RNA-seq normal tissues
- Description: RNA-seq was performed of tissue samples from 95 human individuals representing 27 different tissues in order to determine tissue-specificity of all protein-coding genes
- BioProject: PRJEB4337
- Publication: PMID 24309898
- Analysis date: Wed Jun 15 11:32:44 2016

Genet er hypermethyleret i Vega 2014

(er ikke slået op i Vega 2017 S1, måske er det der?)

Samples

Man kunne gå videre her og se hvad betydning genet har.

Bibliography

Related articles in PubMed

1. Identification of novel PPARgamma target genes in primary human adipocytes.
   Perera RJ, *et al.* Gene, 2006 Mar 15. PMID 16380219
2. Evidence for 26 distinct acyl-coenzyme A synthetase genes in the human genome.
   Watkins PA, *et al.* J Lipid Res, 2007 Dec. PMID 17762044
3. Mitochondrial Protein Interaction Mapping Identifies Regulators of Respiratory Chain Function.
   Floyd BJ, *et al.* Mol Cell, 2016 Aug 18. PMID 27499296, Free PMC Article
4. Genetic variants in nuclear-encoded mitochondrial genes influence AIDS progression.
   Hendrickson SL, *et al.* PLoS One, 2010 Sep 21. PMID 20877624, Free PMC Article
5. The secreted protein discovery initiative (SPDI), a large-scale effort to identify novel human secreted and transmembrane proteins: a bioinformatics assessment.
   Clark HF, *et al.* Genome Res, 2003 Oct. PMID 12975309, Free PMC Article

ETFB idenne artikel

Format: Abstract

BMC Med Genomics. 2018 Apr 3;11(1):37. doi: 10.1186/s12920-018-0356-8.

Patient with multiple acyl-CoA dehydrogenase deficiency disease and ETFDH mutations benefits from riboflavin therapy: a case report.

Goh LL[1], Lee Y[2], Tan ES[3], Lim JSC[4], Lim CW[1], Dalan R[5,6,7].

Author information

Abstract

BACKGROUND: Lipid storage myopathy (LSM) is a diverse group of lipid metabolic disorders with great variations in the clinical phenotype and age of onset. Classical multiple acyl-CoA dehydrogenase deficiency (MADD) is known to occur secondary to mutations in electron transfer flavoprotein dehydrogenase (ETFDH) gene. Whole exome sequencing (WES) with clinical correlations can be useful in identifying genomic alterations for targeted therapy.

CASE PRESENTATION: We report a patient presented with severe muscle weakness and exercise intolerance, suggestive of LSM. Diagnostic testing demonstrated lipid accumulation in muscle fibres and elevated plasma acyl carnitine levels. Exome sequencing of the proband and two of his unaffected siblings revealed compound heterozygous mutations, c.250G > A (p.Ala84Thr) and c.770A > G (p.Tyr257Cys) in the ETFDH gene as the probable causative mutations. In addition, a previously unreported variant c.1042C > T (p.Arg348Trp) in ACOT11 gene was found. This missense variant was predicted to be deleterious but its association with lipid storage in muscle is unclear. The diagnosis of MADD was established and the patient was treated with riboflavin which resulted in rapid clinical and biochemical improvement.

CONCLUSIONS: Our findings support the role of WES as an effective tool in the diagnosis of highly heterogeneous disease and this has important implications in the therapeutic strategy of LSM treatment.

KEYWORDS: ETFDH; Lipid storage myopathy; Multiple acyl-CoA dehydrogenase deficiency; Whole exome sequencing

PMID: 29615056 DOI: 10.1186/s12920-018-0356-8

Grant support

LinkOut - more resources

ETFB side 6

FADS2 fatty acid desaturase 2 [*Homo sapiens* (human)]

Gene ID: 9415, updated on 4-Mar-2018

hypermethyleret Vega 2017, 57
mir 1908 hypomethyleret i CD4+T cells Brenu 2014

Summary
enome Browsers
enome Data Viewer
ap Viewer
riation Viewer (GRCh37.p13)
riation Viewer (GRCh38)
00 Genomes Browser (GRCh37.p13)
nsembl
CSC

Official Symbol	FADS2 provided by HGNC
Official Full Name	fatty acid desaturase 2 provided by HGNC
Primary source	HGNC:HGNC:3575
See related	Ensembl:ENSG00000134824 MIM:606149; Vega:OTTHUMG00000163794
Gene type	protein coding
RefSeq status	REVIEWED
Organism	Homo sapiens
Lineage	Eukaryota; Metazoa; Chordata; Craniata; Vertebrata; Euteleostomi; Mammalia; Eutheria; Euarchontoglires; Primates; Haplorrhini; Catarrhini; Hominidae; Homo
Also known as	D6D; DES6; TU13; FADSD6; LLCDL2; SLL0262
Summary	The protein encoded by this gene is a member of the fatty acid desaturase (FADS) gene family. Desaturase enzymes regulate unsaturation of fatty acids through the introduction of double bonds between defined carbons of the fatty acyl chain. FADS family members are considered fusion products composed of an N-terminal cytochrome b5-like domain and a C-terminal multiple membrane-spanning desaturase portion, both of which are characterized by conserved histidine motifs. This gene is clustered with family members at 11q12-q13.1; this cluster is thought to have arisen evolutionarily from gene duplication based on its similar exon/intron organization. Alternative splicing results in multiple transcript variants encoding different isoforms. [provided by RefSeq, Jul 2013]
Expression	Broad expression in adrenal (RPKM 104.8), brain (RPKM 64.0) and 16 other tissues See more
Orthologs	mouse all

Genomic context

See FADS2 in Genome Data Viewer Map Viewer

Location: 11q12.2

Exon count: 13

Annotation release	Status	Assembly	Chr	Location
108	current	GRCh38.p7 (GCF_000001405.33)	11	NC_000011.10 (61816203..61867354)
105	previous assembly	GRCh37.p13 (GCF_000001405.25)	11	NC_000011.9 (61583675..61634826)

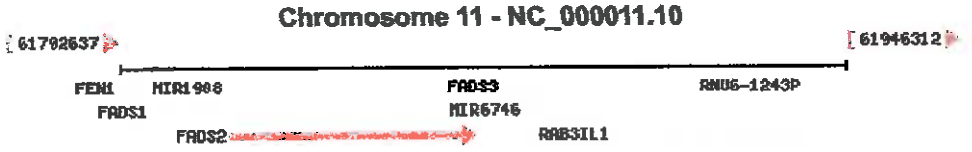

Genomic regions, transcripts, and products

Go to reference sequence details

Genomic Sequence: NC_000011.10 Chromosome 11 Reference GRCh38.p7 Primary Assembly ▼

FAM13A family with sequence similarity 13 member A [*Homo sapiens* (human)]

Gene ID: 10144, updated on 4-Mar-2018

genehspression opregulerd Nguyen 2017
Gen hypermethylerd Vega 2017, 57

Summary
enome Browsers
enome Data Viewer
ap Viewer
iriation Viewer (GRCh37.p13)
iriation Viewer (GRCh38)
)00 Genomes Browser (GRCh37.p13)
nsembl
CSC

Official Symbol	FAM13A provided by HGNC
Official Full Name	family with sequence similarity 13 member A provided by HGNC
Primary source	HGNC:HGNC:19367
See related	Ensembl:ENSG00000138640 MIM:613299; Vega:OTTHUMG00000161006
Gene type	protein coding
RefSeq status	VALIDATED
Organism	Homo sapiens
Lineage	Eukaryota; Metazoa; Chordata; Craniata; Vertebrata; Euteleostomi; Mammalia; Eutheria; Euarchontoglires; Primates; Haplorrhini; Catarrhini; Hominidae; Homo
Also known as	FAM13A1; ARHGAP48
Expression	Ubiquitous expression in fat (RPKM 21.4), thyroid (RPKM 14.6) and 25 other tissues See more
Orthologs	mouse all

Genomic context

Sammenhæng til COPD

See FAM13A in Genome Data Viewer Map Viewer

Location: 4q22.1

Exon count: 31

Annotation release	Status	Assembly	Chr	Location
108	current	GRCh38.p7 (GCF_000001405.33)	4	NC_000004.12 (88725954..89111398, complement)
105	previous assembly	GRCh37.p13 (GCF_000001405.25)	4	NC_000004.11 (89647105..90032549, complement)

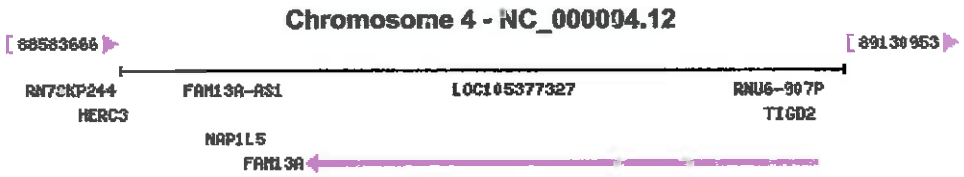

Genomic regions, transcripts, and products

Go to reference sequence details

Genomic Sequence: NC_000004.12 Chromosome 4 Reference GRCh38.p7 Primary Assembly

Go to nucleotide: Graphics FASTA GenBank

NC_000004.12 Find:

Genes, NCBI Homo sapiens Annotation Release 108, 2016-06-07

FAM13A side 1

FAM13A, A Fatty Acid Oxidation Switch in Mitochondria

Friend or Foe in Chronic Obstructive Pulmonary Disease Pathogenesis?

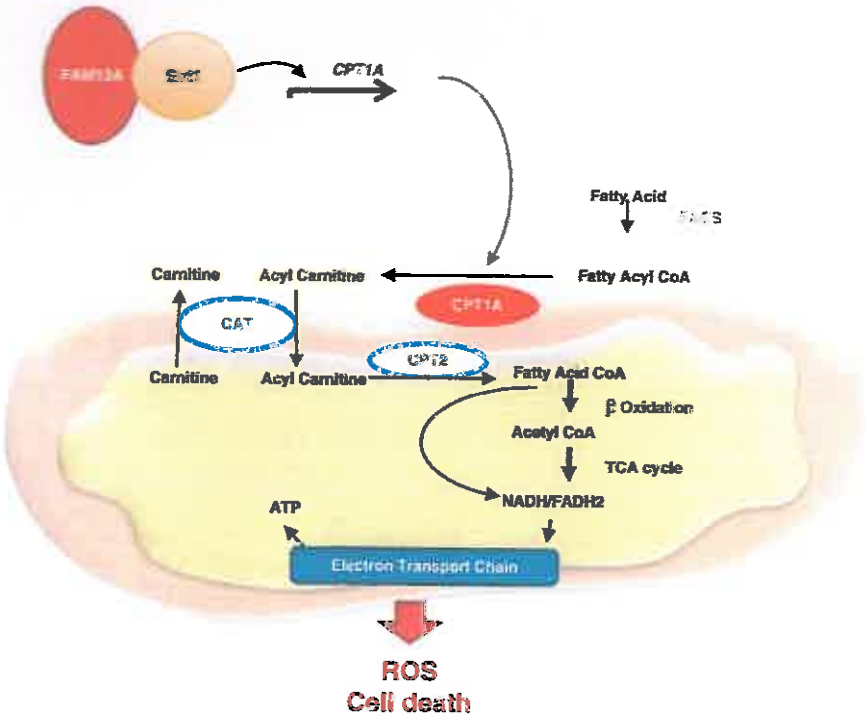

Figure 1. *FAM13A* regulates the CPT1A–FAO pathway in chronic obstructive pulmonary disease (COPD). *FAM13* locus has been shown to be associated with increased expression of *FAM13A* and higher risk for COPD. FAM13 in association with SIRT1 induces the expression of *CPT1A*, a key enzyme that regulates fatty acid oxidation (FAO) in the mitochondria. Up-regulation of CPT1A promotes FAO and high production of ROS, leading to lung epithelial cell death; this is an important pathogenic mechanism that might lead to COPD. CAT, carnitine translocase; CoA, coenzyme A; CPT1A, carnitine palmitoyltransferase 1; CPT2, carnitine palmitoyltransferase 2; FACS, fatty acyl-CoA synthase; FADH2, flavin adenin dinucleotide; FAM13A, family with sequence similarity 13 member A; NADH, nicotinamide adenine dinucleotide reduced; ROS, reactive oxygen species; SIRT1, sirtuin 1; TCA, tricarboxylic acid cycle.

in isolated type 2 epithelial cells from mice exposed to CS (8). In addition, cell and mouse models often fail to consider that COPD is frequently a disease of the elderly, and metabolic changes occur in the lung and other tissues with aging. Thus, studies in alveolar epithelial cells derived from patients with COPD might confer better understanding of the metabolic adaptations to chronic stress, as well as their consequences in cell survival.

The studies by Jiang and colleagues solidify the link between mitochondrial function and COPD that has been previously suggested. Cloonan and colleagues showed that another commonly replicated COPD risk gene, *IREB2*, also has links to mitochondrial function (13). As with *FAM13A*, *IREB2* expression is increased in the lungs of patients with COPD, and mice without an *IREB2* gene were protected from CS-induced COPD. Exposure to CS has also been linked to other alterations in mitochondrial function and homeostasis, including increased ROS production, reduced biogenesis, disrupted mitochondrial fusion, and altered mitophagy (14, 15).

FAM13 has previously been shown to negatively regulate β-catenin activity, promoting its degradation (16). However, inhibition of β-catenin in airway epithelial cell lines did not alter FAO, suggesting FAM13 promotes tissue destruction and impaired repair capacity by a different mechanism. The work by Jiang et al represents a step forward in the identification of pathogenic mechanisms in COPD and the correlation with genetic susceptibility to this disease. Future studies are required to fully clarify the cellular and metabolic responses of human lung cells to chronic stress and disease (Figure 1). ■

Author disclosures are available with the text of this article at www.atsjournals.org.

Gregory A. Hawkins, Ph.D.
Center for Genomics and Personalized Medicine Research
Wake Forest School of Medicine
Winston-Salem, North Carolina

Ana L. Mora, M.D.
Division of Pulmonary, Allergy, and Critical Care Medicine
Vascular Medicine Institute
University of Pittsburgh
Pittsburgh, Pennsylvania

ORCID IDs: 0000-0002-8239-2428 (G.A.H.); 0000-0003-1653-8318 (A.L.M.).

References

1. Rhoades RA. Influence of starvation on the lung: effect on glucose and palmitate utilization. *J Appl Physiol* 1975;38:513–516.
2. Scholz RW, Rhoades RA. Lipid metabolism by rat lung in vitro: effect of starvation and re-feeding on utilization of [U-^{14}C]glucose by lung slices. *Biochem J* 1971;124:257–264.
3. Lehwald N, Tao GZ, Jang KY, Papandreou I, Liu B, Liu B, Pysz MA, Willmann JK, Knoefel WT, Denko NC, *et al.* β-Catenin regulates hepatic mitochondrial function and energy balance in mice. *Gastroenterology* 2012;143:754–764.
4. Hancock DB, Soler Artigas M, Gharib SA, Henry A, Manichaikul A, Ramasamy A, Loth DW, Imboden M, Koch B, McArdle WL, *et al.*

FAM13A side 2

FKBP5 FK506 binding protein 5 [*Homo sapiens* (human)]

Gene ID: 2289, updated on 18-Mar-2018

↑ 5'UTR Vega 2017, S7

Summary
enome Browsers
enome Data Viewer
ap Viewer
ariation Viewer (GRCh37.p13)
ariation Viewer (GRCh38)
00 Genomes Browser (GRCh37.p13)
nsembl
CSC

Official Symbol	FKBP5 provided by HGNC
Official Full Name	FK506 binding protein 5 provided by HGNC
Primary source	HGNC:HGNC:3721
See related	Ensembl:ENSG00000096060 MIM:602623; Vega:OTTHUMG00000014576
Gene type	protein coding
RefSeq status	REVIEWED
Organism	Homo sapiens
Lineage	Eukaryota; Metazoa; Chordata; Craniata; Vertebrata; Euteleostomi; Mammalia; Eutheria; Euarchontoglires; Primates; Haplorrhini; Catarrhini; Hominidae; Homo
Also known as	P54; AIG6; FKBP51; FKBP54; PPIase; Ptg-10
Summary	The protein encoded by this gene is a member of the immunophilin protein family, which play a role in immunoregulation and basic cellular processes involving protein folding and trafficking. This encoded protein is a cis-trans prolyl isomerase that binds to the immunosuppressants FK506 and rapamycin. It is thought to mediate calcineurin inhibition. It also interacts functionally with mature hetero-oligomeric progesterone receptor complexes along with the 90 kDa heat shock protein and P23 protein. This gene has been found to have multiple polyadenylation sites. Alternative splicing results in multiple transcript variants. [provided by RefSeq, Mar 2009]
Expression	Broad expression in fat (RPKM 97.5), lymph node (RPKM 33.3) and 18 other tissues See more
Orthologs	mouse all

Genomic context

See FKBP5 in Genome Data Viewer Map Viewer

Location: 6p21.31

Exon count: 13

Annotation release	Status	Assembly	Chr	Location
108	current	GRCh38.p7 (GCF_000001405.33)	6	NC_000006.12 (35573585..35728583, complement)
105	previous assembly	GRCh37.p13 (GCF_000001405.25)	6	NC_000006.11 (35541362..35696360, complement)

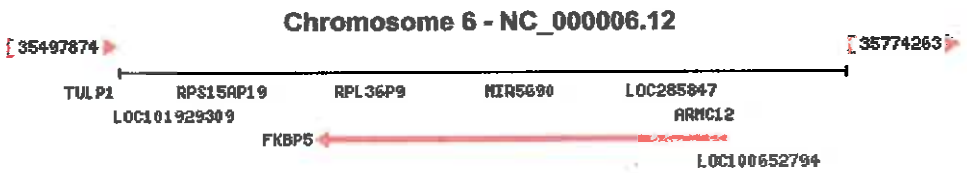

Genomic regions, transcripts, and products

Go to reference sequence details

Genomic Sequence: NC_000006.12 Chromosome 6 Reference GRCh38.p7 Primary Assembly

FKBP5 side 1

Yu HM, *et al.* Gene, 2017 Sep 5. PMID 28629826

3. A FKBP5 mutation is associated with Paget's disease of bone and enhances osteoclastogenesis.
   Lu B, *et al.* Exp Mol Med, 2017 May 19. PMID 28524179, Free PMC Article
4. Methylation matters: FK506 binding protein 51 (FKBP5) methylation moderates the associations of FKBP5 genotype and resistant attachment with stress regulation.
   Mulder RH, *et al.* Dev Psychopathol, 2017 May. PMID 28401840, Free PMC Article
5. FKBP5 genotype and early life stress exposure predict neurobehavioral outcomes for preterm infants.
   D'Agata AL, *et al.* Dev Psychobiol, 2017 Apr. PMID 28247564

See all (247) citations in PubMed

See citations in PubMed for homologs of this gene provided by HomoloGene

GeneRIFs: Gene References Into Functions What's a GeneRIF?

1. GxE interaction between child maltreatment and FKBP5 on dissociative symptoms in adolescence.
2. Children with high attachment insecurity and homozygous FKBP5 minor alleles manifest maladaptive emotion regulation and depressive symptoms.
3. This study demonstrated that FKBP5 Messenger RNA Increases After Adolescence in Human Dorsolateral Prefrontal Cortex.
4. A novel FKBP5 1V55L mutation is associated with Paget's disease in a Chinese family. Mutant FKBP51V55L promotes osteoclastogenesis.
5. A negative correlation between basal levels of FKBP5 methylation and serum cortisol was observed.
6. Study found an additive interaction effect between FKBP5's rs1360780 variant and the graph-theoretical metrics of hippocampal connectivity to influence depression risk. Data reveals alterations of the communication patterns between the hippocampus and the rest of the brain in depression, effects potentially driven by overall familial factors (genes plus shared twin environment) and modified by the FKBP5 gene.
7. This study demonstrated suggest that FKBP5 in the GR pathway may be a point of vulnerability to early-life adversity, as seen in this group of non-traumatized young adults.
8. Psychological stress impaired immediate recall in rs1360780, rs3800373 and rs9296158 allele carriers.
9. Association of FKBP5 haplotype with risk of suicide attempt.
10. This study provides initial evidence that the risk alleles of the FKBP5 polymorphism are associated with different resting-state activity in a frontotemporal-parietal network, and may point to mechanisms underpinning high-risk carriers' vulnerability to severe stress reactions.

Submit: New GeneRIF Correction See all GeneRIFs (184)

Phenotypes

Find tests for this gene in the NIH Genetic Testing Registry (GTR)

Review eQTL and phenotype association data in this region using PheGenI

Associated conditions

Description	Tests
Major depressive disorder MedGen: C1269683, OMIM: 608516, GeneReviews: Not available	Compare labs

Slide fra Ron Davis (i relation til FKBP5)

27 Clinical Lab Tests (>200 Total) Significantly Different Between Patients and Controls

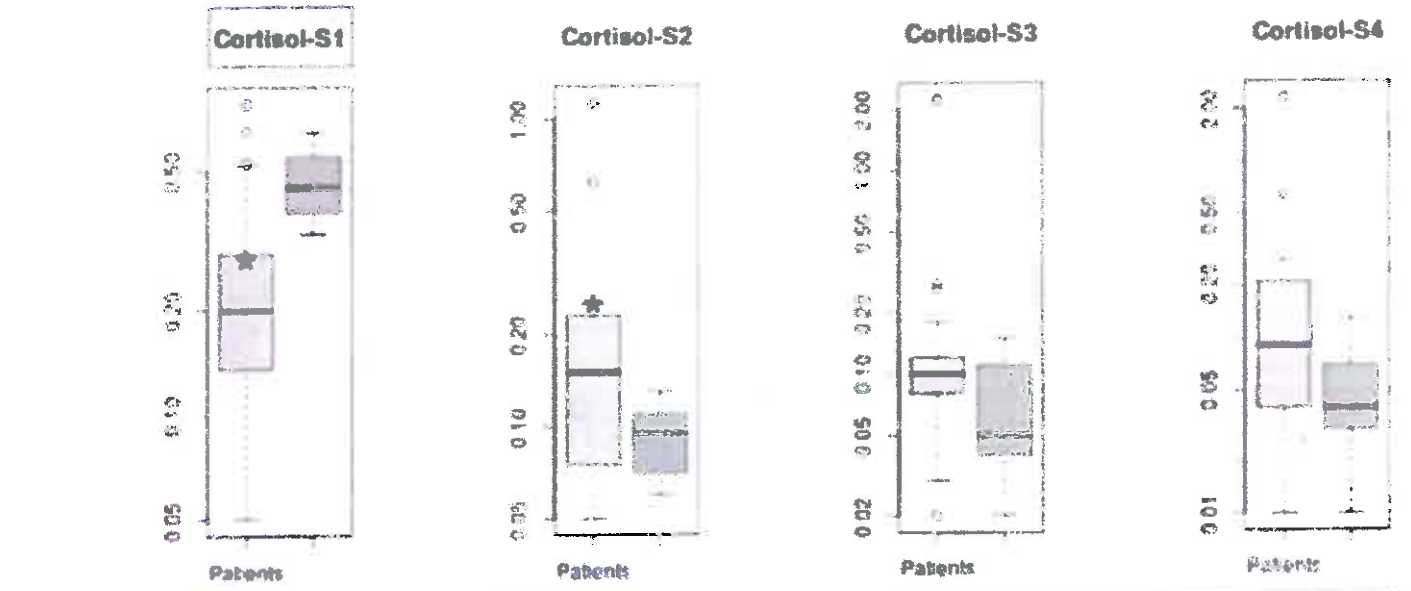

↑

ME patienter har lavt cortisol-niveau om morgenen, senere på dagen øges det.

FKBP5 side 3

HADH hydroxyacyl-CoA dehydrogenase [*Homo sapiens* (human)]

Gene ID: 3033, updated on 5-Nov-2017

3'UTR hypo Vega 2017 S6 s1

Hide sidebar >>

Summary
enome Browsers
enome Data Viewer
ap Viewer
riation Viewer (GRCh37.p13)
riation Viewer (GRCh38)
00 Genomes Browser (GRCh37.p13)
nsembl
CSC

Official Symbol	HADH provided by HGNC
Official Full Name	hydroxyacyl-CoA dehydrogenase provided by HGNC
Primary source	HGNC:HGNC:4799
See related	Ensembl:ENSG00000138796 MIM:601609; Vega:OTTHUMG00000131810
Gene type	protein coding
RefSeq status	REVIEWED
Organism	Homo sapiens
Lineage	Eukaryota; Metazoa; Chordata; Craniata; Vertebrata; Euteleostomi; Mammalia; Eutheria; Euarchontoglires; Primates; Haplorrhini; Catarrhini; Hominidae; Homo
Also known as	HAD; HCDH; HHF4; HADH1; SCHAD; HADHSC; MSCHAD
Summary	This gene is a member of the 3-hydroxyacyl-CoA dehydrogenase gene family. The encoded protein functions in the mitochondrial matrix to catalyze the oxidation of straight-chain 3-hydroxyacyl-CoAs as part of the beta-oxidation pathway. Its enzymatic activity is highest with medium-chain-length fatty acids. Mutations in this gene cause one form of familial hyperinsulinemic hypoglycemia. The human genome contains a related pseudogene of this gene on chromosome 15. [provided by RefSeq, May 2010]
Orthologs	mouse all

Genomic context

See HADH in Genome Data Viewer Map Viewer

Location: 4q25

Exon count: 11

Annotation release	Status	Assembly	Chr	Location
108	current	GRCh38.p7 (GCF_000001405.33)	4	NC_000004.12 (107989714..108035175)
105	previous assembly	GRCh37.p13 (GCF_000001405.25)	4	NC_000004.11 (108910870..108956331)

Chromosome 4 - NC_000004.12

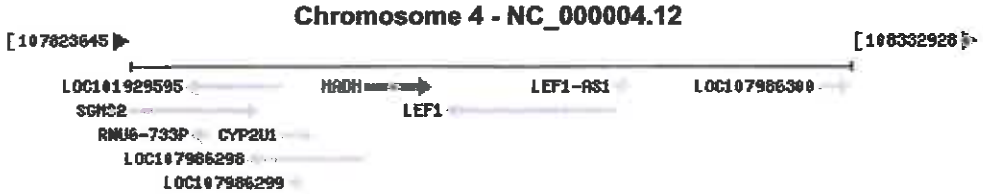

Genomic regions, transcripts, and products

Go to reference sequence details

Genomic Sequence: NC_000004.12 Chromosome 4 Reference GRCh38.p7 Primary Assembly

Go to nucleotide: Graphics FASTA GenBank

NC_000004.12 | Find:

HMGCL 3-hydroxymethyl-3-methylglutaryl-CoA lyase [*Homo sapiens* (human)]

Gene ID: 3155, updated on 21-Dec-2016

Summary

↑ hypermethylated Vega 2014

Official Symbol	HMGCL provided by HGNC
Official Full Name	3-hydroxymethyl-3-methylglutaryl-CoA lyase provided by HGNC
Primary source	HGNC:HGNC:5005
See related	Ensembl:ENSG00000117305 MIM:613898; Vega:OTTHUMG00000002963
Gene type	protein coding
RefSeq status	REVIEWED
Organism	Homo sapiens
Lineage	Eukaryota; Metazoa; Chordata; Craniata; Vertebrata; Euteleostomi; Mammalia; Eutheria; Euarchontoglires; Primates; Haplorrhini; Catarrhini; Hominidae; Homo
Also known as	HL
Summary	The protein encoded by this gene belongs to the HMG-CoA lyase family. It is a mitochondrial enzyme that catalyzes the final step of leucine degradation and plays a key role in ketone body formation. Mutations in this gene are associated with HMG-CoA lyase deficiency. Alternatively spliced transcript variants encoding different isoforms have been found for this gene. [provided by RefSeq, Oct 2009]
Orthologs	mouse all

Genomic context

See HMGCL in Genome Data Viewer Map Viewer

Location: 1p36.11

Exon count: 9

Annotation release	Status	Assembly	Chr	Location
108	current	GRCh38.p7 (GCF_000001405.33)	1	NC_000001.11 (23801877..23825459, complement)
105	previous assembly	GRCh37.p13 (GCF_000001405.25)	1	NC_000001.10 (24128367..24165110, complement)

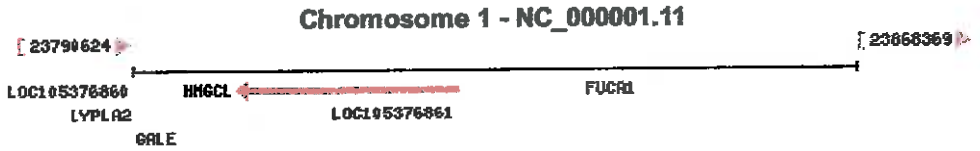

Genomic regions, transcripts, and products

Go to reference sequence details

Genomic Sequence: NC_000001.11 Chromosome 1 Reference GRCh38.p7 Primary Assembly

Go to nucleotide: Graphics FASTA GenBank

OSBPL6 oxysterol binding protein like 6 [*Homo sapiens* (human)]

Gene ID: 114880, updated on 4-Feb-2018

5'UTR hypometylerat } vega 2017
TSS200 hypermethyrat } tabel 57
relaterat til ME patienters livs-kvalitet

Summary
enome Browsers
enome Data Viewer
ap Viewer
riation Viewer (GRCh37.p13)
riation Viewer (GRCh38)
00 Genomes Browser (GRCh37.p13)
nsembl
CSC

Official Symbol	OSBPL6 provided by HGNC
Official Full Name	oxysterol binding protein like 6 provided by HGNC
Primary source	HGNC:HGNC:16388
See related	Ensembl:ENSG00000079156 MIM:606734; Vega:OTTHUMG00000132579
Gene type	protein coding
RefSeq status	REVIEWED
Organism	Homo sapiens
Lineage	Eukaryota; Metazoa; Chordata; Craniata; Vertebrata; Euteleostomi; Mammalia; Eutheria; Euarchontoglires; Primates; Haplorrhini; Catarrhini; Hominidae; Homo
Also known as	ORP6
Summary	*This gene encodes a member of the oxysterol-binding protein (OSBP) family, a group of intracellular lipid receptors. Most members contain an N-terminal pleckstrin homology domain and a highly conserved C-terminal OSBP-like sterol-binding domain. Transcript variants encoding different isoforms have been identified.* [provided by RefSeq, Jul 2008]
Expression	Broad expression in brain (RPKM 4.0), skin (RPKM 2.6) and 21 other tissues See more
Orthologs	mouse all

Genomic context

See OSBPL6 in Genome Data Viewer Map Viewer

Location: 2q31.2

Exon count: 30

Annotation release	Status	Assembly	Chr	Location
108	current	GRCh38.p7 (GCF_000001405.33)	2	NC_000002.12 (178194479..178399433)
105	previous assembly	GRCh37.p13 (GCF_000001405.25)	2	NC_000002.11 (179059208..179264160)

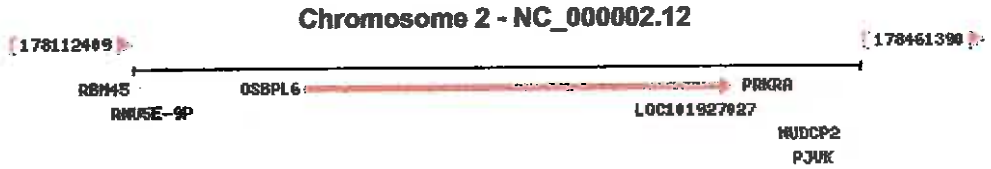

Genomic regions, transcripts, and products

Go to reference sequence details

Genomic Sequence: NC_000002.12 Chromosome 2 Reference GRCh38.p7 Primary Assembly

Go to nucleotide: Graphics FASTA GenBank

OXNAD1 oxidoreductase NAD binding domain containing 1 [*Homo sapiens* (human)]

OXNAD1 hypo Vega 2017 S7, RFTN1 ↑

Gene ID: 92106, updated on 11-Mar-2018

YBEY sidder ved siden af PCNT på chr 11
D2HGDH + OXNAD1 interagerer med YBEY

enome Browsers
enome Data Viewer
ap Viewer
ıriation Viewer (GRCh37.p13)
ıriation Viewer (GRCh38)
)00 Genomes Browser (GRCh37.p13)
ısembl
CSC

Summary

Official Symbol	OXNAD1 provided by HGNC
Official Full Name	oxidoreductase NAD binding domain containing 1 provided by HGNC
Primary source	HGNC:HGNC:25128
See related	Ensembl:ENSG00000154814 Vega:OTTHUMG00000129867
Gene type	protein coding
RefSeq status	VALIDATED
Organism	Homo sapiens
Lineage	Eukaryota; Metazoa; Chordata; Craniata; Vertebrata; Euteleostomi; Mammalia; Eutheria; Euarchontoglires; Primates; Haplorrhini; Catarrhini; Hominidae; Homo
Expression	Ubiquitous expression in lymph node (RPKM 2.7), appendix (RPKM 1.8) and 24 other tissues See more
Orthologs	mouse all

Genomic context

See OXNAD1 in Genome Data Viewer Map Viewer

Location: 3p25.1-p24.3

Exon count: 19

Annotation release	Status	Assembly	Chr	Location
108	current	GRCh38.p7 (GCF_000001405.33)	3	NC_000003.12 (16265160..16386979)
105	previous assembly	GRCh37.p13 (GCF_000001405.25)	3	NC_000003.11 (16306667..16379000)

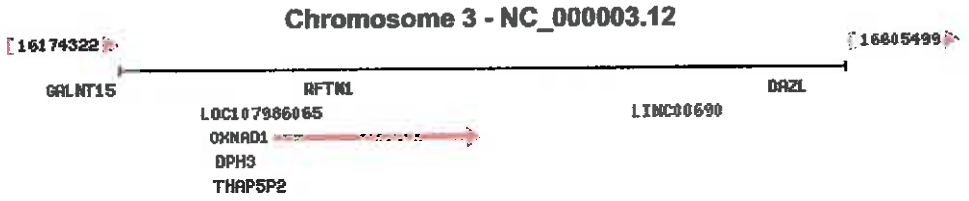

Genomic regions, transcripts, and products

Go to reference sequence details

Genomic Sequence: NC_000003.12 Chromosome 3 Reference GRCh38.p7 Primary Assembly ▼

Go to nucleotide: Graphics FASTA GenBank

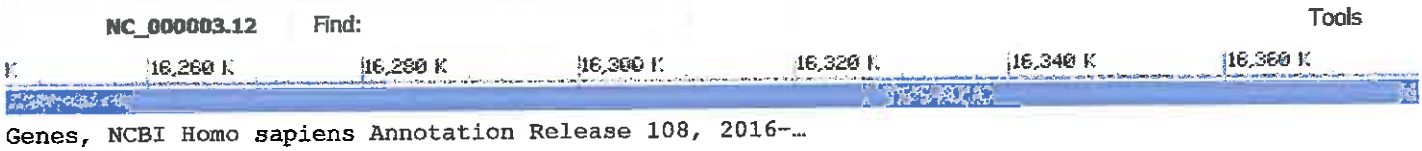

Genes, NCBI Homo sapiens Annotation Release 108, 2016-…

OXNAD1 side 1

Conserved Domains (1) summary

cd00322 Location:48 → 282 FNR_like; Ferredoxin reductase (FNR), an FAD and NAD(P) binding protein, was intially identified as a chloroplast reductase activity, catalyzing the electron transfer from reduced iron-sulfur protein ferredoxin to NADP+ as the final step in the electron transport ...

8. NM_001352983.1 → NP_001339912.1 **oxidoreductase NAD-binding domain-containing protein 1 isoform 3**

Status: VALIDATED

Source sequence(s) AC090948, AC090953, CR739022

Conserved Domains (1) summary

cd00322 Location:48 → 282 FNR_like; Ferredoxin reductase (FNR), an FAD and NAD(P) binding protein, was intially identified as a chloroplast reductase activity, catalyzing the electron transfer from reduced iron-sulfur protein ferredoxin to NADP+ as the final step in the electron transport ...

9. NM_138381.4 → NP_612390.1 **oxidoreductase NAD-binding domain-containing protein 1 isoform 2 precursor**

See identical proteins and their annotated locations for NP_612390.1

Status: VALIDATED

Source sequence(s) AC090953, BC007285, BC008322, HY044078
Consensus CDS CCDS2630.1
UniProtKB/Swiss-Prot Q96HP4
Related ENSP00000285083.5, OTTHUMP00000160306, ENST00000285083.9

Conserved Domains (1) summary

cd00322 Location:75 → 309 FNR_like; Ferredoxin reductase (FNR), an FAD and NAD(P) binding protein, was intially identified as a chloroplast reductase activity, catalyzing the electron transfer from reduced iron-sulfur protein ferredoxin to NADP+ as the final step in the electron transport ...

RNA

1. NR_148217.1 **RNA Sequence**

Status: VALIDATED

Source sequence(s) AC090948, AC090953, BQ180851

2. NR_148218.1 **RNA Sequence**

Status: VALIDATED

Source sequence(s) AC090948, AC090953, BQ180851

3. NR_148219.1 **RNA Sequence**

Status: VALIDATED

Source sequence(s) AC090948, AC090953, BQ180851

4. NR_148220.1 **RNA Sequence**

Status: VALIDATED

Source sequence(s) AC090948, AC090953, CR739022

PFKFB3 6-phosphofructo-2-kinase/fructose-2,6-biphosphatase 3 [*Homo sapiens* (human)]

hypermethylerot body, Vega 2017,57

Gene ID: 5209, updated on 29-Mar-2018

enome Browsers
Summary
enome Data Viewer
ap Viewer
riation Viewer (GRCh37.p13)
riation Viewer (GRCh38)
00 Genomes Browser (GRCh37.p13)
nsembl
CSC

Official Symbol	PFKFB3 provided by HGNC
Official Full Name	6-phosphofructo-2-kinase/fructose-2,6-biphosphatase 3 provided by HGNC
Primary source	HGNC:HGNC:8874
See related	Ensembl:ENSG00000170525 MIM:605319; Vega:OTTHUMG00000017621
Gene type	protein coding
RefSeq status	REVIEWED
Organism	Homo sapiens
Lineage	Eukaryota; Metazoa; Chordata; Craniata; Vertebrata; Euteleostomi; Mammalia; Eutheria; Euarchontoglires; Primates; Haplorrhini; Catarrhini; Hominidae; Homo
Also known as	PFK2; IPFK2; iPFK-2
Summary	The protein encoded by this gene belongs to a family of bifunctional proteins that are involved in both the synthesis and degradation of fructose-2,6-bisphosphate, a regulatory molecule that controls glycolysis in eukaryotes. The encoded protein has a 6-phosphofructo-2-kinase activity that catalyzes the synthesis of fructose-2,6-bisphosphate (F2,6BP), and a fructose-2,6-biphosphatase activity that catalyzes the degradation of F2,6BP. This protein is required for cell cycle progression and prevention of apoptosis. It functions as a regulator of cyclin-dependent kinase 1, linking glucose metabolism to cell proliferation and survival in tumor cells. Several alternatively spliced transcript variants encoding different isoforms have been found for this gene. [provided by RefSeq, Apr 2016]
Expression	Biased expression in fat (RPKM 188.2), bone marrow (RPKM 67.0) and 9 other tissues See more
Orthologs	mouse all

Genomic context

See PFKFB3 in Genome Data Viewer Map Viewer

Location: 10p15.1

Exon count: 20

Annotation release	Status	Assembly	Chr	Location
109	current	GRCh38.p12 (GCF_000001405.38)	10	NC_000010.11 (6144878..6254648)
105	previous assembly	GRCh37.p13 (GCF_000001405.25)	10	NC_000010.10 (6186843..6277508)

Chromosome 10 - NC_000010.11

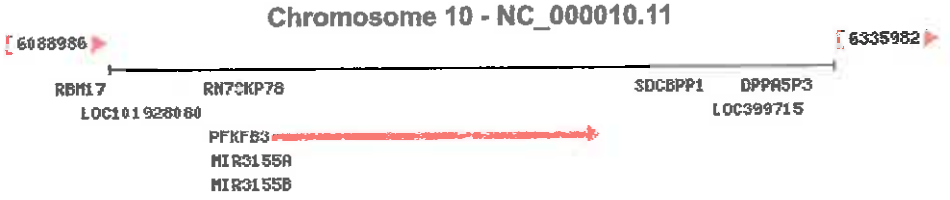

Genomic regions, transcripts, and products

PHYH phytanoyl-CoA 2-hydroxylase [*Homo sapiens* (human)]

Gene ID: 5264, updated on 5-Nov-2017

= phytanoyl coA 2 oxoglutarate dioxy genase

hypermethylated Vega 2017

Summary
enome Browsers
enome Data Viewer
ap Viewer
riation Viewer (GRCh37.p13)
riation Viewer (GRCh38)
00 Genomes Browser (GRCh37.p13)
nsembl
CSC

Official Symbol	PHYH provided by HGNC
Official Full Name	phytanoyl-CoA 2-hydroxylase provided by HGNC
Primary source	HGNC:HGNC:8940
See related	Ensembl:ENSG00000107537 MIM:602026; Vega:OTTHUMG00000017693
Gene type	protein coding
RefSeq status	REVIEWED
Organism	Homo sapiens
Lineage	Eukaryota; Metazoa; Chordata; Craniata; Vertebrata; Euteleostomi; Mammalia; Eutheria; Euarchontoglires; Primates; Haplorrhini; Catarrhini; Hominidae; Homo
Also known as	RD; LN1; PAHX; LNAP1; PHYH1
Summary	This gene is a member of the PhyH family and encodes a peroxisomal protein that is involved in the alpha-oxidation of 3-methyl branched fatty acids. Specifically, this protein converts phytanoyl-CoA to 2-hydroxyphytanoyl-CoA. Mutations in this gene have been associated with Refsum disease (RD) and deficient protein activity has been associated with Zellweger syndrome and rhizomelic chondrodysplasia punctata. Alternate transcriptional splice variants, encoding different isoforms, have been characterized. [provided by RefSeq, Jul 2008]
Expression	Broad expression in liver (RPKM 137.6), kidney (RPKM 65.7) and 17 other tissues See more
Orthologs	mouse all

Genomic context

Proves: L-ascorbic acid binding

See PHYH in Genome Data Viewer Map Viewer

Location: 10p13

Exon count: 10

Interaktion: FKBP4, PEX7, ELAVL1, TP53, WRAP73

Annotation release	Status	Assembly	Chr	Location
108	current	GRCh38.p7 (GCF_000001405.33)	10	NC_000010.11 (13277796..13300130, complement)
105	previous assembly	GRCh37.p13 (GCF_000001405.25)	10	NC_000010.10 (13319796..13342133, complement)

Chromosome 10 - NC_000010.11

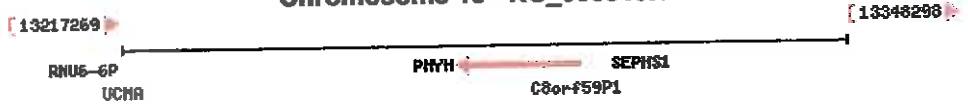

Genomic regions, transcripts, and products

Go to reference sequence details

Genomic Sequence: NC_000010.11 Chromosome 10 Reference GRCh38.p7 Primary Assembly

Go to nucleotide: Graphics FASTA GenBank

NC_000010.11 Find:

POR cytochrome p450 oxidoreductase [*Homo sapiens* (human)]

Gene ID: 5447, updated on 29-Mar-2018

hypomethylated Vega 2014+2017

Important!

Summary
enome Browsers
enome Data Viewer
ap Viewer
riation Viewer (GRCh37.p13)
riation Viewer (GRCh38)
00 Genomes Browser (GRCh37.p13)
ısembl
CSC

Official Symbol	POR provided by HGNC
Official Full Name	cytochrome p450 oxidoreductase provided by HGNC
Primary source	HGNC:HGNC:9208
See related	Ensembl:ENSG00000127948 MIM:124015; Vega:OTTHUMG00000130413
Gene type	protein coding
RefSeq status	REVIEWED
Organism	Homo sapiens
Lineage	Eukaryota; Metazoa; Chordata; Craniata; Vertebrata; Euteleostomi; Mammalia; Eutheria; Euarchontoglires; Primates; Haplorrhini; Catarrhini; Hominidae; Homo
Also known as	CPR; CYPOR; P450R
Summary	This gene encodes an endoplasmic reticulum membrane oxidoreductase with an FAD-binding domain and a flavodoxin-like domain. The protein binds two cofactors, FAD and FMN, which allow it to donate electrons directly from NADPH to all microsomal P450 enzymes. Mutations in this gene have been associated with various diseases, including apparent combined P450C17 and P450C21 deficiency, amenorrhea and disordered steroidogenesis, congenital adrenal hyperplasia and Antley-Bixler syndrome. [provided by RefSeq, Jul 2008]
Expression	Ubiquitous expression in liver (RPKM 99.7), adrenal (RPKM 78.6) and 25 other tissues See more
Orthologs	mouse all

Genomic context

See POR in Genome Data Viewer Map Viewer

Location: 7q11.23

Exon count: 16

Annotation release	Status	Assembly	Chr	Location
109	current	GRCh38.p12 (GCF_000001405.38)	7	NC_000007.14 (75915102..75986855)
105	previous assembly	GRCh37.p13 (GCF_000001405.25)	7	NC_000007.13 (75544420..75616173)

Chromosome 7 - NC_000007.14

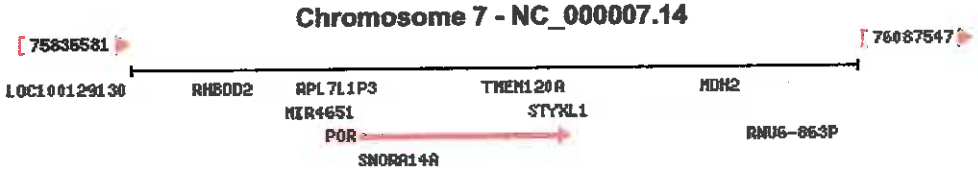

Genomic regions, transcripts, and products

Go to reference sequence details

Genomic Sequence: NC_000007.14 Chromosome 7 Reference GRCh38.p12 Primary Assembly ▼

✓ las artikler og viden **Go to nucleotide:** Graphics FASTA GenBank

PPCDC phosphopantothenoylcysteine decarboxylase [*Homo sapiens* (human)]

Gene ID: 60490, updated on 29-Mar-2018

hypermethylerct body Vega 2017, S7

Summary
enome Browsers
enome Data Viewer
ap Viewer
riation Viewer (GRCh37.p13)
riation Viewer (GRCh38)
00 Genomes Browser (GRCh37.p13)
nsembl
CSC

Official Symbol	PPCDC provided by HGNC
Official Full Name	phosphopantothenoylcysteine decarboxylase provided by HGNC
Primary source	HGNC:HGNC:28107
See related	Ensembl:ENSG00000138621 MIM:609854; Vega:OTTHUMG00000142824
Gene type	protein coding
RefSeq status	VALIDATED
Organism	Homo sapiens
Lineage	Eukaryota; Metazoa; Chordata; Craniata; Vertebrata; Euteleostomi; Mammalia; Eutheria; Euarchontoglires; Primates; Haplorrhini; Catarrhini; Hominidae; Homo
Also known as	coaC; MDS018; PPC-DC
Summary	Biosynthesis of coenzyme A (CoA) from pantothenic acid (vitamin B5) is an essential universal pathway in prokaryotes and eukaryotes. PPCDC (EC 4.1.1.36), one of the last enzymes in this pathway, converts phosphopantothenoylcysteine to 4-prime-phosphopantetheine (Daugherty et al., 2002 [PubMed 11923312]).[supplied by OMIM, Mar 2008]
Expression	Ubiquitous expression in bone marrow (RPKM 1.6), appendix (RPKM 1.5) and 25 other tissues See more
Orthologs	mouse all

Genomic context

See PPCDC in Genome Data Viewer Map Viewer

Location: 15q24.2

Exon count: 10

Annotation release	Status	Assembly	Chr	Location
109	current	GRCh38.p12 (GCF_000001405.38)	15	NC_000015.10 (75023544..75060180)
105	previous assembly	GRCh37.p13 (GCF_000001405.25)	15	NC_000015.9 (75315927..75343067)

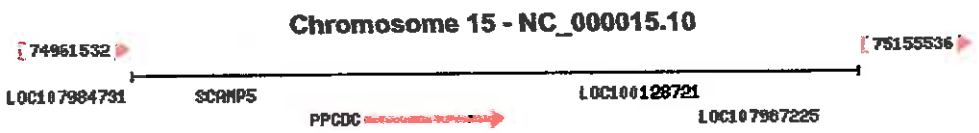

Genomic regions, transcripts, and products

Go to reference sequence details

Genomic Sequence: NC_000015.10 Chromosome 15 Reference GRCh38.p12 Primary Assembly

Go to nucleotide: Graphics FASTA GenBank

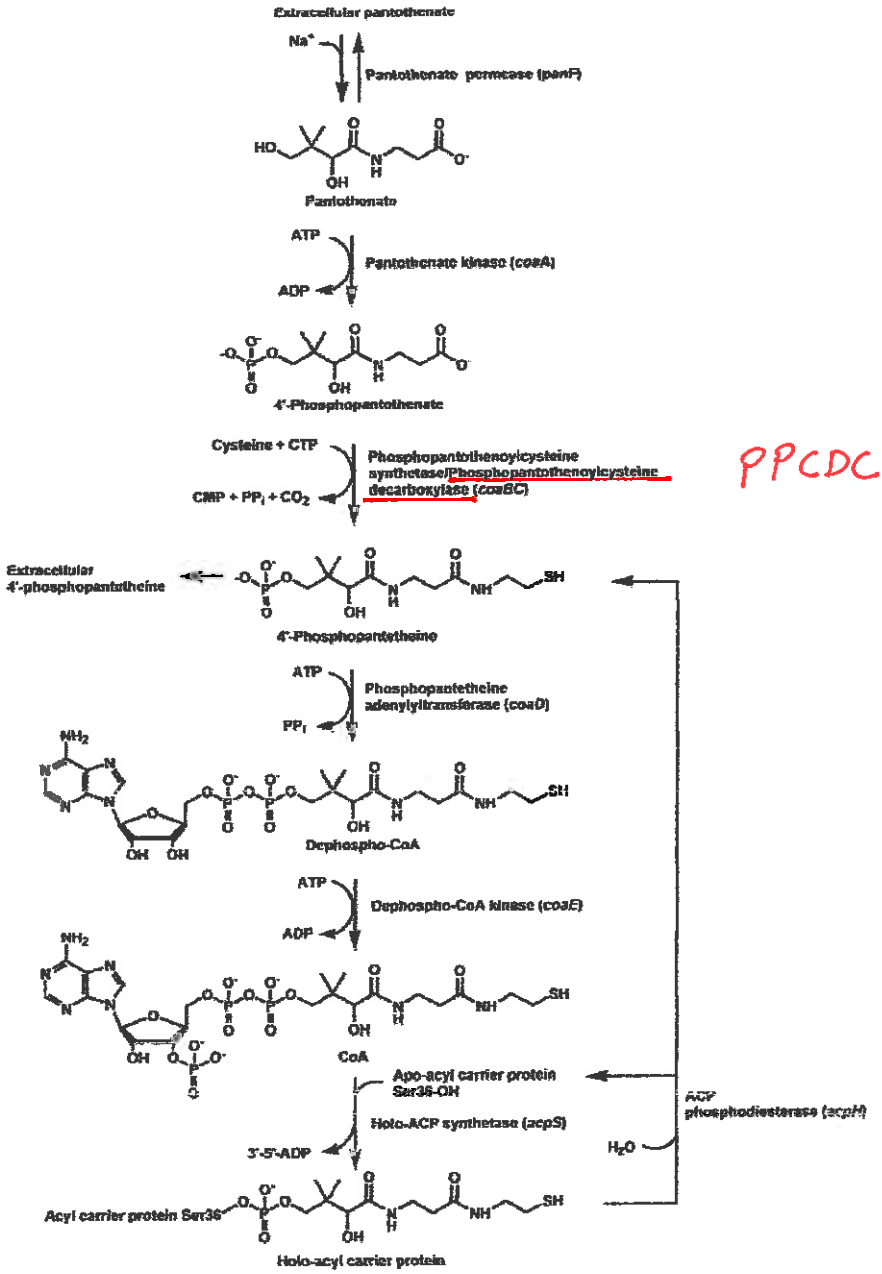

Figure 2.

Pathway for CoA biosynthesis and the addition of the prosthetic group to ACP. Active uptake of pantothenate by a sodium-dependent permease (the *panF* gene product) is an alternate route to intracellular pantothenate, which is then either used for CoA biosynthesis or exported from the cells by a separate transport system. Pantothenate kinase (the *coaA* gene product) is the first, and most highly regulated, step in CoA biosynthesis and is regulated by feedback inhibition by CoA and its thioesters. Cysteine is then added to 4′-phosphopanthenate to generate 4′-phosphopantothenoylcysteine, which is then

PPCDC side2

SORCS2 sortilin related VPS10 domain containing receptor 2 [*Homo sapiens* (human)]

hypermethylated Vega 2014

Gene ID: 57537, updated on 29-Mar-2018

enome Browsers
enome Data Viewer
ap Viewer
riation Viewer (GRCh37.p13)
riation Viewer (GRCh38)
00 Genomes Browser (GRCh37.p13)
nsembl
CSC

Summary

Official Symbol	SORCS2 provided by HGNC
Official Full Name	sortilin related VPS10 domain containing receptor 2 provided by HGNC
Primary source	HGNC:HGNC:16698
See related	Ensembl:ENSG00000184985 MIM:606284; Vega:OTTHUMG00000159981
Gene type	protein coding
RefSeq status	REVIEWED
Organism	Homo sapiens
Lineage	Eukaryota; Metazoa; Chordata; Craniata; Vertebrata; Euteleostomi; Mammalia; Eutheria; Euarchontoglires; Primates; Haplorrhini; Catarrhini; Hominidae; Homo
Summary	This gene encodes one family member of vacuolar protein sorting 10 (VPS10) domain-containing receptor proteins. The VPS10 domain name comes from the yeast carboxypeptidase Y sorting receptor Vps10 protein. Members of this gene family are large with many exons but the CDS lengths are usually less than 3700 nt. Very large introns typically separate the exons encoding the VPS10 domain; the remaining exons are separated by much smaller-sized introns. These genes are strongly expressed in the central nervous system. [provided by RefSeq, Jul 2008]
Expression	Broad expression in brain (RPKM 4.7), kidney (RPKM 2.0) and 20 other tissues See more
Orthologs	mouse all

Genomic context

See SORCS2 in Genome Data Viewer Map Viewer

Location: 4p16.1

Exon count: 29

Annotation release	Status	Assembly	Chr	Location
109	current	GRCh38.p12 (GCF_000001405.38)	4	NC_000004.12 (7192607..7742837)
105	previous assembly	GRCh37.p13 (GCF_000001405.25)	4	NC_000004.11 (7194374..7744564)

Chromosome 4 - NC_000004.12

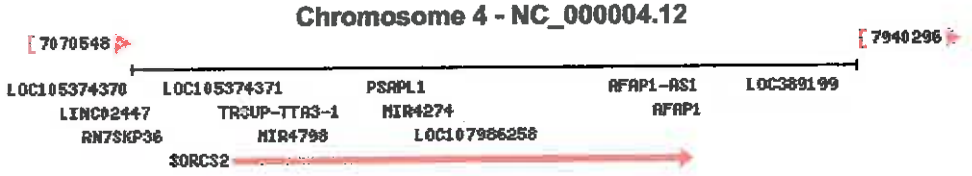

Genomic regions, transcripts, and products

Go to reference sequence details

Genomic Sequence: NC_000004.12 Chromosome 4 Reference GRCh38.p12 Primary Assembly ▼

Go to nucleotide: Graphics FASTA GenBank

SORL1 sortilin related receptor 1 [*Homo sapiens* (human)]

Gene ID: 6653, updated on 31-Oct-2016

Summary

Official Symbol	SORL1 provided by HGNC
Official Full Name	sortilin related receptor 1 provided by HGNC
Primary source	HGNC:HGNC:11185
See related	Ensembl:ENSG00000137642 HPRD:03595; MIM:602005; Vega:OTTHUMG00000166057
Gene type	protein coding
RefSeq status	REVIEWED
Organism	Homo sapiens
Lineage	Eukaryota; Metazoa; Chordata; Craniata; Vertebrata; Euteleostomi; Mammalia; Eutheria; Euarchontoglires; Primates; Haplorrhini; Catarrhini; Hominidae; Homo
Also known as	LR11; LRP9; SORLA; gp250; SorLA-1; C11orf32
Summary	This gene encodes a mosaic protein that belongs to at least two families: the vacuolar protein sorting 10 (VPS10) domain-containing receptor family, and the low density lipoprotein receptor (LDLR) family. The encoded protein also contains fibronectin type III repeats and an epidermal growth factor repeat. The encoded preproprotein is proteolytically processed to generate the mature receptor, which likely plays roles in endocytosis and sorting. Mutations in this gene may be associated with Alzheimer's disease. [provided by RefSeq, Feb 2016]
Annotation information	Note: In some of the published literature, this gene has been incorrectly associated with the LRP9 alias, but the LRP9 alias more correctly refers to Gene ID 26020, LRP10. [05 May 2010]
Orthologs	mouse all

Genomic context

See SORL1 in Genome Data Viewer Map Viewer

Location: 11q24.1

Exon count: 53

Annotation release	Status	Assembly	Chr	Location
108	current	GRCh38.p7 (GCF_000001405.33)	11	NC_000011.10 (121452203..121633762)
105	previous assembly	GRCh37.p13 (GCF_000001405.25)	11	NC_000011.9 (121322912..121504471)

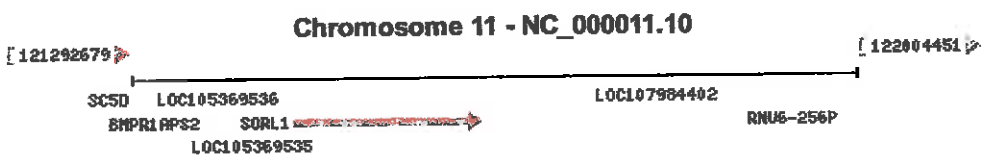

Genomic regions, transcripts, and products

Go to reference sequence details

Genomic Sequence: NC_000011.10 Chromosome 11 Reference GRCh38.p7 Primary Assembly

Go to nucleotide: Graphics FASTA GenBank

SORT1 sortilin 1 [*Homo sapiens* (human)]

Gene ID: 6272, updated on 29-Mar-2018

hypermethylerat TSS1500, Vega2017§7

Summary
enome Browsers
enome Data Viewer
ap Viewer
riation Viewer (GRCh37.p13)
riation Viewer (GRCh38)
00 Genomes Browser (GRCh37.p13)
nsembl
CSC

Official Symbol	SORT1 provided by HGNC
Official Full Name	sortilin 1 provided by HGNC
Primary source	HGNC:HGNC:11186
See related	Ensembl:ENSG00000134243 MIM:602458, Vega:OTTHUMG00000011999
Gene type	protein coding
RefSeq status	REVIEWED
Organism	Homo sapiens
Lineage	Eukaryota; Metazoa; Chordata; Craniata; Vertebrata; Euteleostomi; Mammalia; Eutheria; Euarchontoglires; Primates; Haplorrhini; Catarrhini; Hominidae; Homo
Also known as	NT3; Gp95; NTR3; LDLCQ6
Summary	This gene encodes a member of the VPS10-related sortilin family of proteins. The encoded preproprotein is proteolytically processed by furin to generate the mature receptor. This receptor plays a role in the trafficking of different proteins to either the cell surface, or subcellular compartments such as lysosomes and endosomes. Expression levels of this gene may influence the risk of myocardial infarction in human patients. Alternative splicing results in multiple transcript variants. [provided by RefSeq, Oct 2015]
Expression	Broad expression in brain (RPKM 47.1), testis (RPKM 30.3) and 22 other tissues See more
Orthologs	mouse all

proteomstudie spinal normal-CFS-post Lyme
4 - 7 - 9

Genomic context

Interaktion med SLAM

See SORT1 in Genome Data Viewer Map Viewer

Location: 1p13.3; 1p21.3-p13.1

Exon count: 23

Annotation release	Status	Assembly	Chr	Location
109	current	GRCh38.p12 (GCF_000001405.38)	1	NC_000001.11 (109309565..109397945, complement)
105	previous assembly	GRCh37.p13 (GCF_000001405.25)	1	NC_000001.10 (109852187..109940563, complement)

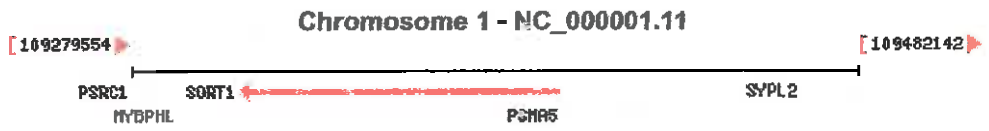

Genomic regions, transcripts, and products

Go to reference sequence details

Genomic Sequence: NC_000001.11 Chromosome 1 Reference GRCh38.p12 Primary Assembly

Go to nucleotide: Graphics FASTA GenBank

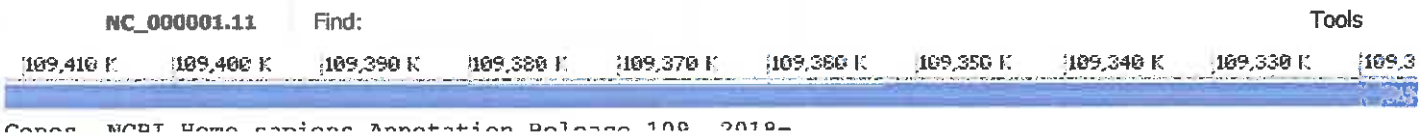

UCP2 uncoupling protein 2 [*Homo sapiens* (human)]

Gene ID: 7351, updated on 2-Apr-2018

↓hypomethylered Vega 2014
→ Søg efter dem i Vega 2017

Summary
enome Browsers
enome Data Viewer
ap Viewer
riation Viewer (GRCh37.p13)
riation Viewer (GRCh38)
00 Genomes Browser (GRCh37.p13)
isembl
CSC

Official Symbol	UCP2 provided by HGNC
Official Full Name	uncoupling protein 2 provided by HGNC
Primary source	HGNC:HGNC:12518
See related	Ensembl:ENSG00000175567 MIM:601693; Vega:OTTHUMG00000163095
Gene type	protein coding
RefSeq status	REVIEWED
Organism	Homo sapiens
Lineage	Eukaryota; Metazoa; Chordata; Craniata; Vertebrata; Euteleostomi; Mammalia; Eutheria; Euarchontoglires; Primates; Haplorrhini; Catarrhini; Hominidae; Homo
Also known as	UCPH; BMIQ4; SLC25A8
Summary	Mitochondrial uncoupling proteins (UCP) are members of the larger family of mitochondrial anion carrier proteins (MACP). UCPs separate oxidative phosphorylation from ATP synthesis with energy dissipated as heat, also referred to as the mitochondrial proton leak. UCPs facilitate the transfer of anions from the inner to the outer mitochondrial membrane and the return transfer of protons from the outer to the inner mitochondrial membrane. They also reduce the mitochondrial membrane potential in mammalian cells. Tissue specificity occurs for the different UCPs and the exact methods of how UCPs transfer H+/OH- are not known. UCPs contain the three homologous protein domains of MACPs. This gene is expressed in many tissues, with the greatest expression in skeletal muscle. It is thought to play a role in nonshivering thermogenesis, obesity and diabetes. Chromosomal order is 5'-UCP3-UCP2-3'. [provided by RefSeq, Jul 2008]
Expression	Broad expression in lymph node (RPKM 136.6), spleen (RPKM 105.7) and 20 other tissues See more
Orthologs	mouse all

Genomic context

See UCP2 in Genome Data Viewer Map Viewer

Location: 11q13.4

Exon count: 7

Annotation release	Status	Assembly	Chr	Location
109	current	GRCh38.p12 (GCF_000001405.38)	11	NC_000011.10 (73974671..73982872, complement)
105	previous assembly	GRCh37.p13 (GCF_000001405.25)	11	NC_000011.9 (73685716..73693889, complement)

Chromosome 11 - NC_000011.10

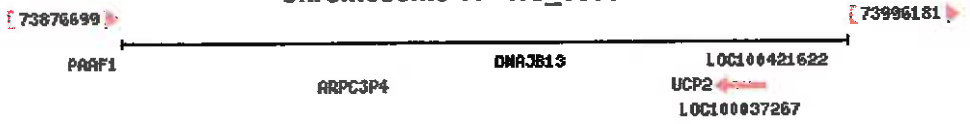

Genomic regions, transcripts, and products

Go to reference sequence details

UCP side 1

Figure 1. Ferrar et al. J Clin Endocrinol Metab 2017

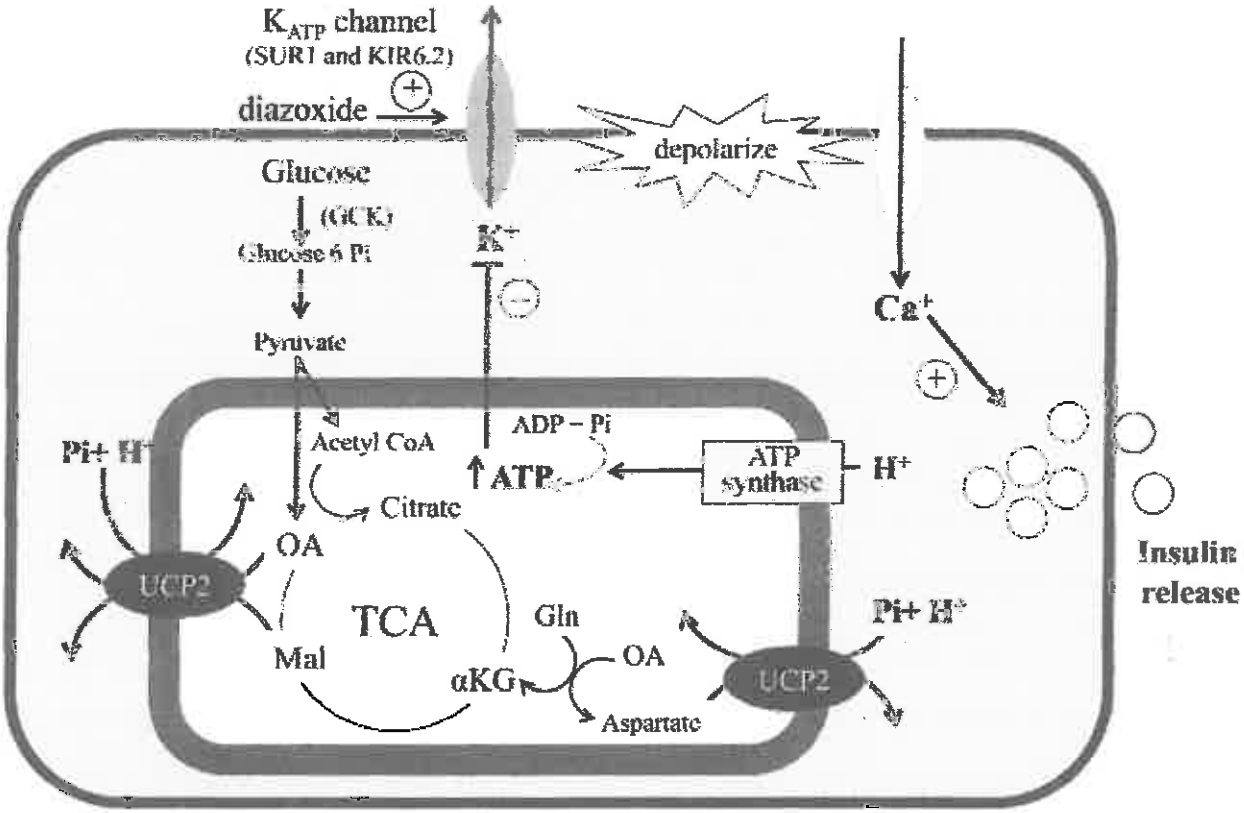

UCP2 modulates β-cell insulin secretion. UCP2 activity increases oxaloacetate to enhance glucose oxidation and restrain the oxidation of amino acids via glutamate metabolism to α-ketoglutarate. αKG: αketoglutarate; acetyl CoA, acetyl coenzyme A; ADP, adenosine 5′-diphosphate; ATP, adenosine triphosphate; GCK, glucokinase; Gln, glutamine; KIR6.2/SUR1, adenosine triphosphate–dependent potassium channel; Mal, malate; OA, oxaloacetate; Pi, phosphate; TCA, tricarboxylic acid.

UCP side 2

UCP3 uncoupling protein 3 [*Homo sapiens* (human)]

Gene ID: 7352, updated on 29-Mar-2018

↓ hypomethylierd Vega 2014

→ Sog effekt dann i Vega 2017

Summary
enome Browsers
enome Data Viewer
ap Viewer
riation Viewer (GRCh37.p13)
riation Viewer (GRCh38)
00 Genomes Browser (GRCh37.p19)
sembl
CSC

Official Symbol	UCP3 provided by HGNC
Official Full Name	uncoupling protein 3 provided by HGNC
Primary source	HGNC:HGNC:12519
See related	Ensembl:ENSG00000175564 MIM:602044; Vega:OTTHUMG00000168109
Gene type	protein coding
RefSeq status	REVIEWED
Organism	Homo sapiens
Lineage	Eukaryota; Metazoa; Chordata; Craniata; Vertebrata; Euteleostomi; Mammalia; Eutheria; Euarchontoglires; Primates; Haplorrhini; Catarrhini; Hominidae; Homo
Also known as	SLC25A9
Summary	Mitochondrial uncoupling proteins (UCP) are members of the larger family of mitochondrial anion carrier proteins (MACP). UCPs separate oxidative phosphorylation from ATP synthesis with energy dissipated as heat, also referred to as the mitochondrial proton leak. UCPs facilitate the transfer of anions from the inner to the outer mitochondrial membrane and the return transfer of protons from the outer to the inner mitochondrial membrane. They also reduce the mitochondrial membrane potential in mammalian cells. The different UCPs have tissue-specific expression; this gene is primarily expressed in skeletal muscle. This gene's protein product is postulated to protect mitochondria against lipid-induced oxidative stress. Expression levels of this gene increase when fatty acid supplies to mitochondria exceed their oxidation capacity and the protein enables the export of fatty acids from mitochondria. UCPs contain the three solcar protein domains typically found in MACPs. Two splice variants have been found for this gene.[provided by RefSeq, Nov 2008]
Expression	Low expression observed in reference dataset See more
Orthologs	mouse all

Genomic context

See UCP3 in Genome Data Viewer Map Viewer

Location: 11q13.4

Exon count: 7

Annotation release	Status	Assembly	Chr	Location
109	current	GRCh38.p12 (GCF_000001405.38)	11	NC_000011.10 (74000281..74009237, complement)
105	previous assembly	GRCh37.p13 (GCF_000001405.25)	11	NC_000011.9 (73711326..73720282, complement)

Chromosome 11 - NC_000011.10

Genomic regions, transcripts, and products